

**RESPONSE OF RICE (*ORYZA SATIVA* L.) TO
HYDROXYAPATITE NANOPARTICLES
AS SOURCE OF PHOSPHORUS AND
CALCIUM FERTILIZER**



Sirinapa Pongpeera

**A Thesis Submitted in Partial Fulfillment of the Requirements for the
Degree of Doctor of Philosophy in Environmental Biology**

Suranaree University of Technology

Academic Year 2020

การตอบสนองของข้าว (*Oryza sativa* L.) ต่อการใช้อนุภาคนาโนของไฮดรอกซีอะพาไทต์เป็นแหล่งของปุ๋ยฟอสฟอรัสและแคลเซียม



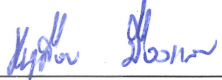
นางสาวศิริินภา พงษ์พีระ

วิทยานิพนธ์นี้เป็นส่วนหนึ่งของการศึกษาตามหลักสูตรปริญญาวิทยาศาสตรดุษฎีบัณฑิต
สาขาวิชาชีววิทยาลิ่งแวดล้อม
มหาวิทยาลัยเทคโนโลยีสุรนารี
ปีการศึกษา 2563

**RESPONSE OF RICE (*ORYZA SATIVA* L.) TO HYDROXYAPATITE
NANOPARTICLES AS SOURCE OF PHOSPHORUS
AND CALCIUM FERTILIZER**

Suranaree University of Technology has approved this thesis submitted in partial fulfillment of the requirements for the Degree of Doctor of Philosophy.

Thesis Examining Committee



(Assoc. Prof. Dr. Nooduan Muangsan)

Chairperson



(Asst. Prof. Dr. Duangkamol Maensiri)

Member (Thesis Advisor)



(Prof. Dr. Piyada Theerakulpisut)

Member



(Asst. Prof. Dr. Sodchol Wonprasaid)

Member



(Asst. Prof. Dr. Santi Watthana)

Member



(Assoc. Prof. Dr. Worawat Meevasana)



(Assoc. Prof. Ft. Lt. Dr. Kontorn Chamniprasart)

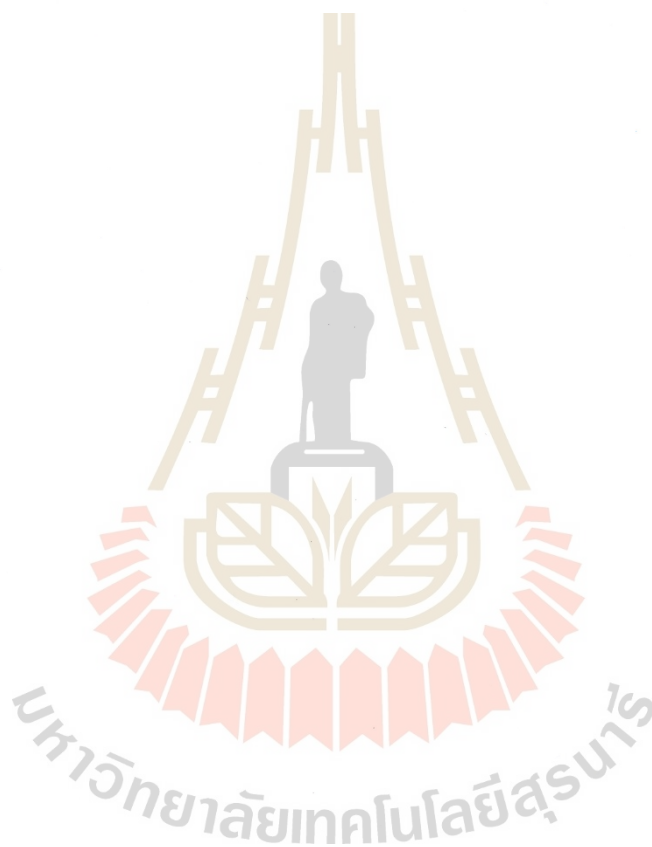
Vice Rector for Academic Affairs
and Internationalization

Dean of Institute of Science

ศิริินภา พงษ์พีระ : การตอบสนองของข้าว (*Oryza sativa* L.) ต่อการใช้อนุภาคนาโนของไฮดรอกซีอะพาไทต์เป็นแหล่งของปุ๋ยฟอสฟอรัสและแคลเซียม (RESPONSE OF RICE (*ORYZA SATIVA* L.) TO HYDROXYAPATITE NANOPARTICLES AS SOURCE OF PHOSPHORUS AND CALCIUM FERTILIZER) อาจารย์ที่ปรึกษา : ผู้ช่วยศาสตราจารย์ ดร.ดวงกมล แม่นศิริ, 142 หน้า.

ไฮดรอกซีอะพาไทต์ (Hydroxyapatite; HAp) ($\text{Ca}_{10}(\text{PO}_4)_6(\text{OH})_2$) เป็นเกลือแคลเซียมฟอสเฟตที่เสถียรที่สุด มีศักยภาพในการใช้เป็นปุ๋ยทางเลือกสำหรับส่งเสริมการเจริญเติบโตของพืช อย่างไรก็ตาม ไฮดรอกซีอะพาไทต์ไม่สามารถละลายได้ง่าย มีการตั้งสมมติฐานว่าไฮดรอกซีอะพาไทต์ ที่มีขนาดเล็กจะละลายน้ำได้ดีขึ้น และด้วยเหตุนี้จึงเหมาะสมที่จะนำมาใช้เป็นปุ๋ยทางเลือกได้ อนุภาคนาโนไฮดรอกซีอะพาไทต์ที่ใช้ในงานวิจัยถูกสังเคราะห์โดยเทคนิคโซลเจลในสารละลายว่านหางจระเข้ และศึกษาลักษณะของอนุภาคโดยใช้เทคนิค XRD TEM SEM/EDX และ FT-Raman อนุภาคนาโนไฮดรอกซีอะพาไทต์ หลังจากแช่ในน้ำเป็นเวลา 30 วัน ถูกนำมาตรวจสอบการละลาย ติดตามการปลดปล่อยธาตุฟอสเฟตและแคลเซียมไอออน โดยใช้เทคนิค Ion Chromatography (IC) ผลการวิจัยพบว่าภายใน 30 วัน อนุภาคนาโนไฮดรอกซีอะพาไทต์ที่มีความเข้มข้น 100 มิลลิกรัมต่อลิตร สามารถปลดปล่อยฟอสเฟต 3.30 มิลลิกรัมต่อลิตร และปลดปล่อยแคลเซียมไอออนได้ 3.18 มิลลิกรัมต่อลิตร ซึ่งชี้ให้เห็นถึงความเป็นไปได้ในการใช้อนุภาคนาโนไฮดรอกซีอะพาไทต์เป็นปุ๋ยที่ปลดปล่อยธาตุอาหารออกมาช้า ๆ ขณะเดียวกันในการศึกษาผลของอนุภาคนาโนไฮดรอกซีอะพาไทต์ต่อการงอกและการเจริญของต้นกล้า ได้ใช้เวลา 7 วัน ในการติดตาม เมล็ดสัมพัทธ์กับอนุภาคนาโนไฮดรอกซีอะพาไทต์เทียบกับปุ๋ยเชิงพาณิชย์สูตร (18-46-0 และ 15-15-15) ที่ความเข้มข้น 100 500 และ 1,000 มิลลิกรัมต่อลิตร วัดการงอก ความยาวรากและความยาวยอด ปริมาณมาลอนไดคิไฮด์ และการตายของเซลล์ พบว่าอนุภาคนาโนไฮดรอกซีอะพาไทต์สามารถเพิ่มเปอร์เซ็นต์การงอกได้สูงถึง 98 เปอร์เซ็นต์ที่ 100 มิลลิกรัมต่อลิตร ความยาวรากได้รับการกระตุ้นอย่างมากที่ 100 และ 500 มิลลิกรัมต่อลิตร ในขณะที่ความยาวของยอดไม่ได้รับผลกระทบในเชิงลบ ขณะเดียวกันผลของอนุภาคนาโนไฮดรอกซีอะพาไทต์ ไม่ส่งผลทำให้เซลล์ตาย นอกจากนี้ในงานวิจัยนี้ได้มีการติดตามการตอบสนองทางสรีรวิทยาของข้าว ในระยะการเจริญเติบโต ความสูงของต้นข้าว ความกว้างของใบ จำนวนรวง จำนวนเมล็ดต่อรวง น้ำหนักเมล็ด จำนวน 1,000 เมล็ด ได้ทำการบันทึกหลัง 130 วัน นอกจากนี้ยังมีการศึกษาคุณภาพของเมล็ดข้าว โดยศึกษาปริมาณอะมิโลส แป้งในเมล็ด และกลิ่นหอมของข้าว (2-Acetyl-1-pyrroline) ใช้อนุภาคนาโนไฮดรอกซีอะพาไทต์และปุ๋ยเชิงพาณิชย์ (18-46-0 และ 15-15-15) 100 500 และ 1,000 มิลลิกรัมต่อกิโลกรัมของดินในการปลูกข้าว ผลการสังเกตพบว่า มีพารามิเตอร์บางอย่างของการเจริญเติบโตของพืชที่ไม่ได้รับผลกระทบ ขณะที่บางส่วนได้รับผลกระทบในทางลบจากอนุภาคนา-

โนไฮดรอกซีอะพาไทต์ คุณภาพของผลผลิตพบว่าที่ได้รับอนุภาคนาโนไฮดรอกซีอะพาไทต์ดีกว่าในกลุ่มการทดลองอื่น พารามิเตอร์คุณภาพของผลผลิตที่ดีขึ้น ได้แก่ จำนวนเมล็ดต่อรวง น้ำหนัก 1,000 เมล็ด ปริมาณแป้ง ปริมาณอะมิโลส และกลิ่นหอมของเมล็ด ผลการวิจัยโดยรวมยืนยันว่าอนุภาคนาโนไฮดรอกซีอะพาไทต์ ที่สังเคราะห์ขึ้นโดยใช้วุ้นหางจรเข้ไม่เป็นอันตรายต่อข้าวและมีศักยภาพในการนำมาใช้เป็นปุ๋ยนาโนฟอสฟอรัสในการเกษตรได้ ข้อเสนอแนะเพิ่มเติมในการศึกษาเกี่ยวกับอนุภาคนาโนไฮดรอกซีอะพาไทต์ จะเสนอให้ตรวจสอบและติดตามถึงผลกระทบต่อสิ่งแวดล้อม การชะล้างผ่านดินและผลเสียที่อาจเกิดขึ้นต่อจุลินทรีย์ในดินเป็นต้น



สาขาวิชาชีววิทยา
ปีการศึกษา 2563

ลายมือชื่อนักศึกษา สินันท์ พงษ์มิตร
ลายมือชื่ออาจารย์ที่ปรึกษา อนุ

SIRINAPA PONGPEERA : RESPONSE OF RICE (*ORYZA SATIVA* L.) TO
HYDROXYAPATITE NANOPARTICLES AS SOURCE OF PHOSPHORUS
AND CALCIUM FERTILIZER. THESIS ADVISOR : ASST. PROF.
DUANGKAMOL MAENSIRI, Ph.D. 142 PP.

HYDROXYAPATITE/NANO-FERTILIZER/GERMINATION/GROWTH /2AP

Hydroxyapatite (HAp) ($\text{Ca}_{10}(\text{PO}_4)_6(\text{OH})_2$) is the most stable calcium phosphate salt. It has the potential to serve as an alternative fertilizer for enhancing plant growth. Nonetheless, HAp does not easily dissolve. It was hypothesized that HAp with a smaller size would dissolve better and hence would be more suitable to serve as an alternative fertilizer. HAp nanoparticles were used in this research synthesized by the sol-gel technique in aloe vera extract, and characterized using XRD, TEM, SEM/EDX, and FT-Raman techniques. HAp nanoparticles left in water for 30 days were investigated for dissolution. The determination of released PO_4^{3-} and Ca^{2+} was conducted using ion chromatography technique. The results indicated that within 30 days, HAp nanoparticles at 100 mg/L released 3.30 mg/L of PO_4^{3-} and 3.18 mg/L of Ca^{2+} , suggesting that it is possible to use HAp nanoparticles as fertilizer that slowly release nutrients. Effect of HAp nanoparticles on germination and seedling were studied for 7 days. Seeds were exposed to HAp nanoparticles compared with commercial fertilizers (18-46-0 and 15-15-15) at concentrations of 100, 500, and 1000 mg/L. Germination, root and shoot length, malondialdehyde level, and cell death were measured. HAp nanoparticles was found that it increased the germination to be as high as 98% at 100 mg/L. Interestingly, the results showed that the root length was

strongly stimulated at 100 and 500 mg while the shoot length did not show any effect. HAp nanoparticles did not cause cell death. In this study, physiological responses were monitored on vegetative stages. Height and leaf width, the number of panicles, the number of grains per panicle, the weights of 1000 grains were recorded in 130 days. In addition, the quality of grains was studied including amylose content, starch in seed, and aroma in seed (2-Acetyl-1-pyrroline). HAp nanoparticles and commercial fertilizers (18-46-0 and 15-15-15) at 100, 500, and 1000 mg/kg in soil were used to treat the rice plants. The results revealed that some parameters of vegetative growth were not affected and some were negatively affected by HAp nanoparticles. Yield quality was found to be better in the HAp nanoparticles treated groups. The better yield and quality parameters included the number of grains per panicle, weight of 1000 grains, starch content, amylose content, and seed aroma. Overall results confirmed that synthesized HAp nanoparticles in Aloe vera extract are not harmful to rice and has potential to be used as phosphorus nanofertilizer in agriculture. Further study on the HAp nanoparticle is suggested to include the monitoring of effects on the environment, leaching through soil, and possible adverse effect on soil microorganisms.

School of Biology

Academic Year 2020

Student's Signature



Advisor's Signature



ACKNOWLEDGEMENTS

I am sincerely grateful to my thesis advisor, Asst. Prof. Dr. Duangkamol Maensiri for her invaluable help, encouragement, valuable suggestion, and support throughout my project. I will be forever grateful.

The author wishes to acknowledge Suranaree University of Technology for the scholarship supporting this study.

I wish to thank Nakhon Ratchasima Rice research center, Nakhon Ratchasima province, for rice grains and kindly provided in this research.

I am also grateful to all the faculty and staff members of the school of Biology and colleagues of the Center for Scientific and Technology Equipment Building 2 Suranaree University of Technology for their help and assistance throughout this research work.

Finally, I wish to thank my family for their unfaltering faith in my ability and encouragement throughout this research.

Sirinapa Pongpeera

CONTENTS

	Page
ABSTRACT IN THAI	I
ABSTRACT IN ENGLISH	III
ACKNOWLEDGEMENT	V
CONTENTS	VI
LIST OF TABLES	XI
LIST OF FIGURES	XIII
LIST OF ABBREVIATIONS	XIX
CHAPTER	
I INTRODUCTION	1
1.1 Background Problem	1
1.2 Research Objectives	4
1.3 Research Hypothesis	4
1.4 Scope and Limitation of the Study	5
1.5 Expected Results	5
II LITERATURE REVIEWS	7
2.1 Agriculture and Fertilizer Use	7
2.2 Calcium Fertilizer	10
2.3 Phosphorus Fertilizer	12
2.4 Application of Nanomaterial in Agriculture	15

CONTENTS (Continued)

		Page
	2.5 Hydroxyapatite Nanoparticle and Their potential Use as Nanofertilizers	18
	2.6 Nanotechnology and Agriculture in the Future	25
III	MATERIALS AND METHODS	28
	3.1 The Synthesis of Hydroxyapatite Nanoparticles Using Aloe Vera Extract by Sol Gel Method	28
	3.2 Characterization of the Resulted Hydroxyapatite Nanoparticles	29
	3.2.1 X-ray diffraction analysis	29
	3.2.2 Transmission electron microscope	29
	3.2.3 Scanning electron microscopy with energy dispersive X-Ray analysis	30
	3.2.4 Fourier transform and Raman spectrometer	31
	3.3 Determination of Size Distribution and Dissolution of Hydroxyapatite Nanoparticles in Solutions	31
	3.3.1 Preparation of particles in solution	31
	3.3.2 Determination of size distribution	31
	3.3.3 Determination of zeta potential	32
	3.3.4 Dissolution of Ca^{2+} and PO_4^{3-} from HAp nanoparticles.....	32

CONTENTS (Continued)

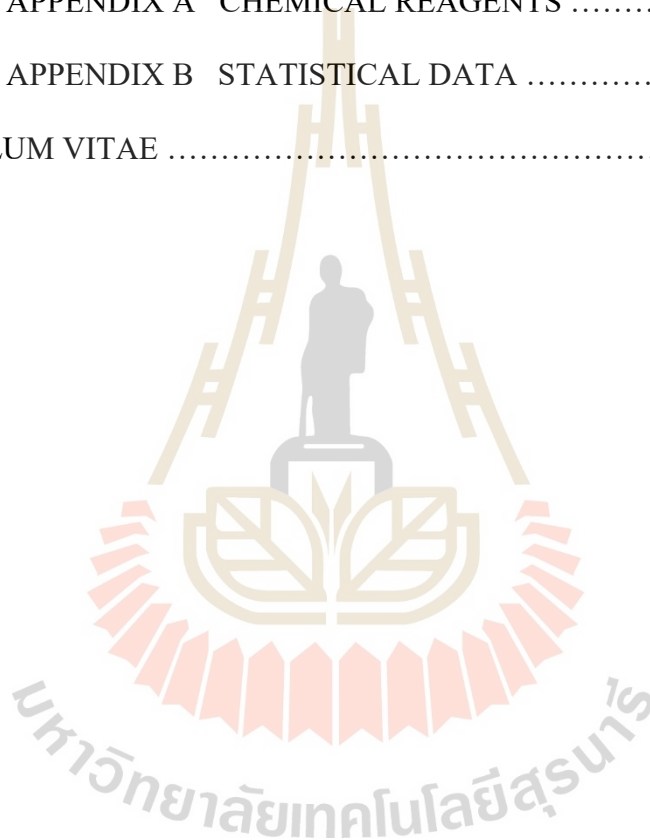
	Page
3.4 Tests for the Potential of Hydroxyapatite Nanoparticle in Enhancing Seed Germination and Seedling Growth and Plant Stress	33
3.4.1 Treating materials	33
3.4.2 Germination test	33
3.4.3 Determination of relative water content	34
3.4.4 Determination of malondiadehyde	35
3.4.5 Determination of cell death evaluation	35
3.5 Tests for the Potential of Hydroxyapatite Nanoparticle in Enhancing Growth of Rice	36
3.5.1 Plant harvest and sample collection	36
3.5.2 Determination of starch in seed using SEM/EDX	37
3.5.3 Determination of amylose content in seeds	38
3.5.4 Determination of aroma in rice seeds using gas chromatography	38
 IV RESULTS AND DISCUSSIONS	
4.1 Characterization of Synthesized Hydroxyapatite Nanoparticles	40
4.1.1 Analysis of crystalline size and structure of hydroxyapatite using analysis of XRD patterns	41

CONTENTS (Continued)

	Page
4.1.2 Elemental composition of the synthesized nanoparticles determined by using scanning electron microscopy techniques and energy dispersive x-ray spectrometer	45
4.1.3 Size and shape of the synthesized hydroxyapatite nanoparticles	48
4.1.4 Functional groups on hydroxyapatite nanoparticles synthesized from using aloe vera extract	50
4.2 Dissolution of Plant Nutrients from HAp Nanoparticle	53
4.2.1 Size and distribution of HAp nanoparticles in colloidal solution	54
4.2.2 Dissolution of HAp nanoparticles	63
4.3 Germination and Seedling Growth	64
4.4 Plant Stress	75
4.5 Growth	87
4.6 Yield Quality	95
4.6.1 Starch in seed	96
4.6.2 Amylose in seed	97
4.6.3 Acetyl-1-pyrroline in rice grains	102
4.6.4 Morphology in seed	105
V CONCLUSION	112

CONTENTS (Continued)

	Page
REFERENCES	114
APPENDICES	128
APPENDIX A CHEMICAL REAGENTS	129
APPENDIX B STATISTICAL DATA	132
CURRICULUM VITAE	142



LIST OF TABLES

Table	Page
2.1	Comparison of effectiveness of phosphorus from different source13
2.2	Types of apatite18
2.3	Stoichiometric of apatite19
2.4	The syntheses of HAp nanoparticle22
2.5	Green syntheses of nanoparticles using plant extract24
4.1	Crystallite size and structure of the synthesized hydroxyapatite nanoparticles42
4.2	Elements detected in hydroxyapatite nanoparticles46
4.3	The weight of the calcium and phosphorus component in HAp powder were detected by using X- Ray spectrum element46
4.4	Functional groups found on the synthesized of hydroxyapatite nanoparticles51
4.5	Size and distribution of hydroxyapatite nanoparticles in solutions56
4.6	Dissolution of calcium ion (Ca^{2+}) and phosphate (PO_4^{3-}) from HAp nanoparticles in solutions63
4.7	Effect of HAp nanoparticles and commercial fertilizers at different concentrations on germination, relative water content, root and shoot length66

LIST OF TABLES (Continued)

Table		Page
4.8	Effect of HAp nanoparticles and commercial fertilizers at different concentrations	80
4.9	Height and leaf width, number of panicle of rice in the experiment	90
4.10	Weight of 1000 grains and grains per panicle of rice in the experiments	93
4.11	Starch content in seed	97
4.12	Amylose content of rice grains from different treatments	99
4.13	2-Acetyl-1-Pyrroline (2-AP) in rice seed from different treatments	103

LIST OF FIGURES

Figure	Page
2.1	Rice exporting countries in the world8
2.2	Fertilizers use in the world8
2.3	Generic pathways for plant to stress11
2.4	Generic pathway for calcium regulated gene expression and the stress response12
2.5	Algal bloom as an effect of increasing total phosphorus loading in freshwater lake14
2.6	Cyanobacteria bloom15
2.7	Urea-hydroxyapatite nanohybrids for slow release of nitrogen17
3.1	The arrangement of rice grains in the petri dish, with the arrowhead beir the germ portion34
3.2	The measurements of height of rice plant37
4.1	The diffraction peaks of hydroxyapatite nanoparticles synthesized by aloe vera extract43
4.2	The diffraction peaks of hydroxyapatite nanoparticles synthesized by aloe vera extract in 2 θ peaks at 25.8° and 28.8° XRD patterns43
4.3	The diffraction peaks of hydroxyapatite nanoparticles synthesized by aloe vera extract in 2 θ peaks at 28.8°, 30.6°, 31.7°,32.1°, 32.9°, and 34.03° XRD patterns44

LIST OF FIGURES (Continued)

Figure	Page
4.4	The diffraction peaks of hydroxyapatite nanoparticles synthesized by aloe vera extract in 2θ peaks at 46.68° and 49.46° XRD patterns44
4.5	EDX spectrums showed of calcium and phosphorus value47
4.6	Rod shape of hydroxyapatite nanoparticles48
4.7	Plot presenting size distribution of the synthesized HAp nanoparticles49
4.8	The peak vibration modes the synthesized of HAp nanoparticles50
4.9	Mechanisms for the formation of HAp nanoparticle53
4.10	Hydrodynamic sizes of HAp nanoparticles at 100 mg/L55
4.11	Hydrodynamic sizes of HAp nanoparticles at 500 mg/L55
4.12	Hydrodynamic sizes of HAp nanoparticles at 1000 mg/L56
4.13	Zeta potential at concentration 100 mg of HAp nanoparticles59
4.14	Zeta potential at concentration 500 mg of HAp nanoparticles59
4.15	Zeta potential at concentration 1000 mg of HAp nanoparticles60
4.16	pH of HAp nanoparticle in solutions61
4.17	Conductivity of HAp nanoparticle in solutions62
4.18	Electrophoretic mobility of HAp nanoparticles in solutions62
4.19	Effect of HAp nanoparticles and commercial fertilizers at different concentrations on seed germination67

LIST OF FIGURES (Continued)

Figure	Page
4.20	Effect of HAp nanoparticles and commercial fertilizers at different concentrations on relative water content70
4.21	Effect of HAp nanoparticles and commercial fertilizers at different concentrations on root length72
4.22	Effect of HAp nanoparticles and commercial fertilizers at different concentrations on shoot length74
4.23	Roots of seeds exposed to the control condition and treatments with 100, 500, and 1000 mg/L77
4.24	Roots of seeds exposed to the commercial fertilizer 18-46-0 at 100, 500 and 1000 mg/L77
4.25	Roots of seeds exposed to commercial fertilizer 15-15-15 at 100, 500, and 1000 mg/L78
4.26	Effect of HAp nanoparticles and commercial fertilizer at different concentrations 100, 500, and 1000 mg/L on malondialdehyde81
4.27	Effect of HAp nanoparticles and commercial fertilizer at different concentration 100, 500, and 1000 mg/L on cell death82
4.28	Cell death of root in control (DI water) and HAp nanoparticles at 100, 500 and 1000 mg/L84
4.29	Cell death of root in commercial fertilizer1 18-46-0 at 100, 500, and 1000 mg/L84

LIST OF FIGURES (Continued)

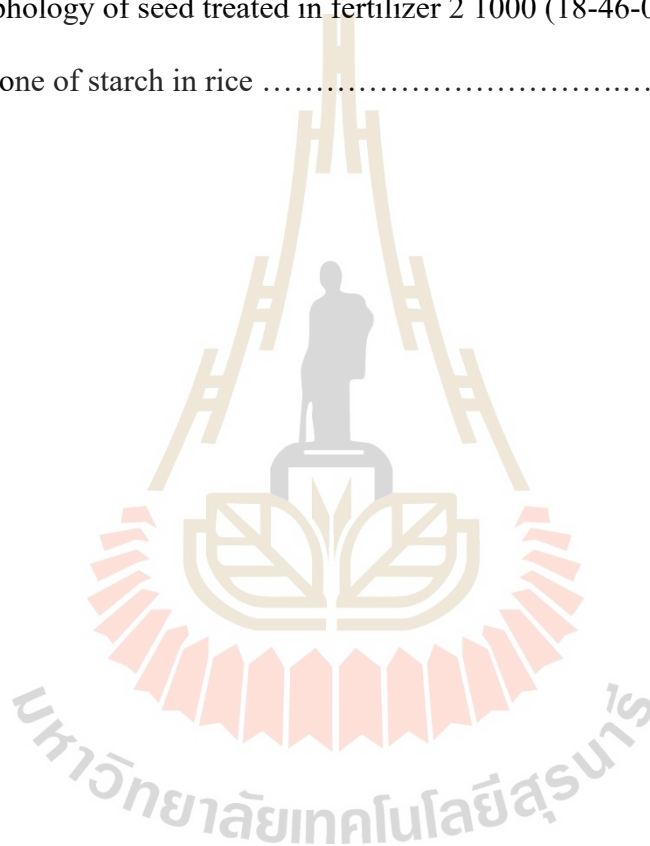
Figure	Page
4.30	Cell death of root in commercial fertilizer1 15-15-15 at 100, 500, and 1000 mg/L85
4.31	Cell death of root in control and HAp nanoparticles at 100, 500, and 1000 mg/L85
4.32	Cell death of root in commercial fertilizer1 (18-46-0) at 100, 500, and 1000 mg/L86
4.33	Cell death of root in commercial fertilizer 2 (15-15-15) at 100, 500, and 1000 mg/L86
4.34	Growth phases and stages in rice plant87
4.35	Physiology of rice after 35, 60, and 90 days88
4.36	Physiology of rice after 130 days89
4.37	Height of rice plants exposed to HAp nanoparticles and commercial fertilizers in soil91
4.38	Leaf width of rice plants exposed to HAp nanoparticles and commercial fertilizers in soil92
4.39	The number of panicle exposed to HAp nanoparticles and commercial fertilizers in soil92
4.40	Number of grain per panicle of rice exposed to HAp nanoparticles and commercial fertilizers in soil94

LIST OF FIGURES (Continued)

Figure	Page
4.41	Weight of 1000 grains of rice exposed to HAp nanoparticles and commercial fertilizers95
4.42	Effect of HAp nanoparticles and commercial fertilizer1 (18-46-0) and fertilizer2 (15-15-15) at different concentrations100
4.43	Relative color board derived from apparent amylose content characterization101
4.44	Amylose in seed with the iodine solution101
4.45	Morphology of seed treated in control and aleurone of starch in rice107
4.46	Morphology of seed treated in HAp 100 mg and aleurone starch107
4.47	Morphology of seed treated in HAp 500 mg and aleurone of starch108
4.48	Morphology of seed treated in HAp 1000 mg and aleurone of starch108
4.49	Morphology of seed treated in fertilizer 1 100 (18-46-0) and aleurone of starch109
4.50	Morphology of seed treated in fertilizer 1 500 (18-46-0) and aleurone of starch in rice109
4.51	Morphology of seed treated in fertilizer 1 1000 (18-46-0) and aleurone of starch in rice110
4.52	Morphology of seed treated in fertilizer 2 100 (18-46-0) and aleurone of starch in rice110

LIST OF FIGURES (Continued)

Figure		Page
4.53	Morphology of seed treated in fertilizer 2 500 (18-46-0) and aleurone of starch in rice	111
4.54	Morphology of seed treated in fertilizer 2 1000 (18-46-0) and aleurone of starch in rice	111



LIST OF ABBREVIATIONS

°C	=	Degree Celsius
cm	=	Centimeter
DI	=	Distilled water
DW	=	Dry weight
FW	=	Fresh weight
g	=	Gram
FHW	=	Hour
MDA	=	Malondialdehyde
l	=	Liter
mg	=	Milligram
mL	=	Milliliter
D.nm	=	Diameter of nanoparticles
FWHM	=	The full width at half-maximum value of XRD diffraction lines
θ	=	Angle-Bragg angle (°)

CHAPTER I

INTRODUCTION

1.1 Background Problem

The world population is expected to increase to 9.7 billion in 2050 (FAO, 2017) leading to higher demand for food. Farmers use chemical fertilizers to increase productivity. Nitrogen, phosphorus, and potassium are main nutrients for plant. They come from various sources. Nitrogen and potassium can be found in natural or synthetic origin. The source of phosphorus fertilizers are bones, guano and rock phosphate. Commercially available phosphate fertilizers mainly come from rock phosphate. Igneous and sedimentary are two types of rock phosphates. Both types have the same phosphate mineral, i.e., calcium phosphate of the apatite group. Phosphate rock is important to make phosphate fertilizer for enhancing to plant. Phosphate rock minerals are important resources of phosphorus. The use of phosphate fertilizers will probably be limited in the future, due to their non-renewable natural origin (Cordell et al., 2009). For this reason, we have concerned about phosphorus depletion continuously from demand for fertilizer increasing to grow increased products and the use of phosphate fertilizer to efficiently. Thus, the phosphorus release slowly into the soil for the plant can get it continuously (sustaining fertilizers), which means is phosphorus did not run off into the source water before plant uptake to use for mature growth. Recently, nanotechnology caught the attention of the agricultural industry, especially the possible application to improve plant growth and

yield. Various nanoparticles such as zinc, silver, phosphorus, calcium, carbon, copper, etc. Result in conventional agricultural application because of components, with essential nutrient that can convert them to be nanofertilizer (Shang et al., 2019). Good properties of nanofertilizer include the solubility and the slow-release of nutrients. Hence, plants can slowly use the nutrients for growth and development. Some reports show the potential of nanoparticles as a plant growth enhancer, although nanoparticles are hard to dissolve generally. Montalvo and colleagues supported the potential of higher dissolution when decreasing particles to nanoscale were provided (Montalvo et al., 2015). The nanoparticles can easily move in the soil and through into the root plants from the mass flow. Hydroxyapatite (HAp) is one of the apatite groups which are phosphorus and calcium-based compound. It was known to hardly dissolve in water but and soluble in acid. Watanabe and colleagues demonstrated that HAp in water, ammonium, and potassium ion was slowly released phosphate from the dissolution of HAp by cation exchange with calcium and co-dissolved with phosphate (Watanabe et al., 2014). In addition, Kottegoda and colleagues studied a nanohybrid of urea with HAp nanoparticles. It was found that HAp nanoparticles can slowly release nitrogen (Kottegoda et al., 2011). The result suggested that HAp nanoparticles can be a source of plant nutrients. Liu and Lal and co-worker suggested that HAp nanoparticles can be the main source of phosphorus and can greatly enhance soybean growth. To use of HAp with a small particle size may be an alternative way to improve its effectiveness as fertilizer (Liu and Lal, 2014).

HAp is a calcium phosphate-based compound. It has a similar chemical composition to bone and hard tissue. Its biocompatible property is known and it did not appear to be toxic to plant. In addition, it also has phosphorus (P) which is an

important nutrient involving in biological molecule production such as DNA, RNA, and proteins. For calcium ions, it is the key to the strength of tissue cells and in the plant. Calcium deficiency affects the germination of root. It is a secondary messenger and the most multipurpose signaling molecule in all eukaryotic organisms. Some reports are supporting that HAp nanoparticles were not toxic to plant. Liu and Lal developed HAp nanoparticles to improve *Glycine max*, seed yield (Liu and Lal, 2014). Mikhak and colleagues also revealed that HAp nanoparticles can increase cucumber rapidly and can stimulate the highest phosphate uptake to enhance root and shoot in chamomile plants (Mikhak et al., 2017). It can improve the growth parameters and chemical compositions of the baobab plant (Merghany et al., 2019). Moreover, HAp nanoparticles resulted in higher phosphorus content in lettuce (Taşkın et al., 2018) Marchiol and colleagues reported that HAp nanoparticles did not inhibit tomato seed germination but increased root elongation (Marchiol et al., 2019). Pradhan and colleagues showed the efficiency of incorporation of urea with HAp nanoparticles which showed two-fold growth of rice as compared to conventional phosphorus and nitrogen fertilizers (Pradhan et al., 2021).

The synthesis of HAp nanoparticles materials is mostly based on solid-state reaction and wet methods, such as the hydrothermal method and sol-gel method. In this research, HAp nanoparticle synthesized by sol-gel method using aloe vera extract was carried out. Aloe vera gel contains a lot of water and it can associate with metal ions in solution (Femenia et al., 2003). It can be used as a bio-reducing agent, the substrate material for a simple, inexpensive, and environmentally friendly synthesis (Klinkaewnarong et al., 2010). Aloe vera extract plant was first successfully used to synthesize nanoparticles by Maensiri and colleagues (Maensiri et al., 2008). This

method utilized aloe vera plant extract instead of inorganic solvents. In this report, we sought to synthesize HAp nanoparticles with the green synthesis method by using aloe vera and investigated their effect on rice (*Oryza sativa* L.) germination, seedling, and growth. We did experiments to see, if HAp nanoparticles could release plant nutrients slowly and be more suitable to serve as an alternative phosphate fertilizer. Some parameters related to the quality of grain yield were determined.

1.2 Research Objectives

The main objective of this thesis was to investigate the potential of HAp nanoparticles as sustainable fertilizer. Specific objectives were as follows:

- 1.2.1 To monitor HAp nanoparticle solubility.
- 1.2.2 To study the effects of HAp nanoparticle on germination phytotoxicity and stress in rice seedling.
- 1.2.3 To study the effects of HAp nanoparticle on rice plants at vegetative stage.
- 1.2.4 To study the effects of HAp nanoparticles on some grain quality parameters.

1.3 Research Hypothesis

HAp nanoparticles were investigated for their potential as nanofertilizer. If they had potential as nanofertilizer, they would show an adequate level of solubility and release Ca^{2+} and PO_4^{3-} which are plant nutrients. They would not inhibit seed germination and would not show an adverse effect on development and growth and yield. They would not increase stress to a lethal level for plants. Rice was used in this research.

1.4 Scope and Limitation of the Study

HAp nanoparticles were synthesized and characterized. The crystalline size and structure of HAp were analyzed by using XRD. Morphology and size particles were studied by TEM. The elemental phase composition was determined by SEM-EDX and functional group using FT-Raman spectroscopy. This study was focused on the properties of HAp nanoparticles which would suggest their potential as alternative phosphate fertilizers. The release of plant nutrients, solubility, and size dispersion stability in aqueous solutions were measured by Ion chromatography (IC) and NanoSizer. The effects on germination and seedling, phytotoxicity and plant stress were investigated in rice grown in HAp nanoparticles solution compared with commercial fertilizers (18-46-0) and (15-15-15) and control treatment (DI water). In addition, the potential of HAp nanoparticles to enhance growth of rice grown in the soil for 130 days was studied. The parameters were determined such as the number of panicles, yield, the weight of grains per pots, 1000 grain weight, the number of grains per panicle, starch, amylose content, and aromatic of grain rice (2-Acetyl-1-Pyrroline; 2-AP). All the experiment was analyzed using ANOVA by SPSS Statistics 23 (IBM).

1.5 Expected Results

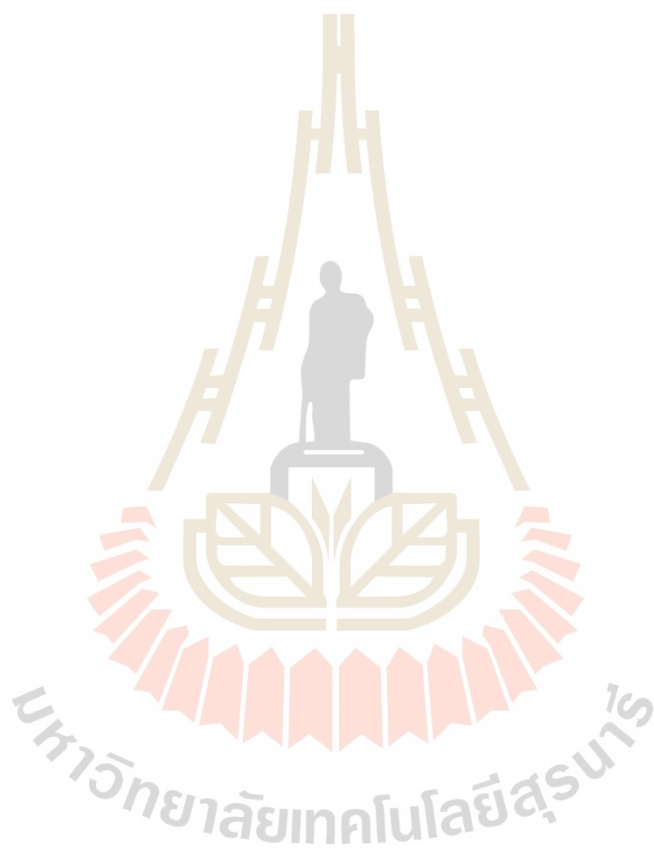
It was expected that this study would provide information on:

1.5.1 The capacity of HAp nanoparticles to slowly release plant nutrients which would suggest the suitability of the particles to serve as alternative phosphorus and calcium fertilizer.

1.5.2 The effect of HAp nanoparticles on seed germination and seedling growth.

1.5.3 The phytotoxicity of HAp nanoparticles on rice seedling rice.

1.5.4 The potential of HAp nanoparticles to enhance growth, yield quality, and the aroma in seed (2-Acetyl-1-Pyrroline).



CHAPTER II

LITERATURE REVIEW

2.1 Agriculture and Fertilizer Use

The global population has been increasing and it is estimated to be 9.6 billion in 2050. The agricultural productivity has to be increased to meet the need of a growing population. The data of global demand for rice, for example, is estimated to increase from 496 million tons in 2020 to 555 million tons in 2035. Consequently, the demand for fertilizers in rice production will also increase (Tuong and Bouman, 2003).

Rice is the 3rd most produced agricultural product after sugarcane and maize. The agriculture sector is the most important in the Thai economy. More than 60% of the population is involved in agriculture. Thailand is one of the top rice exporters in the world, especially Jasmine rice (variety Khao Dawk Mali 105), which is the famous fragrant rice of Thailand (Wongpornchai et al., 2003). Jasmine rice has 23-31% amylose content leading to high cooking quality. Jasmine rice has faced rising competition from countries that are developing varieties of rice with similar qualities. Thailand and Vietnam are the top exporters in Southeast Asia (Figure 2.1). In Thailand, rice is the crop that has the highest fertilizer usage, and the number is expected to rise due to the high demand. This increasing demand for fertilizer usage is not only happening in Thailand, but it is a global trend as shown in Figure 2.2.

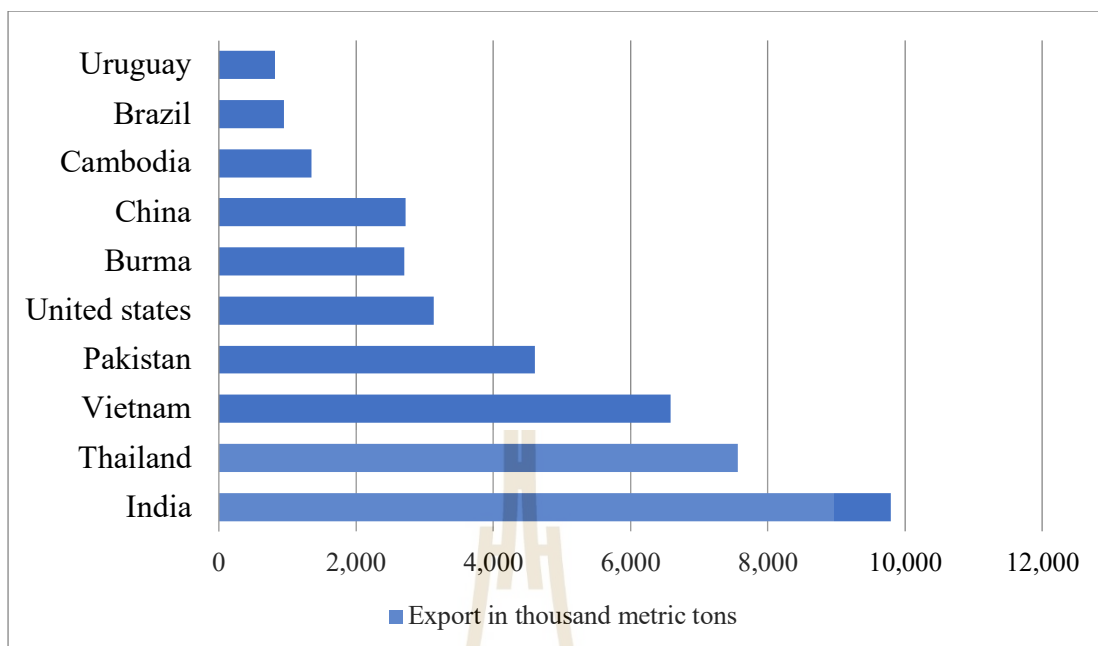


Figure 2.1 Rice exporting countries in the world (Wilkinson, 2015).

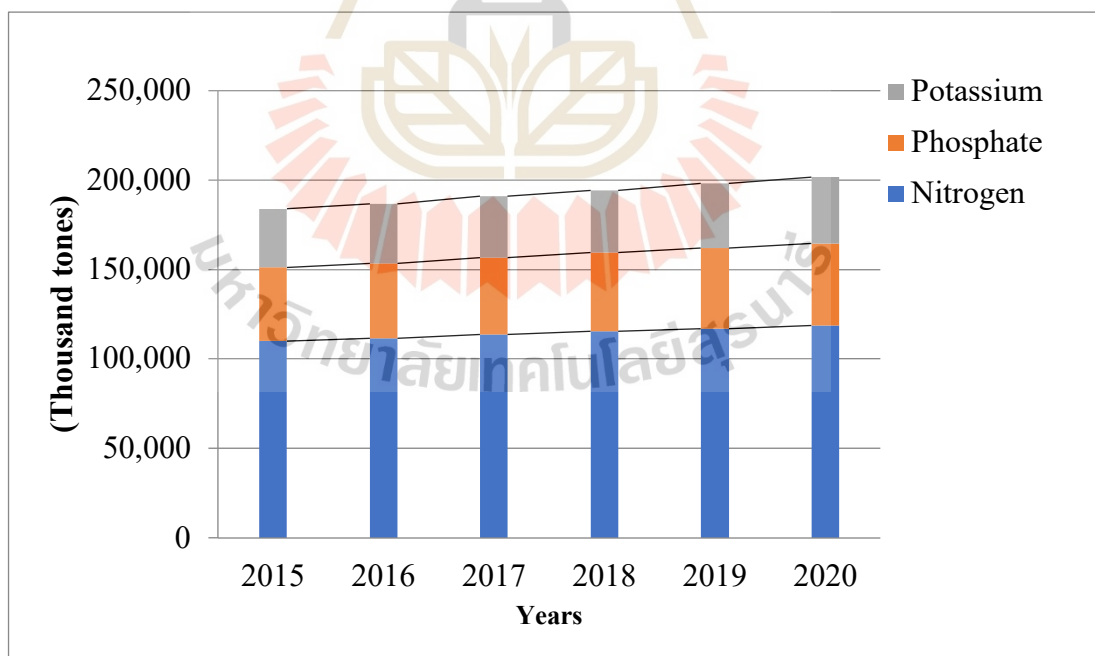


Figure 2.2 Fertilizers use in the world (Bruinsma, 2003).

The demands for fertilizers have increased every year, especially, the demand for nitrogen, phosphorus, and potassium (NPK). During 2015–2020 fertilizer use increased from 184,017 to 201,663 million tons (Alexandratos and Bruinsma, 2012). These elements are fertilizers for stimulating the growth of plants and increasing crop yield. Nitrogen is involved in the syntheses of plant proteins, nucleic acids, and hormones. Phosphorus is also associated with nucleic acids, phospholipids, and various proteins. Potassium is available in the soil and plant can get it directly from the soil. It has a function in the synthesis of protein and major processes in the plant (Razaq et al., 2017). In addition, calcium is also essential in the metabolic process in the plant cell including cell wall, elongation of the cell, enzymatic and hormonal process.

Fertilizers can be categorized into organic and inorganic fertilizers. Organic fertilizers are naturally occurring substances and are manufactured through a natural process. Organic fertilizers increase the abundance of soil organisms by providing organic matter and micronutrients for organisms such as fungi mycorrhiza. Organic fertilizers provide slowly released nutrition and a slow growth rate, while inorganic fertilizers provide rapid nutrition. The inorganic fertilizers are added to the soil to sustain plant growth. Each inorganic fertilizer has a different source and raw materials from which they are derived. Sources of nitrogen such as ammonia can be found in natural gas or air. Potassium chloride is an elementary component of potash. Phosphorus is made from rock phosphate, which is the only raw material of phosphate fertilizer presently. It is expected that future generations will face problems in obtaining phosphate due to the greater demand that comes with the increasing population.

2.2 Calcium Fertilizer

Calcium is important in several metabolic roles within the plant, including root and shoot development, cell wall strength, enzyme activation, and neutralizing organic acids in the plant. Therefore, it plays a significant function in plant growth and development.

2.2.1 Role of calcium in plants

Calcium is an important plant nutrient required for the growth and development of a plant, particularly for root and shoot tips. Ca^{2+} helps in the formation of microtubules and is important for the anaphasic movement of chromosomes. Ca^{2+} is a key divalent cation in cell wall and membranes. Accumulated Ca^{2+} in the cell wall helps bind the cell together. It is also necessary as an intracellular messenger in the cytosol. Ca^{2+} helps decrease the toxic effects of NaCl and reduces stress (Mahajan et al., 2005). Calcium ion (Ca^{2+}) is the second messenger molecule involved in many signaling transduction pathways in plants. There are many extracellular signals and environmental induction such as light, abiotic, and biotic stress factors which cause adjustment of the cellular calcium ion levels, termed as calcium signatures (Tuteja and Mahajan, 2007). The concentration of Ca^{2+} in vacuoles, endoplasmic reticulum, mitochondria, and cell wall are actively balanced by the presence of 'Ca²⁺ stores. Ca^{2+} is present in millimolar concentrations in the cell wall and vacuoles and is released whenever the cell requires it (Tuteja and Mahajan, 2007). Facing environmental stress, plant cells reprogram their cellular setup by activating a network of signaling events that begin with stress perception at the membrane level of the cell and end with cellular response. A generic signal transduction pathway has the following steps as shown in Figure 2.3.

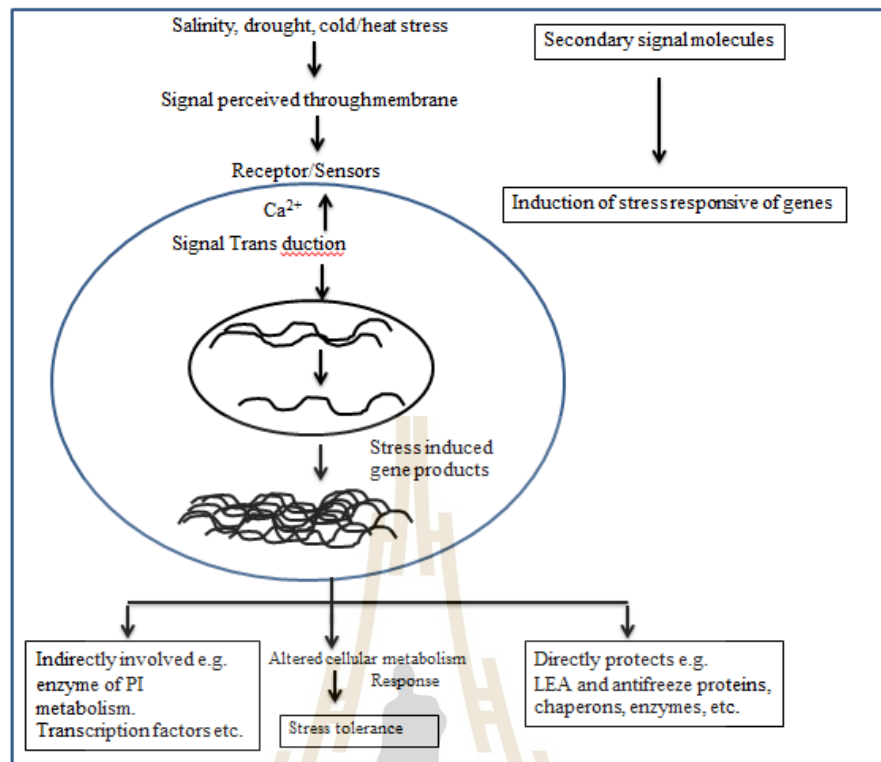


Figure 2.3 Generic pathways for plant to stress (Tuteja and Mahajan, 2007).

The extracellular stress signal is first sensed by the membrane receptors and then activates large and complex signal cascades intracellularly, including the production of secondary signal molecules. The signal cascade results in the expression of several stress-responsive genes, the products of which may provide direct or indirect stress tolerance.

The calcium (Ca^{2+}) level increases in response to the stimuli, and it is recognized by some calcium sensors or Ca^{2+} -binding proteins, which can stimulate protein kinases (Tuteja and Mahajan, 2007). These activated protein kinases can phosphorylate many regulatory proteins and transcription factors. The regulation of gene expression level causes the alteration of metabolism followed by the phenotypic response of stress tolerance (Figure. 2.4).

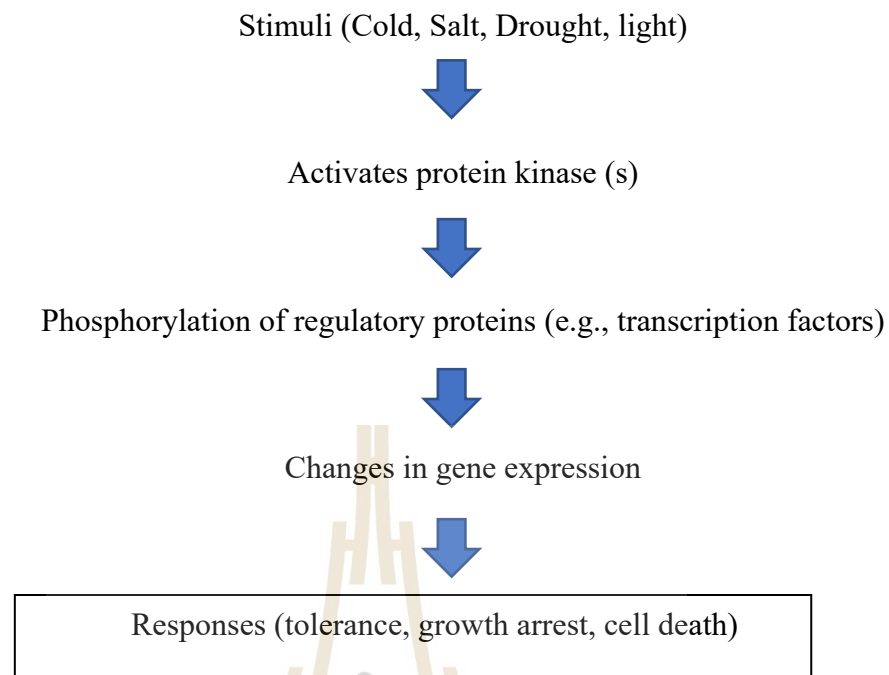


Figure 2.4 Generic pathway for calcium regulated gene expression and the stress response (Tuteja and Mahajan, 2007).

2.3 Phosphorus Fertilizer

Phosphorus is an essential component of every living cell. It involves in metabolic processes, including synthesis of starch and nucleic acids and photosynthesis (Albaum, 1952). Phosphorus has been obtained mainly from phosphate. Due to the world's increasing population, the rate of depletion of phosphate will accelerate. Most of the world's phosphate fertilizers are produced from phosphate rock resources. In agricultural circles, phosphate rocks are also called rock phosphates. Almost all of these resources contain some form of the mineral apatite ($\text{Ca}_5(\text{PO}_4, \pm\text{CO}_3, \pm\text{OH})_3(\text{OH}, \text{F}, \text{Cl})$). Apatite is stable calcium phosphate minerals, similar to the insoluble calcium phosphates naturally occurring in soil.

The first step in phosphorus fertilizer production is mixing crushed phosphate rock with sulfuric acid to produce phosphoric acid. Phosphoric acid is liquid. It reacts with ammonia to result in phosphorus fertilizer such as diammonium phosphate (DAP) and monoammonium phosphate (MAP). Therefore, the price of phosphorus fertilizer depends on the price of phosphate rock and sulfuric acid. Phosphorus fertilizer from different sources was shown to affect differently on wheat yield (Table 2.1). Their effectiveness differs considerably. Research has shown orthophosphate fertilizer (MAP and TSP) to be the best phosphate source. The plant has relatively high demand for orthophosphate fertilizers (H_2PO_4 in acid and HPO_4^{2-} in alkaline).

Table 2.1 Comparison of effectiveness of phosphorus from different source (Thin et al., 2020).

P source	P ₂ O ₅ rate, (mg/pot)	Yield (g/pot)	P uptake (mg)
Control	0	0.89	1.50
MAP (11-48-0)	25	2.51	4.19
TSP (0-45-0)	25	2.78	4.21
PR (Christmas Island)	250	2.39	3.59
PR (Idaho)	250	1.08	2.22

MAP is Monoammonium phosphate
TSP is triple superphosphate
PR is phosphate rock

Since phosphate fertilizer also stimulates the growth of algae and cyanobacteria, the fertilizer runoff into the water reservoir can cause algal bloom (Figure 2.5) which increases oxygen consumption leading to hypoxic conditions of the water. As the temperature increases, the solubility of oxygen decreases. This means the level of dissolved oxygen can drop dramatically in the water reservoirs where algae are

blooming especially on warm days. The low oxygen levels may lead to fish kills and a range of other effects. Agricultural fertilizer causes the increase of phosphorus in water due to the runoff of it from agriculture.

Smith and Schindler (Smith and Schindler, 2009) showed that the concentration of phosphorus levels corresponded with increased algae in water (Figure 2.6). Such algal blooms increase surface or shoreline accumulations and many other problems. It was found that nutrient enrichment in the water (Grand Beach, Lake Winnipeg Canada), causes the bloom of cyanobacteria of surface waters in both freshwater lakes and coastal ecosystems (Figure 2.5 and 2.6).

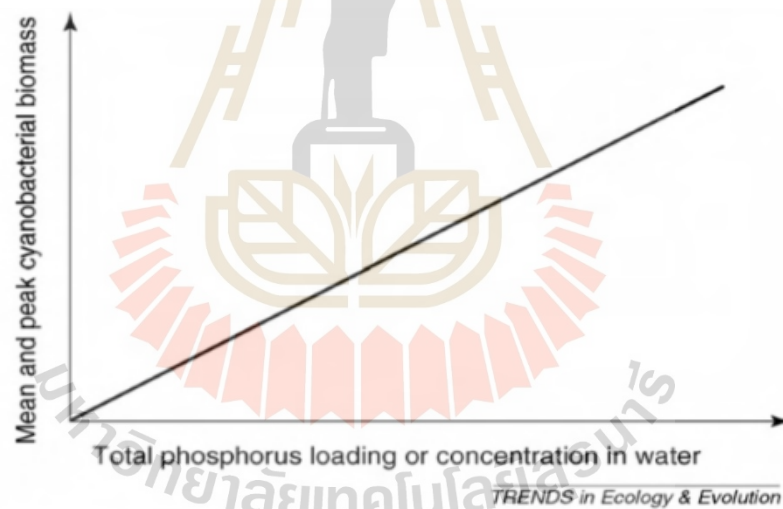


Figure 2.5 Algal bloom as an effect of increasing total phosphorus loading in freshwater lake (Smith and Schindler, 2009).

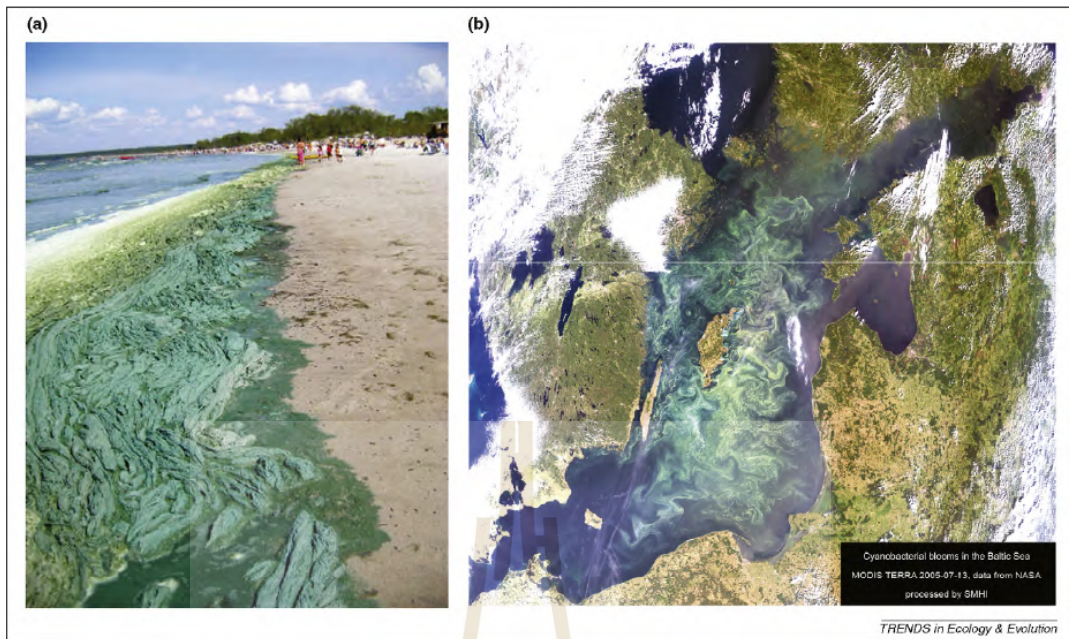


Figure 2.6 Cyanobacteria bloom (a) At Grand Beach, Lake Winnipeg, Canada (b) In the Baltic.

2.4 Application of Nanomaterial in Agriculture

Nanoparticles (NPs) are defined as small materials with a single unit between 1 and 100 nanometers in size in at least one dimension. Nanotechnology, the study and the application of nanoparticles have rapidly grown in the last few years. In this recent times, nanomaterial has become a matter of great interest due to their different functional properties including medicinal, biological, electronic, physical, chemical, thermal, and engineering. Nanoparticles have great potential in many applications, such as cellular therapy, tissue repair, drug delivery, magnetic resonance imaging (MRI), hyperthermia treatment, agricultural sector, and environmental remediation.

If we look at the historical part of agricultural applications of nanotechnology, it came only in recent years. Nanomaterial has great implications in sustainable

agricultural crop production and many studies reported their positive impact on various crops. Mainly, germination of various crops has been reported to be improved in these reports as a result of nanoparticle exposure of seeds. For example, the applications of nSiO₂ in tomato and maize (Siddiqui and Al-Whaibi, 2014), carbon nanotubes in tomato and rice (Khodakovskaya et al., 2013), and hydroxyapatite in soybean (Liu and Lal, 2014) was shown to improve seed germination, root growth, biomass, and chlorophyll. Khodakovskaya and colleagues (Khodakovskaya et al., 2013) reported that multi walled carbon nanotubes promoted photosynthesis and improved growth in tobacco. They suggested the mechanism involved in enhancing cell growth. The water channels (aquaporin) were activated due to the expression of the water channel gene (*NtPIP1*). According to (Yuvakkumar et al., 2011), nano-silica influenced the level of chlorophyll *a* and *b* and dry weight percentage in maize roots and shoots. The higher dry weight percentage in roots reflects the increased accumulation of silica in leaf bundle sheath, which stimulates the factors involved in the synthesis of chlorophyll. The acceleration may be due to increased leaf area that renders better light absorption and photosynthetic activity of chlorophyll *a* and *b*. In addition, Shang and colleagues (Shang et al., 2019) found that zinc oxide nanoparticles could increase barley yield by 91 %, while the conventional ZnSO₄ could give was 31% increase of yield when compared with the control. Jan and colleagues (Jan et al., 2010). supported that zinc oxide nanoparticles positively affected growth and physiological responses such as sprout and root elongation, fresh and dry weight, and photosynthesis.

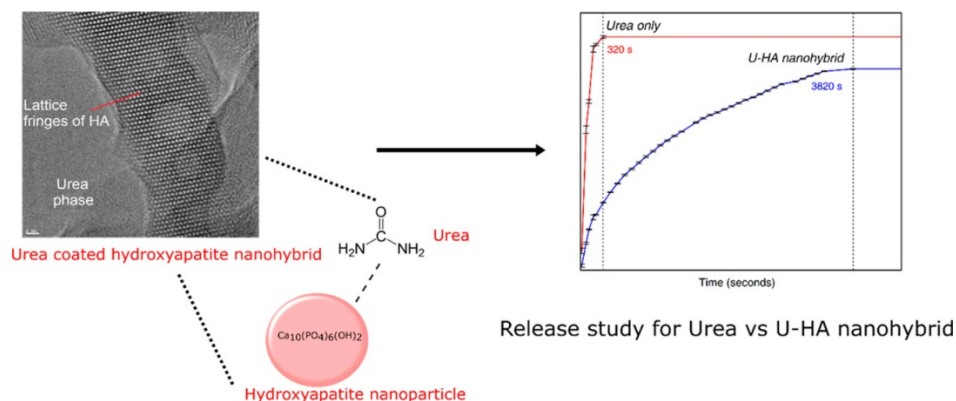


Figure 2.7 Urea-Hydroxyapatite nanohybrids for slow release of nitrogen.

Designs nutrient fertilizer as nanoparticles to supply nutrients for plants are called nanofertilizer. Nano fertilizers are new types of fertilizers resulted from innovative nanotechnology. Some recent research in nanotechnology has demonstrated the promising perspective of nanofertilizer development and application for improving crop growth and yields. Their nano-size is one of the properties that can serve an agricultural purpose leading to the increase in crop yields (Mukhopadhyay, 2014). In addition, their capacity has enhanced the efficiency of fertilizer use; reduce nutrient losses, and/or minimize the adverse environmental impacts that have been the research interests. The downside of using commercial fertilizer is that it hits into the soil all at once and the plant does not uptake nutrient efficiently, due to loss from runoff or by leaching. This is particularly true for phosphorus fertilizer. In contrast, nanoparticle-based phosphorus fertilizer is supposed to have three major advantages over conventional fertilizers in that it does not release phosphorous as quickly as conventional fertilizers. It does not change the soil pH upon phosphorous release and the loss of phosphorus from the soil is low. The slow and steady release of phosphorous allows plants to continuously take up the nutrient as they grow.

Nonetheless, these putative advantages are yet to be confirmed. (Giroto et al., 2017). studied the nanohybrid containing HAp nanoparticles decorated with urea in a 6:1 ratio and found that it displayed significance by slow release of nitrogen. The slow release of urea leads to a reduction in the decomposition in soil (Kottegoda et al., 2017). Therefore, there is an increased interest to develop HAp nanoparticle fertilizers as slow-release and environmentally friendly fertilizers.

2.5 Hydroxyapatite Nanoparticle and Their potential Use as Nanofertilizers

Hydroxyapatite ($\text{Ca}_{10}(\text{PO}_4)_6(\text{OH})_2$) is calcium and phosphate-based compound that belongs to the apatite group, which can be synthesized by various techniques. Apatite group includes hydroxyapatite, fluorapatite and chlorapatite. Members of this family have high concentrations of OH^- , F^- , and Cl^- ions in their crystals which can be easily interchanged between each other to form different apatite (Table 2.2). Hydroxyapatite natural lattice structure is hexagonal; it has a 1.67 stoichiometric ratio of Ca/P which is identical to natural bone apatite (Table 2.3).

Table 2.2 Types of apatite (Palmer et al., 2008).

Apatite type	Formula	Apatite name
Fluorine-rich	$\text{Ca}_5(\text{PO}_4)_3\text{F}$	Fluorapatite
Chlorine-rich	$\text{Ca}_5(\text{PO}_4)_3\text{Cl}$	Chlorapatite
Hydroxyl-rich	$\text{Ca}_5(\text{PO}_4)_3\text{OH}$	Hydroxyapatite
Common Apatite	$\text{Ca}_5(\text{PO}_4)_3(\text{F}, \text{Cl}, \text{OH})$	Apatite

Table 2.3 Stoichiometric of apatite (Koutsopoulos, 2002).

Molecular type	Ca/P ratio	Name
$\text{Ca}(\text{H}_2\text{PO}_4)_2 \cdot \text{H}_2\text{O}$	0.50	Monohydrate calcium phosphate (MCPH)
$\text{Ca}(\text{H}_2\text{PO}_4)_2$	0.50	Monocalcium phosphate (MCP)
$\text{Ca}(\text{HPO}_4) \cdot 2\text{H}_2\text{O}$	1.0	Dicalciumphosphate dehydrate (DCPD)
α - and β - $\text{Ca}_3(\text{PO}_4)_2$	1.50	Tricalcium phosphate (TCP)
$\text{Ca}_4\text{H}(\text{PO}_4)_3 \cdot 2.5 \text{H}_2\text{O}$	1.33	Octacalcium phosphate (OCP)
$\text{Ca}_5(\text{PO}_4)_3(\text{OH})$	1.67	Hydroxyapatite (HAp)

Hydroxyapatite is hard to dissolve but soluble in acids. The good fertilizer properties are the solubility and the slow-release of nutrients so that the plants can slowly use the nutrients through growth and development. There are some reports about the potential of HAp nanoparticles to be used in agriculture. Chunguang and colleagues (Chunguang et al., 2017) evaluated the phytotoxicity of HAp nanoparticles on the spouting of plants and found that the germination percentage and germination index of cucumber increased rapidly with increasing concentration of HAp nanoparticles. Nonetheless, when the concentration was greater than 1000 mg/L, both root growth and shoot growth were inhibited. On the other hand, the results of Ruiqiang and colleague suggested that HAp nanoparticles solutions stabilized with carboxymethyl cellulose (CMC) had affected on root length. The results demonstrated that concentrations at 200–2000 mg/L of HAp nanoparticles stabilized with CMC

stimulated root length of *Solanum lycopersicum* L. (Ruiqiang and Rattan, 2015). Similarly, Liu and Lal reported that apatite nanoparticles in CMC solution could serve as phosphate fertilizers (plant nutritional) for soybean (*Glycine max*). The data showed that nanoparticles increased the growth rate and seed yield in the greenhouse (Liu and Lal, 2014). Furthermore, the report of Kottegoda and colleagues suggested that HAp-urea nanohybrid could release nitrogen. Rice yield increased by 8.2%. This work demonstrates that nanotechnology can be used to develop slow release fertilizers which can significantly reduce the amount of chemicals used while maintaining yield (Kottegoda et al., 2017). Similar to Pradhan and colleagues (Pradhan et al., 2021), their research suggested that urea doped hydroxyapatite nanoparticles can be the controlled-release formulation for rice seed germination and seedling growth (5.99217 ± 0.156). Fresh weight (13.8 ± 0.5) and dry weight (1.6 ± 0.5) were enhanced in the treatment compared to control. In addition, Taskin and colleagues (Taşkın et al., 2018) investigated that HAp nanoparticles gave similar results to water-soluble P source (H_3PO_4) as shown by the growth (dry weight) and phosphorus uptake of lettuce (*Lactuca sativa* L.) grown in two different calcareous alkaline soils. In results showed that HAp seemed to be more effective than that of ordinary phosphorus source on growth (dry weight). Mikhak and colleagues studied the effect of synthetic nano-zeolite (nCp)/nanohydroxyapatite (nHA) on agro-morphological characteristics and phosphorus uptake by chamomile (*Matricaria chamomilla* L.) in sandy soil (Mikhak et al., 2017). The research included four fertilizers namely saturated nano zeolite with ammonium sulfate (nCp-NH₄⁺), rock phosphate (RP), triple superphosphate (TSP) and nano-hydroxyapatite (nHA) in eight different treatment combinations. Among all the treatments, the saturated nano-zeolite with ammonium

sulfate plus nanohydroxyapatite ($n\text{Cp-NH}_4^+ + n\text{HA}$) treatment showed the highest phosphorus content and uptake by both root and shoot in the chamomile plant. In addition, the report of Soliman and colleagues (Soliman et al., 2016) revealed that the foliar application of HAp nanoparticle significantly increased plant height, stem diameter, number of leaves per plant, leaf area, root length, total fresh and dry weight compared to the control in baobab plants grown in sandy soil. Foliar application of HAp nanoparticles provided a significant increase in phosphorus availability to the plant which led to improving growth parameters and chemical compositions of the baobab plant. Although there are quite a few reports on positive effects, adverse effects appeared in some literature.

HAp nanoparticles can be prepared by various techniques such as hydrothermal, sol-gel, and other techniques (Table 2.4). The sol-gel technique has advantages over other techniques as it does not require pH control, high temperature and vigorous agitation or long hydrolysis times, which contribute to it being one of the most commonly, used processing methods for nanomaterial.

Table 2.4 The syntheses of HAp nanoparticle.

Substrates	Size of NPs (nm)	Lattice parameter A°		References
		a (nm)	c (nm)	
HAp from calcium and phosphorus Tris,	15.88	0.96993	0.70281	(Cengiz et al., 2008)
Reference of HAp	26.70	0.97049	0.69427	(Cengiz et al., 2008)
HAp from Ca(NO ₃) ₂ ·4H ₂ O and (NH ₄) ₂ HPO ₄	62 43 79 171	0.95197 0.95277 0.95239 0.95359	0.67410 0.67392 0.67387 0.67473	(Palomas et al., 2018)

Cengiz and colleagues reported for the first time that the HAp nanoparticles could be synthesized by precipitation method in the presence of simulated body fluid solution or calcium phosphorus tris solution. Particle size distributions were significantly different for both samples (Cengiz et al., 2008). Lattice parameters showed that the synthesized particles were in a hexagonal structure. Palomas and colleagues reported the synthesis of nanocrystalline HAp powders by a simple method using aloe vera plant extract solution. Particle size distributions were significantly different for all samples prepared using varying temperatures and were shown to have the hexagonal structure of the HAp nanoparticles with the lattice

parameter (Palomas et al., 2018). In recent years, the development of efficient green chemistry methods for the synthesis of metal nanoparticles has become a major focus of research to find an eco-friendly technique for the production of well-characterized nanoparticles. One of the most considered methods is the production of metal nanoparticles using organisms. Among these organisms, plants seem to be the best candidates as they are suitable for the large-scale biosynthesis of nanoparticles. Nanoparticles produced by plants are more stable and the rate of synthesis is faster than in the case of using microorganisms. Moreover, the nanoparticles are more varied in shape and size in comparison with those produced by other organisms. The advantages of using plant and plant-derived materials for biosynthesis of metal nanoparticles have interested researchers in investigating mechanisms of metal ions uptake and bioreduction by plants, and to understand the possible mechanism of metal nanoparticle formation in plants. Table 2.5 shows examples of nanoparticle green synthesis using plant extract.

Table 2.5 Green syntheses of nanoparticles using plant extract.

Plants	Nanoparticles	Condition	Size of NPs (nm)	Morphology	Reference
Aloe vera L.	Indium oxide (In ₂ O ₃)	400°C	13±1	Spherical, triangular	(Maensiri et al., 2008)
		500°C	15±4		
		600°C	15±3		
Aloe vera L.	Hydroxyapatite	500°C	62	Spherical	(Klinkaewnarong and Maensiri, 2010)
		600°C	43		
		700°C	79		
		800°C	171		
<i>Polyalthia longifolia</i>	Silver	10 ⁻³ M 25°C	50	Spherical	(Kaviya et al., 2011)
		10 ⁻⁴ M and 25°C	20		
		10 ⁻³ M and 60°C	35		
		10 ⁻⁴ M and 60°C	15		

Maensiri and colleagues reported that In₂O₃ nanoparticles with particle sizes of 5–50 nm could be synthesized by a simple, cost-effective, and environmentally friendly route using indium acetylacetonate and aloe vera plant extract solution. It was found that the morphology and size of In₂O₃ materials were affected by the calcination temperature. Aloe vera extract was also successfully used to synthesize nanocrystalline hydroxyapatite (Maensiri et al., 2008). Klinkaewnarong and colleagues reported that nanocrystalline hydroxyapatite powders were synthesized by a simple method using aloe vera plant extract. The morphology tends to change from

a spherical shape to a rod-like shape with increasing calcination temperature (Klinkaewnarong and Maensiri, 2010). Kaviya reported the synthesis of silver nanoparticles (AgNPs) using *Polyalthia longifolia* leaf extract as a reducing and capping agent along with D-sorbitol to increase the stability of the nanoparticles. They found that the smaller particles lead to the greater antimicrobial effects and the antibacterial activity is higher in the case of silver nanoparticles synthesized at 60 °C compared to 25 °C because of them being smaller in size (Kaviya et al., 2011).

2.6 Nanotechnology and Agriculture in the Future

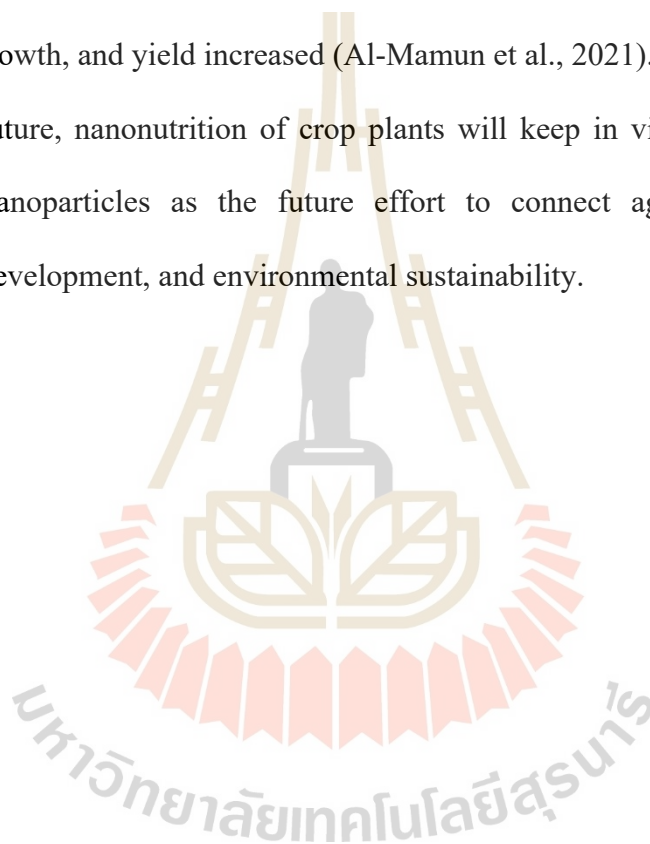
There are reports from the market research platform estimating the global nanotechnology industry will reach approximately 124 billion USD by 2024 (Research and Market, 2020). Nanotechnology applications are expected to increase in agricultural industries due to a growing population expected to hit 9 billion by 2050. The future population is likely to increase. Therefore, it will be necessary to raise productivity in agriculture too. More fertilizer use to promote plant growth is also expected to rise (Mukhopadhyay, 2014). From the literature, nanotechnology has the potential to revolutionize agricultural productivity with novel tools for enhancing crop plants (Suresh et al., 2020). The engineered nanomaterial is being studied as nano fertilizers to increase nutrient efficiency and improve plant nutrition, compared with traditional fertilizers (Chunguang et al., 2017). Nanofertilizer can increase the efficiency of micro- as well as macronutrients of plants. In the literature, various nanoparticles (NPs) and nanomaterials (NMs) have been successfully used for better nutrition of crop plants compared to conventional fertilizers (Shang et al., 2019). This review summarizes these NPs and NMs into macronutrient-based fertilizers and plant-

growth-enhancing nanoparticles. Macronutrients as based fertilizer of one or more nano-sized of these compose N, P, K, Ca, Mg and S. For example, the slow-releasing of nitrogen when urea was coated on zeolite chips (Kottegoda et al., 2011). Similarly, urea-modified HAp nanoparticles were encapsulated under pressure into the cavities of softwood of *Gliricidia sepium*, and were tested for slow and sustainable release of nitrogen into the soil (Kottegoda et al., 2011). HAp as nano phosphorus fertilizers were compared with conventional chemical fertilizers for their role in increasing uptake for plant growth (Shang et al., 2019). The effect of HAp on soybean (*Glycine max*) under greenhouse conditions was studied. It was found that seed treated with HAp was a significant increase in growth rate and seed yield when compared to the conventional chemical fertilizers was observed. The HAp nanoparticles showed no phytotoxicity effect on the growth of lettuce (*Lactuca sativa*). Dry weights of lettuce were grown significantly increased. HAp nanoparticles seem to be more effective than ordinary phosphorus sources (H_3PO_4 -P) (Taşkın et al., 2018). Similarly, in another approach of Tarafdar and colleagues reported that the biosynthesized of phosphorus nanoparticles by using *Aspergillus tubingensis* TFR-5 from tri-calcium phosphate ($Ca_3P_2O_8$) were not tested to have efficacy in improving plant growth, development, and yield and need to be explained the uptake, translocation, and interactions of nano-phosphorus with the other elements were studied in the future (Tarafdar et al., 2012).

Ca nanoparticles ($CaCO_3$) have also been tested for their role in increasing the crop growth and productivity in Hoagland solution were on peanut compared with control (without Ca) and with the soluble source of Ca as $Ca(NO_3)_2$. It was found that Ca nanoparticles can enhance Ca uptake and its transport from root to shoot. Moreover, when there was a combined application of Ca nanoparticles and humic

acid (1 g/L), the maximum increase in seedling dry weight, i.e. 30% and 14% compared to the control and treated with $\text{Ca}(\text{NO}_3)_2$, respectively was observed (Xu et al., 2011). Al-Mamun and colleagues reported the effect of Mg-nanoparticles combined with Fe-nanoparticles (0.5 g/L) on the photosynthetic efficiency of black-eyed pea (*Vigna unguiculata*) was studied. It was found that Mg uptake increases with combined application of Fe and Mg-nanoparticles and helps improved photosynthetic efficiency, growth, and yield increased (Al-Mamun et al., 2021).

In the future, nanonutrition of crop plants will keep in view nanotoxicological effects of nanoparticles as the future effort to connect agricultural efficiency, sustainable development, and environmental sustainability.



CHAPTER III

MATERIALS AND METHODS

3.1 The Synthesis of Hydroxyapatite Nanoparticles Using Aloe Vera Extract by Sol Gel Method

The nanocrystalline hydroxyapatite nanoparticles were synthesized at 600 °C by a simple sol-gel method using aloe vera extract solution according to Klinkaewnarong and colleagues (Klinkaewnarong et al., 2010). In this study, calcium nitrate ($\text{Ca}(\text{NO}_3)_2 \cdot 4\text{H}_2\text{O}$ (99 % purity, BDH), diammonium hydrogen phosphate ($(\text{NH}_4)_2\text{HPO}_4$ (99% purity, BDH)) and aloe vera plant extract were used as the starting materials. The molar ratio of Ca/P was kept at 1.67 to make the resulted material hydroxyapatite. *A. vera* extract solution was prepared from 35 g of fresh aloe vera leaf. Aloe leaves were washed, finely chopped, and boiled in 100 ml of de-ionized water. 39.4 g of calcium nitrate and 11.5 g of diammonium hydrogen phosphate were added in 250 ml of the aloe vera extract under vigorous stir at 30 °C to obtain a well-dissolved solution. No pH adjustment was done. Then, the solution was mixed continuously by stirring at 150 °C until the dried precursor was obtained. To burn away the polymer from plant extract and obtain nanoparticles, heat at 600 °C was applied for 2 hours in the furnace. The resulted nanoparticles were characterized using various methods. The method used to study the crystalline phase was X-ray diffraction (XRD) analysis. Transmission electron microscope (TEM) was used to

analyze the morphology and particle size. The elemental phase composition was studied using scanning electron microscopy - energy dispersive X-ray (SEM-EDX). FT-Raman spectroscopy was used to investigate the functional groups on hydroxyapatite powder.

3.2 Characterization of the Resulted Hydroxyapatite Nanoparticles

3.2.1 X-ray diffraction analysis (XRD)

X-ray diffraction analysis, as its name suggests, is an x-ray based analytical approach used in characterizing materials usually in powdery form. X-ray beam interactions with the atoms of different materials yield unique fingerprints used for material identification. XRD analysis was carried out to furnish information on the crystalline size and crystallinity of the HAp nanoparticles synthesized under different temperature conditions. The x-ray diffraction pattern of the dry nanoparticles powder was obtained using Bruker D2 x-ray diffract meter with Cu K α radiations ($\lambda=1.5406$ °A).

3.2.2 Transmission electron microscope (TEM)

The transmission electron microscope (TEM; FEI TECNAI G2 20 S-Twin) is an essential tool for studies conducted in the material sciences. By using a beam of electrons instead of light, the fine features of specimens such as crystal structure, grain boundaries, shape, and size can be observed. A resolution several magnitudes better than that of a light microscope is owed to the much smaller wavelength of electrons. In this experiment, the transmission electron microscope was used for the analysis of the shape and size of the developed nanoparticles. The powder of HAp nanoparticles was dispersed in deionized water and alcohol. Then, shaking sonication

was applied for 15 minutes, About 3 μL of the hydroxyapatite colloidal samples were placed on carbon-coated copper grids and spread thin, and then left to dry in the oven at 60 °C for about 15 minutes before analysis.

3.2.3 Scanning electron microscopy with energy dispersive X-Ray analysis

Scanning electron microscopy (SEM; Field emission scanning electron microscope; JEOL JSM 7800F) is a type of electron microscope which, by scanning the surface with a focused electron beam, provides images of a sample. Different signals provide details about the topography of the surface and the composition of the sample. In a raster scan pattern, the electron beam scans on the surface of the sample, and the beam angle is combined with the size of the detected signal to make an image. The energy dispersive x-ray analyzer (EDX; JEOL JEM 2010 200kv) is an analytical technique used to provide elemental identification and quantitative compositional information of a sample. By using a beam of X-rays focused into the samples, the number and energy of the X-rays emitted from a specimen can be measured by an energy-dispersive spectrometer. In this experiment, the energy dispersive x-ray analyzer was used for the analysis of the elemental identification such as calcium and phosphorus of hydroxyapatite powder. The powder of HAp nanoparticles samples was cleaned and degreased and dried to eliminate any outgassing from organic contamination and water. The sample was dispersed in a volatile solvent like acetone and alcohol. After being cleaned, samples should be dried completely using an oven or a hot plate or be allowed to air dry. Then, the sample powder was dispersed onto the substrate surface. Carbon tape and copper tape can be used for powder mounting. A spatula was used to distribute the powder lightly and to press lightly to have the sample adhered to the tape. The sample holder was then turned upside down and

tapped to remove loose material or it can alternatively be blown off with a compressed gas.

3.2.4 Fourier transform and Raman spectrometer (FT- Raman)

Fourier transform Raman spectroscopy (Bruker Vertex70-RamII) was carried out to identify the functional groups bound which are involved in hydroxyapatite substrate reduction and stabilization bound to the surface of HAp nanoparticles. The hydroxyapatite synthesized powder at 600 temperature used for FT-Raman analysis with a spectrum covering the wavenumber range 400–4000 cm^{-1} .

3.3 Determination of Size Distribution and Dissolution of Hydroxyapatite Nanoparticles in Solutions

3.3.1 Preparation of particles in solution

Suspension of HAp nanoparticles at various concentrations at 100, 500 and 1000 mg/L were prepared in deionized water (DI-water; 18.23 $\text{m}\Omega\cdot\text{cm}$) and dispersed by ultrasonic vibration (100 W, 40 kHz) for 30 min. Small-sized bars were placed in the suspensions for stirring before use to avoid aggregation of the particles. The samples were shaken at 25 °C and 180 rpm 24 hr. Then, the pH values of the solution were recorded. Finally, the samples were filtered through 0.2 μm membranes to collect samples for size determination using the Nanoparticle Sizer and Zeta Potential Analyzer (Malvern Zetasizer-ZS).

3.3.2 Determination of size distribution

Nanoparticle sizer (Malvern Zetasizer-ZS) analyzed the sample by dynamic light scattering (DLS) method. The refractive index value from the Malvern manual was used to determine the particle size. In addition, other values related to

size distribution were used as the analysis input. The hydrodynamic diameter as the Z-average with the mean of intensity, weighted size distribution, and polydispersity or agglomeration were reported. These results in used to assess the dispersion of nanoparticles qualitatively.

3.3.3 Determination of zeta potential

Zeta potential, pH, conductivity, and electrophoretic mobility were detected by nanosizer (Malvern Zetasizer-ZS). One ml of the suspension was taken using a ten ml syringe. A disposable folded capillary cell was fitted with an electrode on each side for the zeta potential measurements. Once the sample starts to emerge from the other end, the stopper was inserted and any liquid which may have spilled onto the electrodes was removed. The cuvettes were cleaned thoroughly with ethanol and DI water. At least five measurements in the automatic mode were recorded and the averaged zeta potential value was reported.

3.3.4 Dissolution of Ca^{2+} and PO_4^{3-} from HAp nanoparticles

The suspensions were sonicated to help disperse particles well. Sonication was performed for 30 min to avoid aggregation. Ion Chromatograph (IC; Dionex ICS-5000) was utilized to detect the concentration of calcium ion (Ca^{2+}) and phosphate (PO_4^{3-}) dissolved in the solution. The method used was modified from that reported by Ling and Xing (2009).

3.4 Tests for the Potential of Hydroxyapatite Nanoparticle in Enhancing Seed Germination and Seedling Growth and Plant Stress

3.4.1 Treating materials

Khao Dawk Mali 105 was the rice variety used throughout all experiments. Seeds were obtained from the Rice Research and Development Institute, Nakhonratchasima, Thailand. Rice seeds were treated with HAp nanoparticles in the study of germination. Three concentrations of particle suspensions were used including 100, 500, and 1000 mg/L. Commercial phosphate fertilizers with the formulas 18-46-0 and 15-15-15 were prepared at the same concentration range. They would be used to treat seeds and plants also for comparison. DI water was used as control.

3.4.2 Germination test

Rice seeds were sterilized by immersing in 2.5% sodium hypochlorite solution for 15 min. They were rinsed three times with distilled water before soaking in HAp nanoparticle suspensions and solution of commercial fertilizers both formulas at 100, 500, and 1000 mg/L. Twelve seeds treated with each of the solutions were transferred into labeled Petri dishes containing Whatman filter paper number 1. Ten ml of HAp nanoparticle suspensions and both fertilizer solutions were distributed to each of these Petri dishes, followed by incubation for 7 days. The control in which distilled water was also used included. For each treatment, five replicates, each containing twelve grains, were performed. To ensure that all grains had equal access to moisture, the solutions introduced into the Petri dishes were dispensed evenly. The germination percentage was obtained following the formula below (Lin and Xing, 2007). Root and shoot length were measured with Image J software.

$$\text{Germination percentage} = \frac{\text{Number of germinated seeds}}{\text{Number of incubated seeds}} \times 100$$

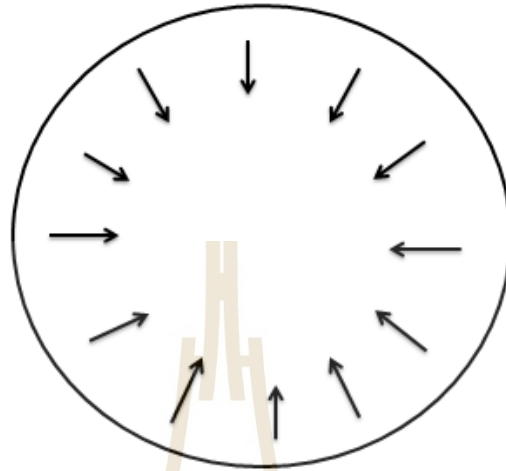


Figure 3.1 The arrangement of rice grains in the petri dish, with the arrowhead being the germ portion.

3.4.3 Determination of relative water content

Relative water content (RWC) of rice seedlings under different treatments were estimated in roots following the equation: $RWC = [(FW - Dw) / (Tw - Dw)] \times 100$. Where FW is the fresh weight of seedlings, Dw is the dry weight of seedlings and Tw is the turgid weight of seedlings. The fresh weight (FW) was measured after 7 days of treatment according to the method of Barrs and Weatherly as cited by Mezer and colleagues. Five seedlings were taken for the measurements. The turgid weight (TW) was taken from the seedlings that had been kept in distilled water for 24 hours in the dark at 4 °C. These seedlings were subsequently dabbed off excess water before weighing to obtain the turgor weight. The dry weight (DW) was measured after the

samples were dried at 105 °C for 2 hours and then kept at 70 °C for 24 hours in a forced air-driven oven to reach a constant weight overnight.

3.4.4 Determination of malondialdehyde (MDA)

Lipid peroxidation is an oxidative process that affects cellular membranes and other molecules that contain lipid. It causes cell damage and its toxicity leads to cell death. As the indicator of lipid peroxidation, the method of Mukherjee and Choundhuri, (1983) was followed. After rice grains had germinated under exposure to various concentrations of HAp nanoparticles suspensions and commercial fertilizer solutions, 0.5 g of the root was taken, grounded, and homogenized in 2 ml in 0.25% thiobarbituric acid (TBA). The homogenate was centrifuged at 10000 rpm for 10 minutes. Then, the supernatant was added to 1.5 mL of 10% (w/v) TCA containing 0.25 (w/v) of 2-thiobarbituric acid (TBA). Samples were incubated at 95 °C (degrees Celsius) for 20 minutes in a water bath. The samples were then centrifuged at 12000 rpm for 5 minutes. The supernatant was taken for the measurement of absorbance at 532 nm and 600 nm using a UV-Vis spectrophotometer. To determine the amount of Malondialdehyde (MDA) in tissue samples, the following formula was applied.

MDA content (nmol) = $(A_{532} - A_{600}) \times 1,000 \times 2 / 155 \times (\text{Fresh weight, FW})$.

3.4.5 Determination of cell death evaluation

Cell death was evaluated based on the method used in Zanardo and colleagues. Three cm of root tips from each experiment were excised and put into 5 mL of Evans blue (0.25% v/v) for 15 minutes. Then, the roots were washed by leaving in distilled water for 30 minutes to get rid of excess and unbound dye. The root tips

were then incubated in 7 mL of N-dimethylformamide at room temperature for 50 minutes in the dark. N-dimethylformamide was used as blank. The release of Evans blue was measured by using an absorbance value at 600 nm.

3.5 Tests for the Potential of Hydroxyapatite Nanoparticle in Enhancing Growth of Rice

3.5.1 Plant harvest and sample collection

HAp nanoparticle suspensions and commercial fertilizers with formulas 18-46-0 and 15-15-15 were prepared at 100, 500, and 1000 mg/L in DI water. Homogeneity was ensured with sonication. After germinations for 7 days in plates and their root and shoot lengths were recorded, the seedlings were transferred and planted in plastic pots in kg of soil mixed with 1 liter of treating suspension/solution at different concentrations. Twelve seeds were placed in one pot. There were 5 plastic pots for each concentration as 5 replicates. Growths of rice exposed to HAp nanoparticles were monitored. The height and width of rice leaves were recorded at day 35 days (Figure. 3.2). The most recent mature leaf (MRML) was used for the measurement by one leaf of every plant in the pots was measured.

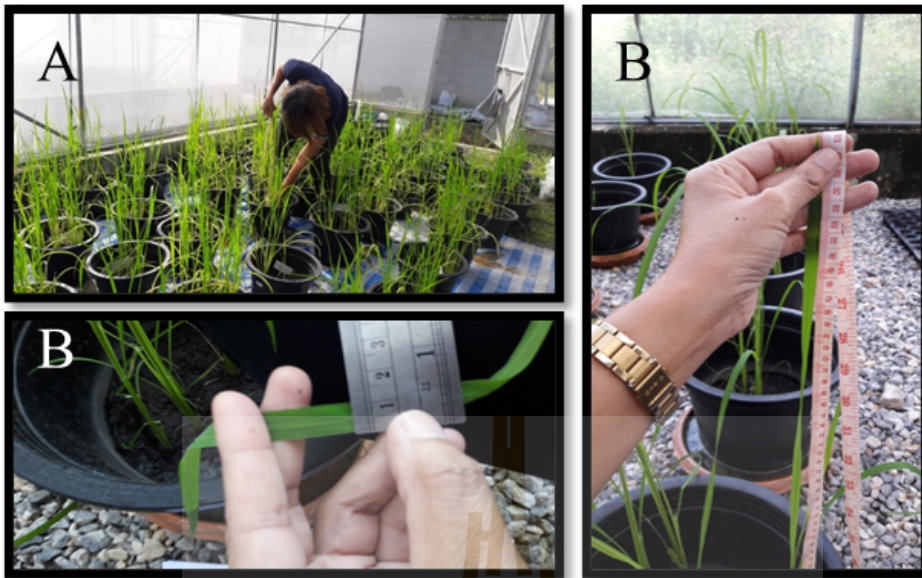


Figure 3.2 The measurements of height of rice plant (A), length of leaf (B) and width of leaf (C).

The number of panicles, the number of grains per panicle, the number of grains per pots, and the weight of 1000 grains were determined within 130 days following the method of the International Research Rice Institute (IRRI). In addition, the quality of grains such as starch, amylose content, and 2AP production were determined. The data were analyzed by One Way Anova and compared by the Duncan test at 0.05 p-value level.

3.5.2 Determination of starch in seed using SEM/EDX

Scanning Electron Microscope (SEM) with energy-dispersive X-ray spectroscopy (EDX) was used to identify elements in the seed. This method helped us identify starch in grains through morphology and elemental carbon and oxygen. Starch is composed of oxygen, hydrogen, and carbon $(C_6H_{10}O_5)_n$, where n ranges

from 300–1000. Therefore, starch is approximately 42.1% carbon, 6.5% hydrogen, and 51.4% oxygen.

3.5.3 Determination of amylose content in seeds

Amylose content value was determined according to the iodometric technique described by Gilbert and Spragg, 1964. For 100 mg of rice, 1 ml of ethanol (95%) and 9 ml of 1N NaOH were added in a volumetric flask (100 ml) and mixed. Samples were heated in a boiling water bath for 10 min to gelatinize the starch and later allowed to cool down to room temperature. Five milliliters of the gelatinized starch solution was then transferred to a 100 ml volumetric flask followed by the addition of 1 ml of 1N acetic acid and 2 ml of iodine solution, with the volume adjusted to 100 ml with distilled water. All the content was thoroughly vortex mixed and allowed to stand for 20 min. The absorbance was measured at 620 nm using a spectrophotometer.

3.5.4 Determination of aroma in rice seeds using gas chromatography

The 2AP content was analyzed following Sansenya and colleagues with some process modifications. 2AP was purchased from BOC Sciences with a purity of 95% to be used as a standard. One g of rice powder was placed into 20 mL headspace vials. The rice samples needed to be prepared fresh and capped immediately. Using a headspace technique, the rice samples were examined. A 5 mg/mL stock solution was prepared by adding 2 mL of methanol-toluene (1:1) to 10 mg of 2AP; this was then diluted to 0.01, 0.05, 0.1, 0.5, 1.0, and 2.5 mg/mL with ethanol. The calibration standards were prepared by adding 1.25, 2.5, 5.0, 10.0, 25.0, 50.0, and 100.0 µg of the 2AP standard to a 20 mL headspace vial containing 1 g of rice blank. We used the gas chromatograph (GC) from Agilent 7890A. Rice samples were incubated with shaking

at 120 °C for 15 minutes, and then 1 mL of gas was removed and injected into the GC injector port with a gas-tight syringe (2.5 mL). The injector was set to 240 °C, and a split mode with a 5:1 split ratio was applied. Helium gas was used at a steady flow rate of 1.5 mL/min as the carrier gas. The following oven temperature program was used: the column temperature was isothermally maintained for 2 min at 40 °C, programmed to a rate of 10 °C/min to 100 °C/min. Then at a rate of 5 °C/min to 150 °C; and finally at a rate of 30 °C/min to 250 °C/min, and the temperature of the column was then isothermally maintained for 15 min at 250 °C. In the electron ionization mode, the mass spectrometer was used with the ion source temperature set at 230 °C and the ionization energy set at 70 eV. To analyze for 2AP, the multi-reaction monitoring (MRM) mode was used. At a flow rate of 2.35 mL/min, helium gas was used as the quenching gas. At a flow rate of 1.5 ml/min, nitrogen gas was used as the collision gas. The precursor ion m/z 111 and the production m/z 83 were selected for 2AP with collision energy of 5 eV. The MS detection dwell time was 30 min.

CHAPTER IV

RESULTS AND DISCUSSIONS

With the increasing requirement of agricultural yield due to the peak in worldwide production that will occur in the next decades, phosphorus (P) is obtaining more interest as a nonrenewable resource (Cordell et al., 2009). Thus, phosphorus has an opportunity reduced every year. Phosphorus has unique characteristics such as its low availability due to slow diffusion and high fixation in soil. While it can be a major limiting factor for plant growth. Even that, chemical phosphorus fertilizer has improved yield production but caused environmental damage in the past decades. So, HAp nanoparticles are alternative to improve phosphorus fertilizer, it has property in solubility and dispersion in the soil led to it can increase the bioavailability is better (Mani and Mondal, 2016). Therefore, we are interested to develop fertilizers with improved performance and environmentally friendly properties by using aloe vera extract for synthesizing HAp nanoparticles. Aloe vera extract as the intermediary to reagents of hydroxyapatite for reduction and stabilization of aqueous phosphate and calcium. Aloe vera leaf extracts have contained flavonoids and tannins to a large part of chemical compounds known as the polyphenols, capable of serving as reducing agents (López et al., 2013).

4.1 Characterization of Synthesized Hydroxyapatite Nanoparticles

In this study, the characterization of HAp powders was carried out to confirm the effectiveness of using aloe vera extract in the sol-gel synthesis process. The HAp powders were calcined at 600 temperatures. The characterizations of HAp nanoparticles powder were investigated by X-ray diffraction (XRD), scanning electron microscopic and energy dispersive X-ray (EDX) spectroscopy, Transmission Electron Microscope (TEM), and FT-Raman analysis to determine the crystallite size, elemental composition, morphology, and functional groups.

4.1.1 Analysis of crystalline size and structure of hydroxyapatite using analysis of XRD patterns

Phase analysis, crystalline size of the HAp powders were conducted using X-ray diffractometer (XRD) and confirmed that $(\text{Ca}(\text{NO}_3)_2 \cdot 4\text{H}_2\text{O})$ and $(\text{NH}_4)_2\text{HPO}_4$ can be formed HAp structure. X-ray diffraction with Cu K α radiation ($\lambda = 1.54060 \text{ nm}$) was studied. The analysis was recorded in the 2θ range of $10\text{-}80^\circ$ at a scan rate of $0.02^\circ/\text{min}$. The XRD patterns are showed peaks revealed to be $(\text{Ca}_{10}(\text{PO}_4)_6(\text{OH})_2)$ (ICSD: 84-1998) in Table 4.1 and Figure 4.1 -4.4. The diffractions of all peak was 25.8° , 28.8° , 30.6° , 31.7° , 32.1° , 32.9° , 34.0° , 46.6° , and 49.4° used to evaluate the mean crystalline size of HAp, which were calculated using the Scherrer equation (Klug and Alexander, 1954).

$$D = K \cdot \lambda / \beta \cdot \cos\theta$$

These demonstrated the consistency of crystal lattices that calculate their physical Where D is the mean diameter of nanoparticles, b is the full width at a half-maximum value of XRD diffraction lines (FWHM), λ is 0.15405 nm of the wavelength of X-ray radiation. θ is the diffraction angle-Bragg angle ($^\circ$) and K is the

content of Scherrer with a value from 0.9 to 1. The result of the crystalline size of HAp nanoparticles calculated from Scherrer equation was about 34 nm and lattice (A°) dimension in the range of $a = 0.9416 \text{ nm}$ $c = 0.6874 \text{ nm}$. These exactly match with the powder diffraction file (PDF Card No. 84-1998 of hexagonal phase).

Table 4.1 Crystallite size and structure of the synthesized hydroxyapatite nanoparticles.

Peaks	Peak positions 2Theta (θ)	Crystalline size	
		FWHM	Crystalline size D (nm)
Peak 1	25.8	0.17989	45.31123802
Peak 2	28.8	0.53991	15.19815526
Peak3	30.6	0.24687	33.3640628
Peak 4	31.7	0.22815	36.2022904
Peak 5	32.1	0.22936	36.04906284
Peak 6	32.9	0.23966	34.56255455
Peak 7	34.0	0.20875	39.8012535
Peak 8	46.6	0.252	34.3316533
Peak 9	49.4	0.25009	34.97136845
Average of crystalline size \pm SD		= 0.26 \pm 0.10	= 34.42 \pm 8.09
Y-Scale		= 96%	
The lattice (A°)	= Hexagonal	$a=0.9416 \text{ nm}$ $c=0.6874 \text{ nm}$	

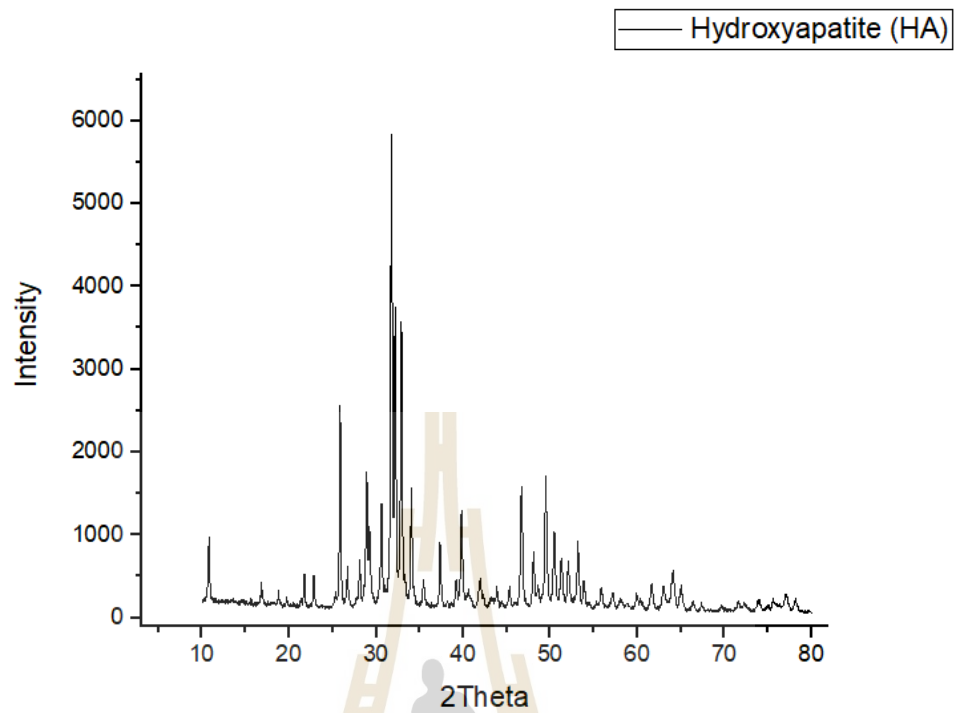


Figure 4.1 The diffraction peaks of hydroxyapatite nanoparticles synthesized by aloe vera extract are shown in 2θ peaks.

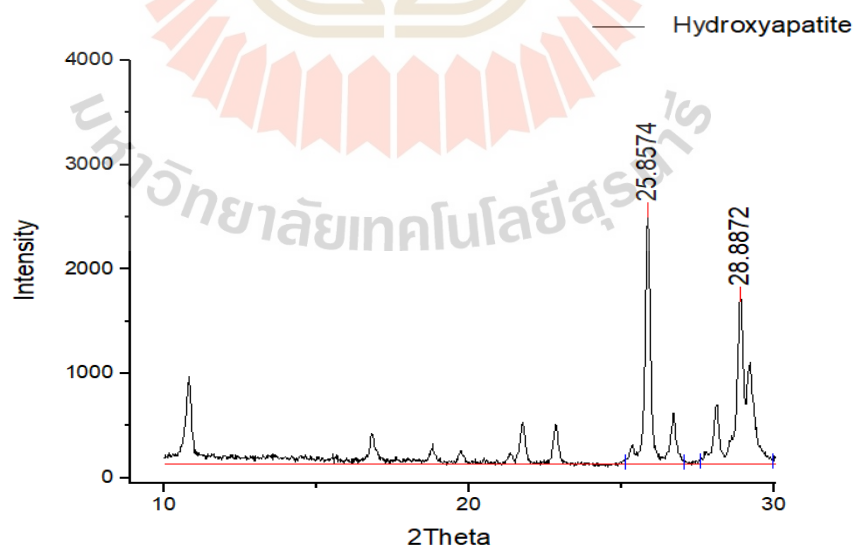


Figure 4.2 The diffraction peaks of hydroxyapatite nanoparticles synthesized by aloe vera extract in 2θ peaks at 25.8° and 28.8° XRD patterns.

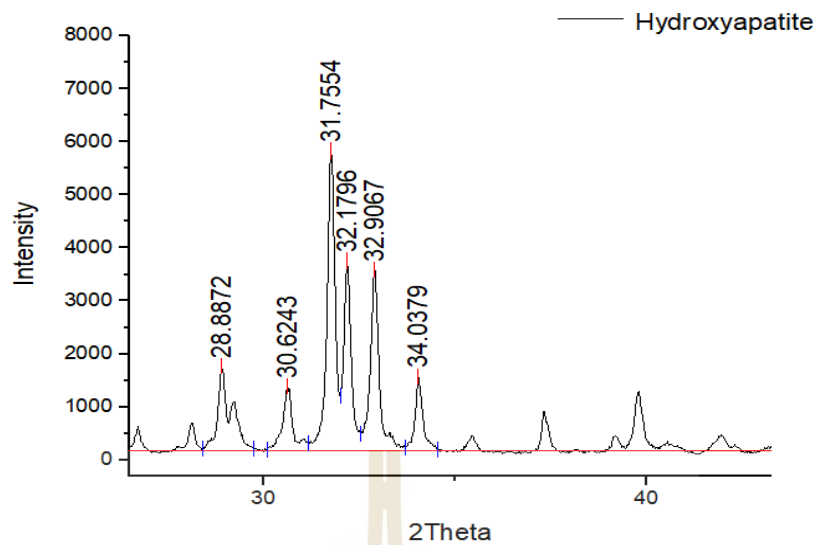


Figure 4.3 The diffraction peaks of hydroxyapatite nanoparticles synthesized by aloe vera extract in 2θ peaks at 28.8° , 30.6° , 31.7° , 32.1° , 32.9° and 34.03° XRD patterns.

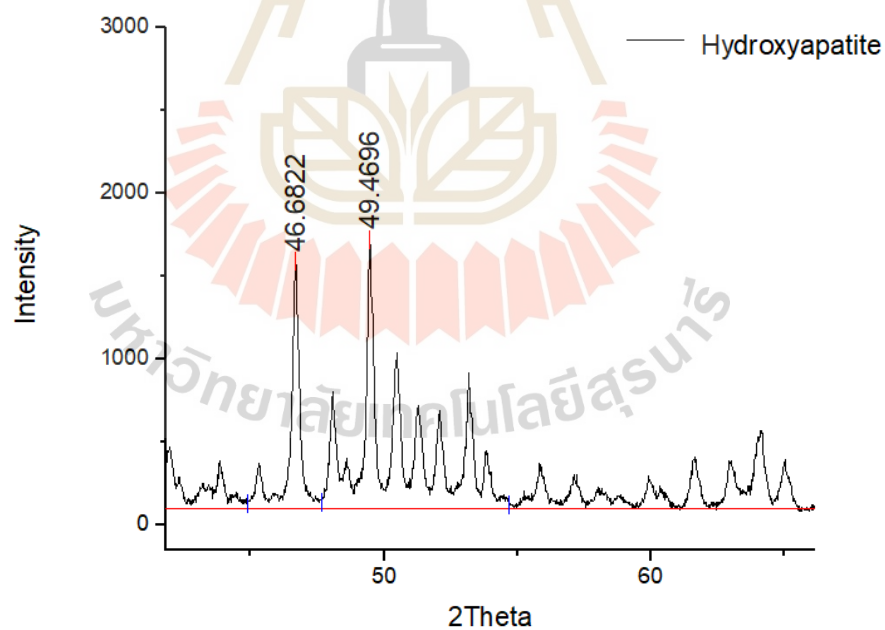


Figure 4.4 The diffraction peaks of hydroxyapatite nanoparticles synthesized by aloe vera extract in 2θ peaks at 46.68° and 49.46° XRD patterns.

The results of the XRD pattern can be confirmed the HAp synthesized using aloe vera in sol-gel synthesis can form HAp nanoparticles. The lattice dimension and crystalline size of HAp powder similar to the result of Klinkeawnarong and co-worker who reported that the crystalline size of their HAp nanoparticles was 43 nm at 600 °C and hexagonal lattice $a = 0.95277$ nm and $c = 0.67392$ nm (Klinkeawnarong et al., 2010). The results similar to Nasiri-Tabrizi and colleagues (Nasiri-Tabrizi et al., 2013) who reported the lattice dimension of the HAp and standard database are found within the range of $a = 0.9418$ nm and $c = 0.6884$ nm. In addition, Sanosh and colleagues demonstrated the HAp powders at 600 °C. XRD a pattern showed size was 39 nm or below, indicating that a high purity of HAp nanoparticles (Sanosh et al., 2009). The small size of HAp was expected to involve in bio-resorption than the fully strong crystalline HAp structure (Jiang et al., 2018).

4.1.2 Elemental composition of the synthesized nanoparticles determined by using scanning electron microscopy techniques and energy dispersive x-ray spectrometer (SEM/EDX)

The calcium and phosphorus components in the HAp powder were detected using the X-Ray spectrum (EDX) in the energy dispersive x-ray (EDX) analysis. Atomic % and weight % of calcium and phosphorus were determined as shown in Table 4.2. EDX showed the composition of calcium and phosphorus in 1-5 spectrums values measured in atomic (%) and weight % are listed in Table 4.3. Figure 4.5 showed the EDX measurement areas were focused and the corresponding peaks. From this study, in spectrum 1-5 the quantities of phosphorus were 16.75, 14.59, 22.32, 20.06, and 21.62 while in calcium were 28.45, 26.08, 39.61, 37.27, and 39.52 measured in weight %. The results as similar to Klinkaewnarong and colleagues

(Klinkaewnarong et al., 2010) confirm that HAp was 39.52% of calcium and 21.02% of phosphorus (% weight), were similar an optimal Ca/P ratio of 1.67 as followed theoretical.

Table 4.2 Elements detected in hydroxyapatite nanoparticles.

Detections	Phosphorus		Calcium		Oxygen		Carbon	
	Weight (%)	Atomic (%)						
Detection 1	16.75	11.56	28.45	15.18	54.81	73.26	-	-
Detection 2	14.59	9.38	26.08	12.96	50.12	62.39	9.21	15.27
Detection 3	22.32	17.63	39.61	24.17	38.07	58.20	-	-
Detection 4	20.06	15.26	37.27	21.90	42.68	62.84	-	-
Detection 5	21.62	16.70	39.52	23.60	35.68	53.37	3.18	6.33
Averages	19.068	14.106	34.186	19.562	44.272	59.2	6.195	10.8

Table 4.3 The weight (%) of the calcium and phosphorus component in HAp powder were detected by using X- Ray spectrum (EDX) element.

Elements	Detection 1	Detection 2	Detection 3	Detection 4	Detection 5
Phosphorus	16.75	14.59	22.32	20.06	21.62
Calcium	28.45	26.08	39.61	37.27	39.52
Ratio (Ca/P)	0.70/0.54	0.65/0.47	1/0.72	0.92/0.64	1/0.69

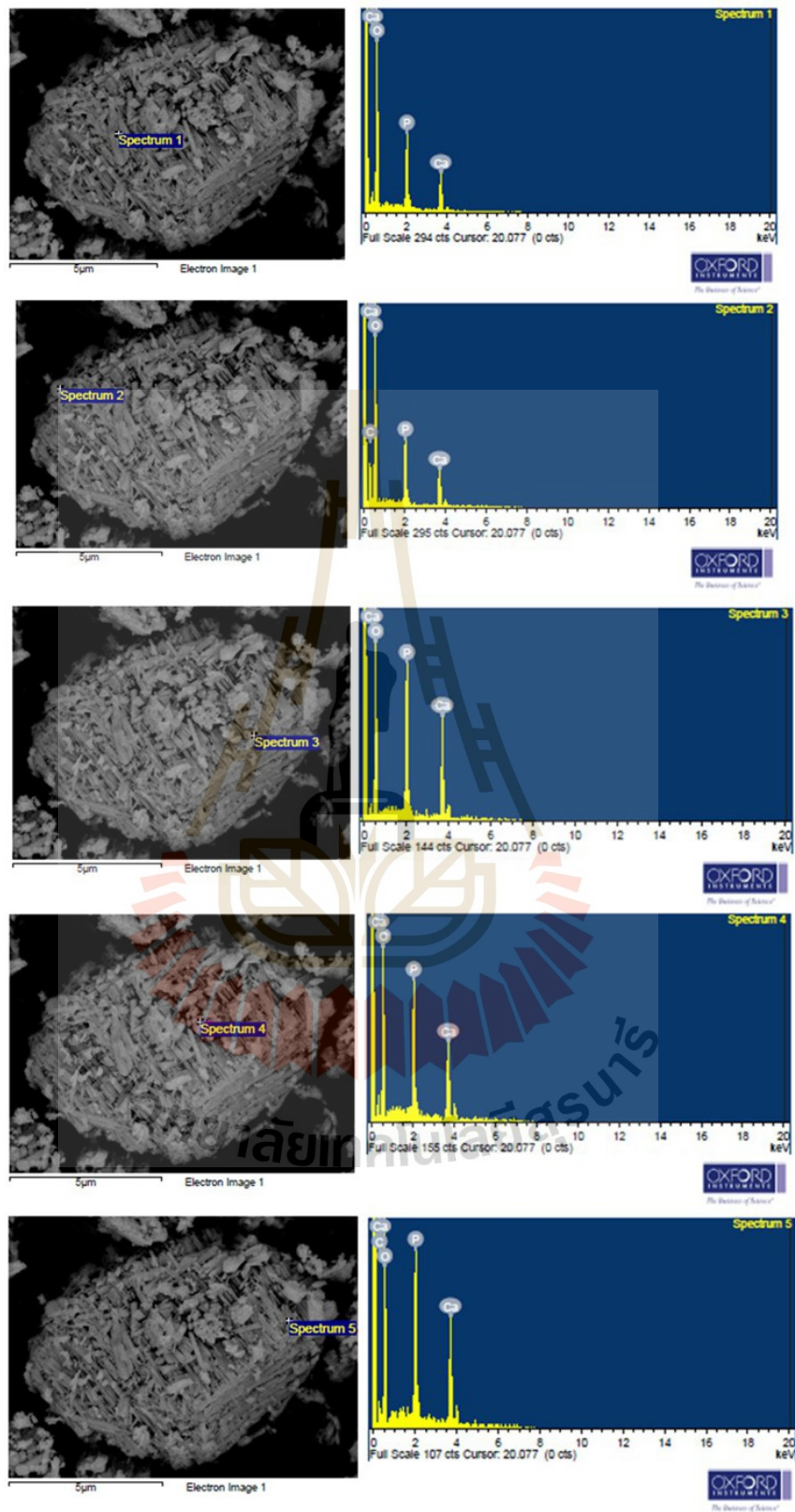


Figure 4.5 EDX spectra showed of calcium and phosphorus value.

4.1.3 Size and shape of the synthesized hydroxyapatite nanoparticles

The size and shape of nanoparticles were examined by Transmission Electron Microscope (TEM). The morphology of particles was revealed and the histogram was derived from image J software to the HAp nanoparticles were rod-like shape (Figure 4.6-4.7) with the diameter range of 8-60 nm. Most of the particles were nanosized.

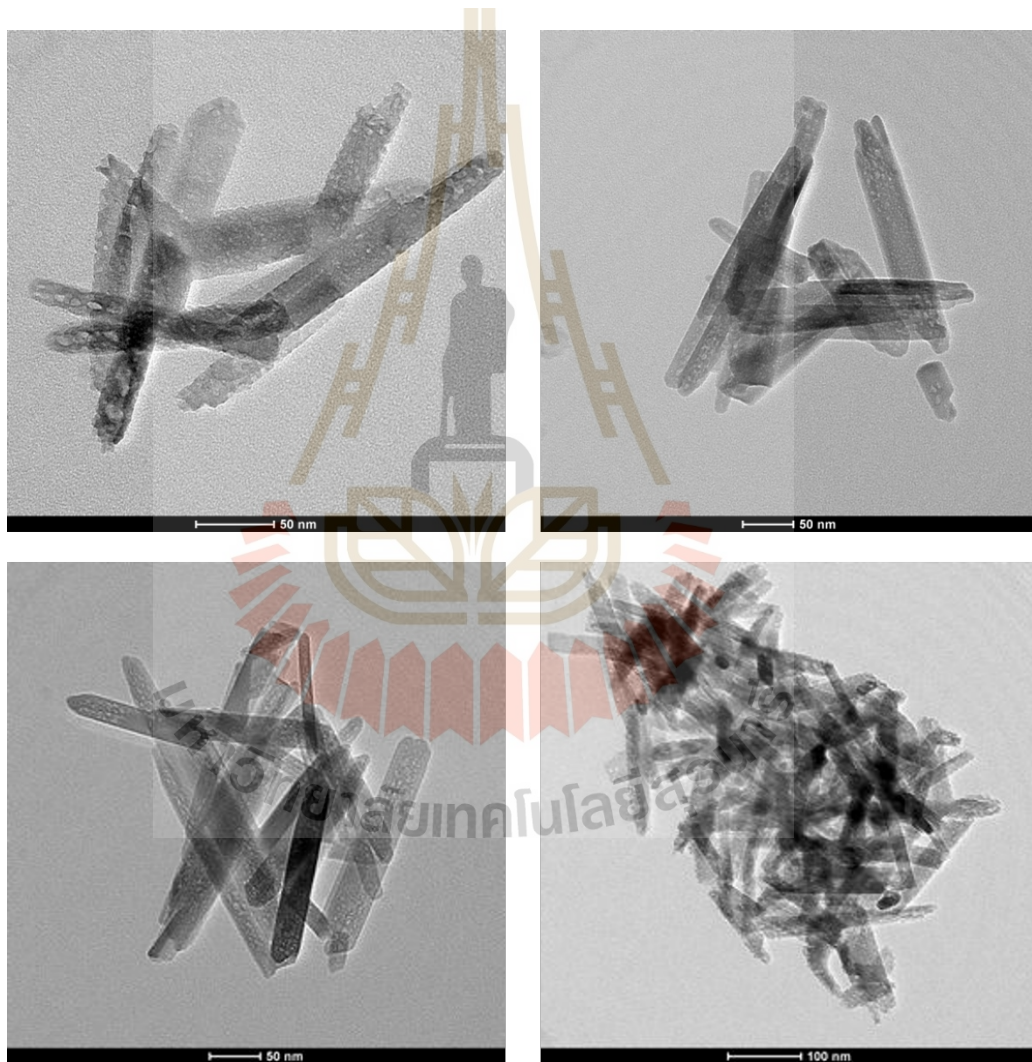


Figure 4.6 Rod shape of hydroxyapatite nanoparticles.

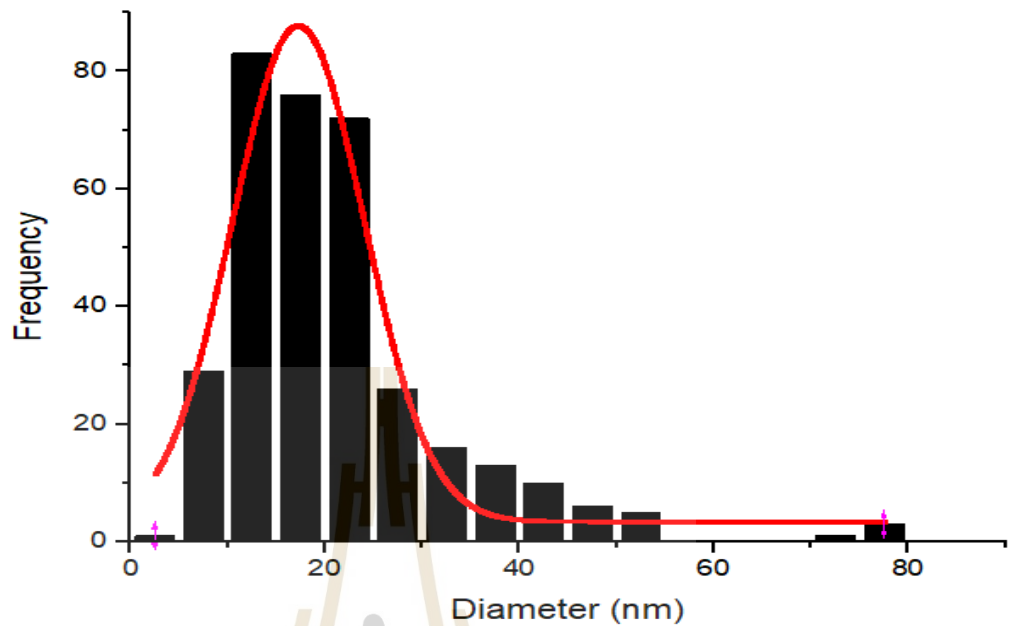


Figure 4.7 Plot presenting size distribution of the synthesized HAp nanoparticles.

These findings showed that 8-60 nm and rod shape were sized for the rod shape of HAp that is responsible for the regulation of single-crystalline shaping of aloe vera extract plant (Tippayawat et al., 2016). Nanocrystalline HAp powders were synthesized by a simple method using aloe vera plant extract, similar to Klinkaewnarong and colleagues (Klinkaewnarong et al., 2010), which reported the change of shape spherical shape to rods as temperature increased. Rod-shaped particles were shown to be dissolved not as well as spherical ones as reported by Misra and colleagues (Misra et al., 2013) reported that the spheres of nanoparticles can dissolve significantly higher dissolution than rod shapes, which is from studies indicated that the shape of the rod can be affected to release calcium and phosphate slowly. Borm and colleagues agree that with a spherical shape, the particle size is

nanoscale, it appears to be unstable, and it can cause too much dissolution (Borm et al., 2006).

4.1.4 Functional groups on hydroxyapatite nanoparticles synthesized from using aloe vera extract

Aloe vera extract played a reducing role in the synthesis of HAP nanoparticles to observe the functional group responsible for stabilizing the nanoparticles. FT-Raman analysis was performed. FT-Raman analysis provides information on the vibrational and rotational modes of motion of a molecule, and hence it is an important technique for the identification and characterization of substances. The peak vibration modes were ranging from 400–4000 cm^{-1} as shown in Figure 4.8.

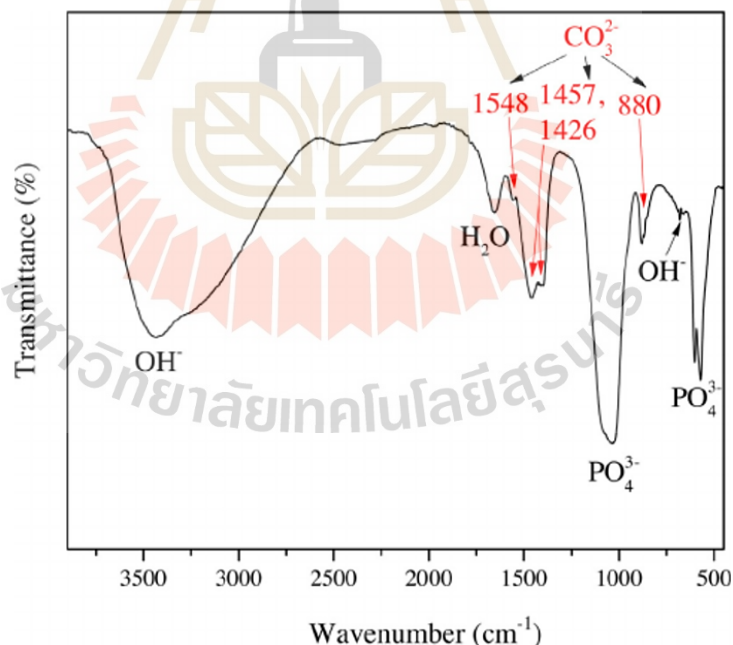


Figure 4.8 The peak vibration modes the synthesized of HAP nanoparticles were ranging from 400–4000 cm^{-1} .

The bending vibration of the phosphate group (PO_4^{3-}) was identified by a peak at 561 cm^{-1} . The band at 1028 cm^{-1} was considered to be the P-O stretching vibrations breathing mode. The broad peak at 875 cm^{-1} was correlated with the presence of HPO_4^{2-} group and 632 cm^{-1} band peak were considered to be weak intensity breathing mode of the O-H absorption band. HAp attributed to the O-P-O bending modes, was referred to by Raman spectra (Silva et al., 1998). The ν_4 (PO_4^{3-}) frequencies at 561 and 602 cm^{-1} were widely associated with the bending character of the O-P-O. The $962 \text{ cm}^{-1} \nu_1$ (PO_4^{3-}) band was a standard carbonated apatite-related phosphate band. Finally, the P-O stretching ν was assigned to the band observed at 1028 and $1087 \text{ cm}^{-1} \nu_3$ (PO_4^{3-}) as shown in Table 4.4.

Table 4.4 Functional group found on the synthesized of hydroxyapatite nanoparticles.

Chemical gr.	Absorption bands, (cm^{-1})	References
CO_3^{2-}	880, 1426, 1457 1548	(Meejoo et al., 2006).
OH-	630, 632	630 and 3540 (Destainville et al., 2003) (Raynaud et al., 2002).
HPO_4^{2-}	875	875 (Destainville et al., 2003) (Raynaud et al., 2002).
	561, 602	560 - 600 ν_4 602, 555 (Destainville et al., 2003) bending mode (Han et al., 2006).
	472	460 ν_2 (Destainville et al., 2003) (Raynaud et al., 2002).
	962	960 ν_1 (Destainville et al., 2003) (Raynaud et al., 2002).
PO_4^{3-}	1028-1087	1020 -1120 ν_3 1000 - 1100 (Destainville et al., 2003) (Raynaud et al., 2002).

We conclude that HAp were synthesized by the method using aloe vera plant extracted solution. Aloe vera extract as reducing agent, HAp was calcined at 600 °C for 2 hr. (Klinkaewnarong, 2010). The phase composition of the calcined was studied by the X-ray diffraction (XRD) technique. The XRD results confirmed the formation of HAp phase, the crystallite size is small and showing the hexagonal structure of HAp with the lattice parameter, a , in a range of 0.9416 nm and c of 0.6874 nm. The particle sizes of the powder were obtained to be 8-60 nm. The morphology was revealed by TEM showing rods shaped. The main based phosphorus and calcium component was confirmed with SEM-EDX. The functional properties of the HAp powders were characterized by FT-Raman. Raman spectrum showed a main peak of the phosphate vibration mode ($\nu_1(\text{PO}_4)$) at $\sim 962\text{cm}^{-1}$ for all the samples. The peaks of the carbonyl functional group and hydroxyl vibration modes were presented to contribute the mechanism of bioreduction processing.

The formation of HAp nanoparticles possible is likely invoked by the carbonyl group, in conjunction with several other functional groups provided by bioactive agents in the aloe vera aqueous extract, initially binding to phosphate ions and calcium ions to form hydroxyapatite complexes. These complexes are then reduced to particles with an oxidation state of zero. Aggregation of particles was decreased and then contributes to the creation of clusters that end up serving as nucleation sites. Eventually, the remainder of metal ions can build up around these centers with a reduction process, next to is referred to as secondary development (Shuai et al., 2020) as shown in Figure 4.9.

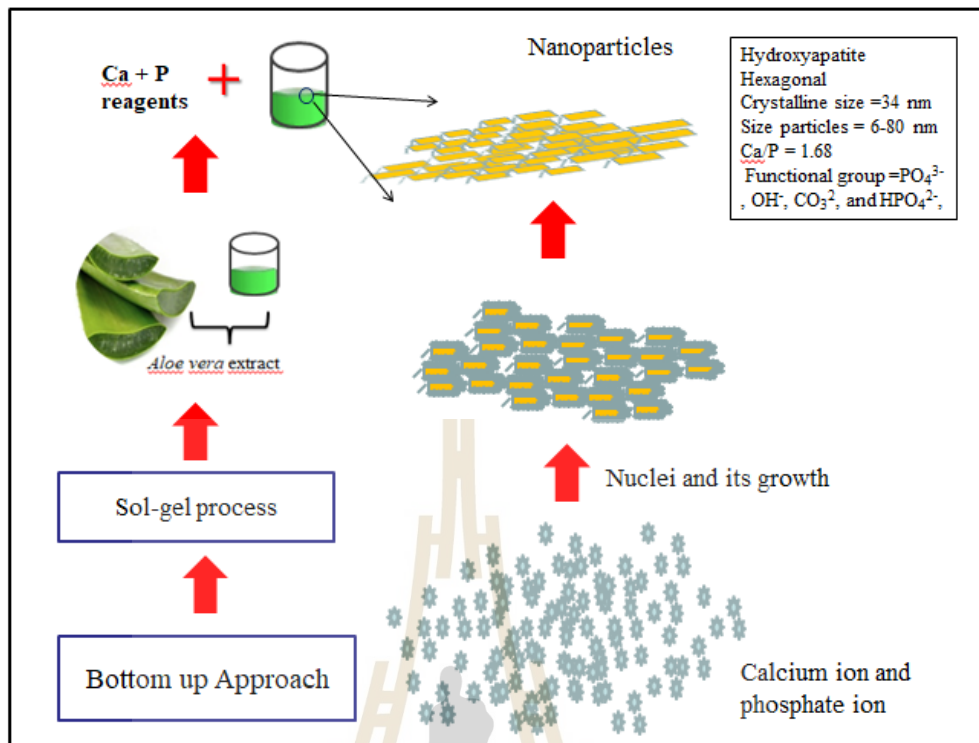


Figure 4.9 Mechanisms for the formation of HAp nanoparticle.

4.2 Dissolution of Plant Nutrients from HAp Nanoparticle

The slow-releasing of a nutrient is an important property of good fertilizer. This property guarantees the efficient utilization of the nutrient released by plants. Hydroxyapatite is calcium and phosphate-based compound. Phosphorus is one of the three main nutrients required by the plant. It is known that phosphorus is hard to dissolve from phosphate fertilizer. Sun and colleagues (Sun et al., 2012) described that solubility increased as particle size was decreased. Although size affects the solubility of the particles, the dissolution properties also depend on the shape and many factors such as zeta potential, pH, and electrophoretic mobility. Since there had not been informed about the dissolutions of HAp nanoparticles; the observation on

dissolution was carried out at various HAp nanoparticles concentrations including 100, 500, and 1,000 mg/L.

4.2.1 Size and distribution of HAp nanoparticles in colloidal solution

The Nanosizer (Malvern) was used to determine the hydrodynamic size of particles and polydispersibility in an aqueous solution. The dynamic light scattering (DLS) technique was commonly used to study the hydrodynamic size of particles in an aqueous solution. DLS has several advantages over other hydrodynamic techniques, that is it can be used under a wide variety of solvent conditions. The DLS instrument will generate a correlation function that is mathematically linked with particle size. The smaller particles disperse faster than larger ones; it is possible to quantify the hydrodynamic size of a particle based on the rate of its Brownian motion (Raval et al., 2019). DLS was measured the particle size of dispersing colloidal samples, by the mechanism of light scattering from a laser that passes through a colloidal solution and analyzes modulation of the intensity of scattered light as a function of time (Lim et al., 2013). In this study, the stability of HAp nanoparticles was detected, and aggregations or agglomerations were presented. Thus, DLS is the ultimate tool to determine and measure the agglomeration state of nanoparticles. The Z- average size and polydispersibility of the particles were revealed as shown in Figure 4.10-4.12 and Table 4.5.

Results

	Size (d.nm):	% Intensity	Width (d.nm):
Z-Average (d.nm): 165.6	Peak 1: 188.2	85.0	48.84
Pdl: 0.428	Peak 2: 53.20	10.9	7.657
Intercept: 0.712	Peak 3: 1681	2.6	298.1
Result quality: Good			

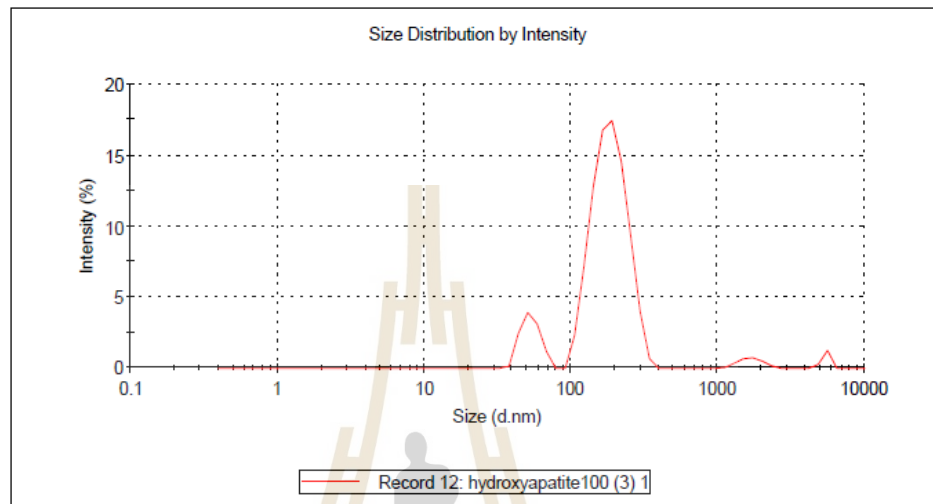


Figure 4.10 Hydrodynamic sizes of HAp nanoparticles at 100 mg/L.

Results

	Size (d.nm):	% Intensity	Width (d.nm):
Z-Average (d.nm): 200.4	Peak 1: 163.3	66.3	52.84
Pdl: 0.373	Peak 2: 485.2	33.7	134.7
Intercept: 0.771	Peak 3: 0.000	0.0	0.000
Result quality: Good			

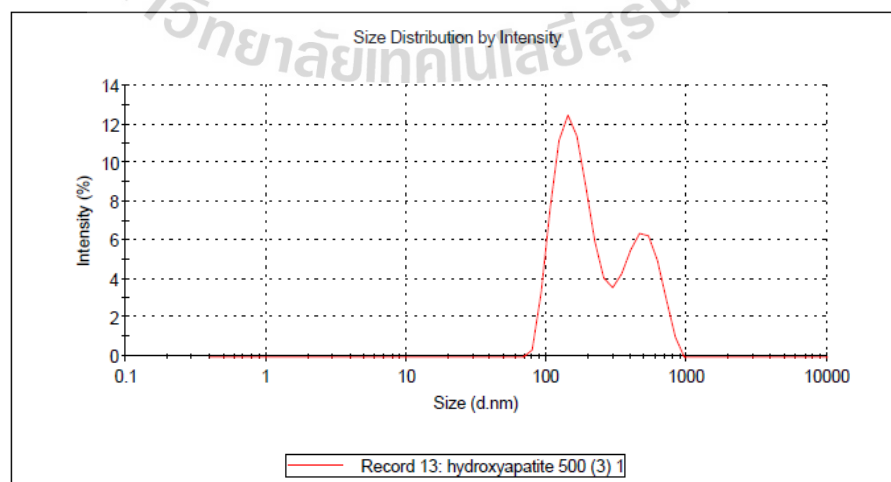


Figure 4.11 Hydrodynamic sizes of HAp nanoparticles at 500 mg/L.

Results

	Size (d.nm):	% Intensity	Width (d.nm):
Z-Average (d.nm): 231.9	Peak 1: 387.8	66.3	104.5
Pdi: 0.386	Peak 2: 111.9	33.7	24.24
Intercept: 0.586	Peak 3: 0.000	0.0	0.000

Result quality : Refer to quality report

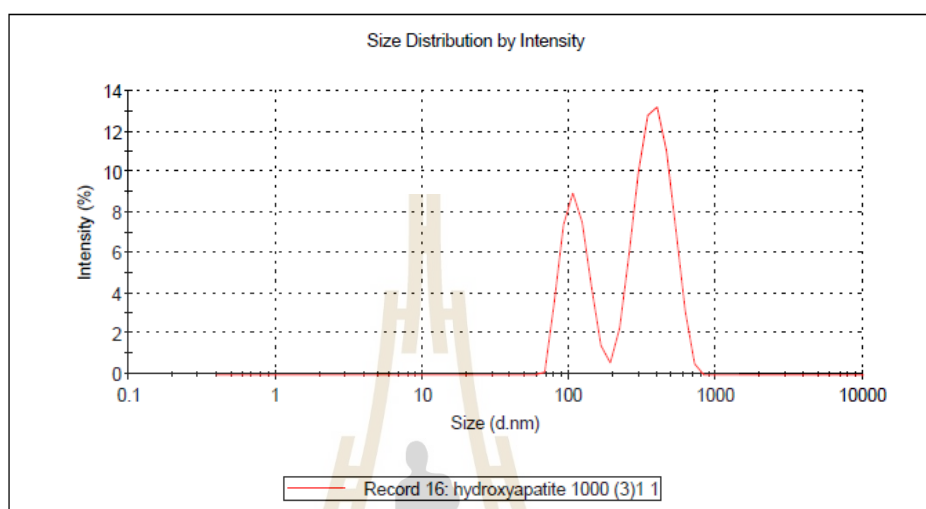


Figure 4.12 Hydrodynamic sizes of HAp nanoparticles at 1,000 mg/L.

Table 4.5 Size and distribution of hydroxyapatite nanoparticles in solutions.

Samples mg/L	Z-Average (d.nm)	PDI (%)	Zeta Potential (mV)	pH	Conductivity mS/cm	Mobility ($\mu\text{mcm}/\text{VS}$)
HA 100	165.6	0.428	-26.4	5.94	0.026	-2.07
HA 500	200.4	0.373	-10.3	6.29	0.132	-0.81
HA 1,000	231.9	0.386	0.34	6.49	0.242	0.026

*PDI (%) = polydispersibility (%), Mobility = electrophoretic, d.nm=diameter in nanometer.

The scattering is related to the hydrodynamic radius (R_h), as in the Stokes–Einstein equation

$$D = kT/6\sqrt{\eta Rh}$$

In the equation, D is diffusion coefficient, k is Boltzmann's constant, T is temperature, η is solvent viscosity, and Rh is the rheodynamic radius of particle solution (Raval et al., 2019). The size distribution range of the particles is depicted as polydispersity index (PDI). PDI is a measurement of the heterogeneity of a sample based on size. PDI values have between 0 and 1, where 1 is the highly heterogeneous population and 0 is the highly homogeneous nanoparticle population. This technique also allows for analyzing nanoparticles as to rods shape (Kumar et al., 2017). Our finding showed the z-average size values and polydispersibility of the particles obtained were 165 d.m and 200.4 d.m with a polydispersity index were 0.428 and 0.373 at 100 and 500 mg/L of HAp nanoparticles respectively. While, at 1,000 mg/L the Z-average values obtained were 231 d.nm. These results indicated that a low concentration of HAp nanoparticles is good distribution than a high concentration. Because, it has a smaller hydrodynamic size in solution and the heterogeneity of a sample based on size is low, it caused to agglomerate slowly rate (Following the theory of Brownian motion). On the other hand, the software reported at 1,000 mg/L has a large hydrodynamic size or sedimenting particles were presented is poor distributions due to high concentration, supermolecular complexes and sedimentation can occur rapidly. Larger size complexes were formed by hydrogen bonding between hydroxyl groups and hydrophobic interactions were provided nanoparticles aggregation (Eliaz and Metoki, 2017).

The measurements of Zeta potential (ZP), pH, conductivity, and electrophoretic mobility using ZetaSizer Nano ZS (Malvern) were carried out to test the stability of the particles. Zeta potential (ZP) measurement is the method for the

measurement of the electrostatic potential at the electrical double layer surrounding a nanoparticle in solution. Zeta potential analysis indicates the stability of nanoparticles in colloids and assessing the surface charge of nanoparticles. This technique is a guideline classifying nanoparticle dispersion with zeta potential values of the solution. It was assessed the surface charge potential of nanoparticles by identifying the positive or negative dimensions of particles are moving toward during electrophoresis (Shah et al., 2017). The technique determines the surface charge of nanoparticles in a colloidal solution. Typically, the values are in the range of +100 to -100 mV. And nanoparticles with zeta potential values between -10 and +10 mV are considered approximately neutral, while nanoparticles with zeta potentials of greater than +30 mV or less than -30 mV are considered strongly cationic and strongly anionic, respectively (Uskokovic et al., 2010). Results as Figure 4.13-4.15 showed that the stability is strongly anionic at 100 mg/L compared to the other two concentrations as indicated by the zeta potential was -26.4 showing that the particles were least agglomerated (Figure 4.13).

Results

	Mean (mV)	Area (%)	Width (mV)
Zeta Potential (mV): -26.4	Peak 1: -26.4	100.0	6.52
Zeta Deviation (mV): 6.52	Peak 2: 0.00	0.0	0.00
Conductivity (mS/cm): 0.0267	Peak 3: 0.00	0.0	0.00

Result quality : **Good**

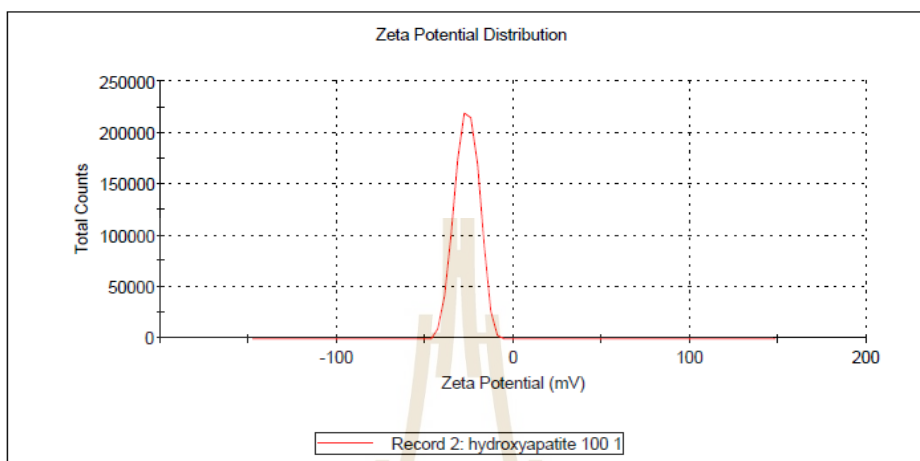


Figure 4.13 Zeta potential at concentration 100 mg of HAp nanoparticles.

Results

	Mean (mV)	Area (%)	Width (mV)
Zeta Potential (mV): -10.3	Peak 1: -10.3	100.0	5.28
Zeta Deviation (mV): 5.28	Peak 2: 0.00	0.0	0.00
Conductivity (mS/cm): 0.132	Peak 3: 0.00	0.0	0.00

Result quality : **Good**

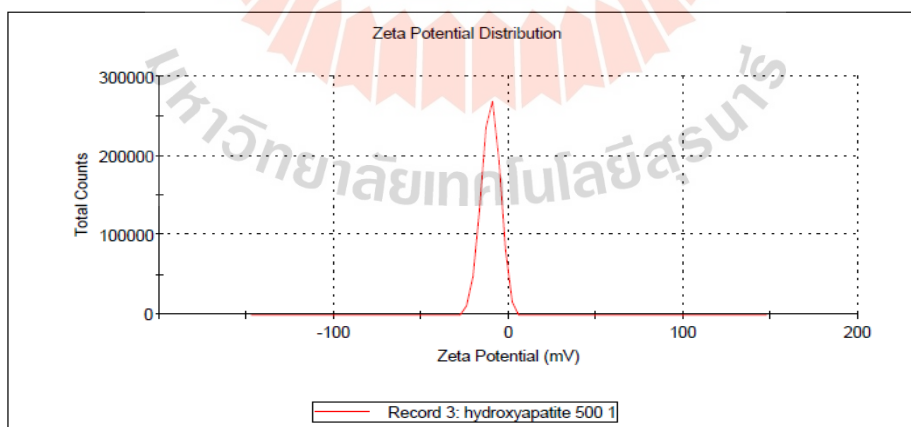


Figure 4.14 Zeta potential at concentration 500 mg of HAp nanoparticles.

Results

	Mean (mV)	Area (%)	Width (mV)
Zeta Potential (mV): 0.340	Peak 1: 0.340	100.0	4.78
Zeta Deviation (mV): 4.78	Peak 2: 0.00	0.0	0.00
Conductivity (mS/cm): 0.242	Peak 3: 0.00	0.0	0.00

Result quality : See result quality report

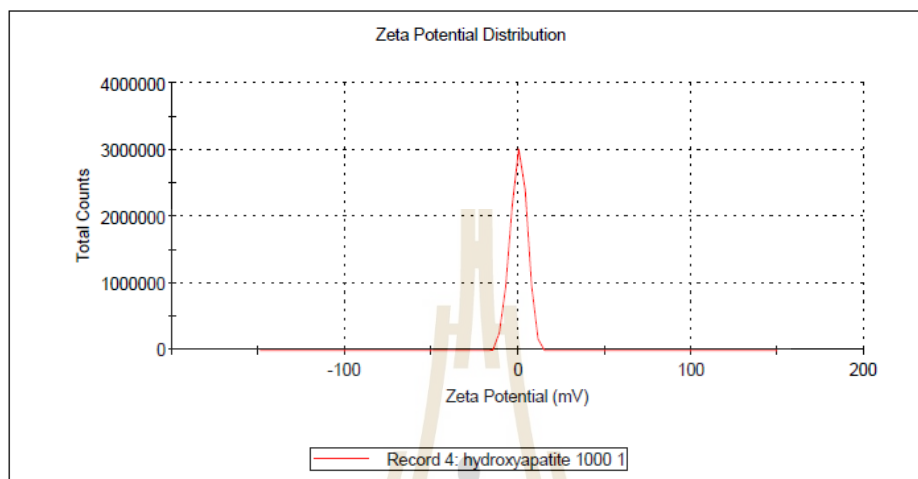


Figure 4.15 Zeta potential at concentration 1,000 mg of HAp nanoparticles.

However, Theory colloid stability depends on the sum of van der Waals attractive forces and electrostatic repulsive forces. The zeta potential provides information on the electrostatic repulsive forces it does not provide any insight on the attractive van der Waals forces (Tadros et al., 2014). Therefore, it is not uncommon to come across stable colloids with low zeta potential at 500 mg/L of HAp nanoparticles was occurred. While, the results at 1,000 mg/L of HAp nanoparticles in colloidal solution has occurred zeta potential 0.34 mV. This concentration provides supramolecular complexes and fast sedimentation due to low stability. Andrade and colleagues (Andrade et al., 2004) describe that the zeta potential into a nearly isoelectric point or 0 value could be caused the van der Waals is low attracting forces. However, the zeta potential only provides indicative evidence towards the nature of the surface charge (positive/negative). While, the pH values and conductivity are

factors relevant for nanoformulations it can change from +ve to -ve and vice versa. The factors of pH and conductivity have affected zeta potential, due to it depends on the concentration of ions in the solution and can be calculated from the ionic strength of the solution (Berg et al., 2009). The results of pH and conductivity at 100 mg/L of HAp nanoparticles confirmed that it had the suitable concentration of the most excellent stability in the solution. pH 5.94, conductivity 0.026 mS/cm and electrophoretic mobility of $-2.07 \mu\text{mcm/VS}$, similarly to Fatehah and colleagues (Fatehah et al., 2014) supported that the low pH values can dissolve nanoparticles increasingly, was $\text{pH} < 6.4$ and $\text{pH} 8.3 < \text{pH} < 10.5$, whereas at pH 6.4 and 9.4, the aggregation has occurred. While, at 1,000 mg/L of HAp nanoparticles in colloidal solution was found aggregation more than other concentrations as shown in Table 4.16-4.18.

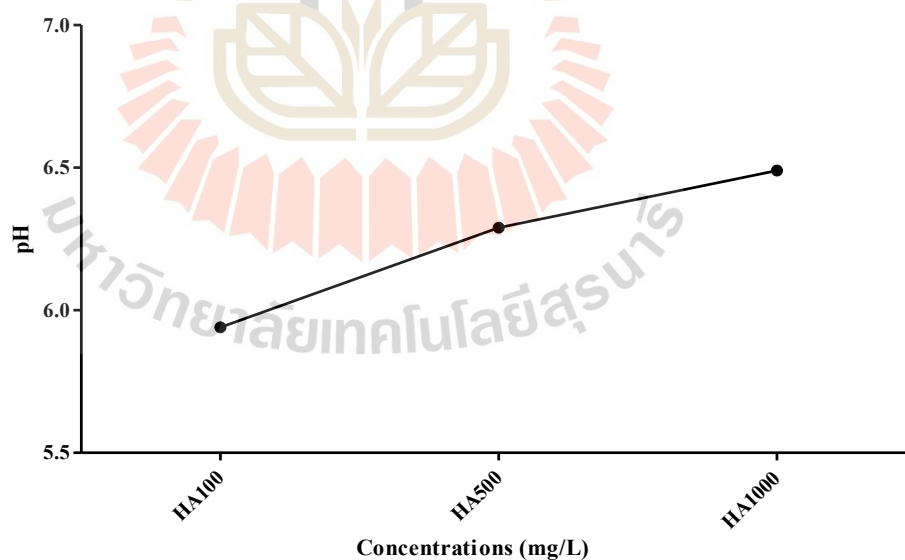


Figure 4.16 pH of HAp nanoparticle in solutions.

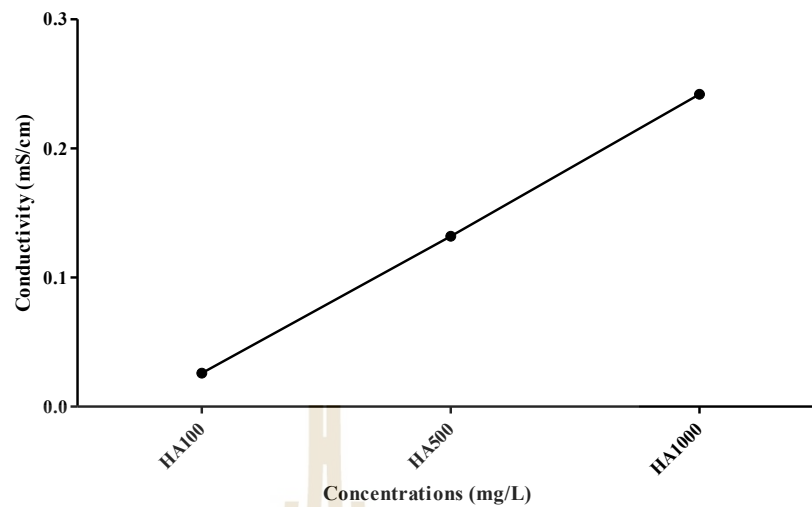


Figure 4.17 Conductivity of HAp nanoparticle in solutions.

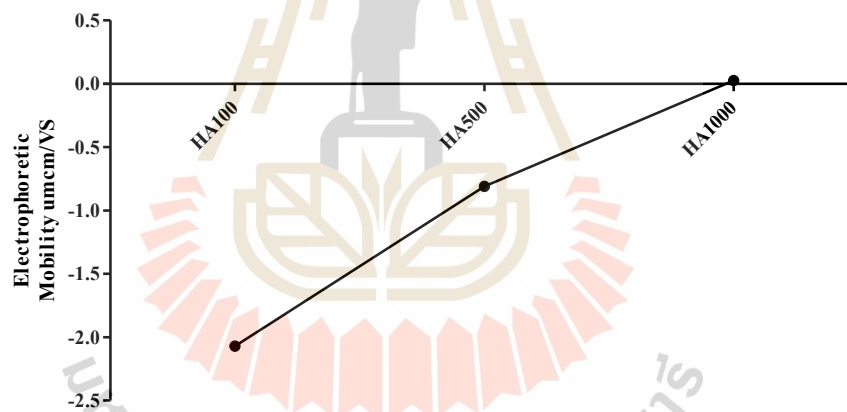


Figure 4.18 Electrophoretic mobility of HAp nanoparticles in solutions.

We concluded that the concentration has influenced the diffusion due to the high concentration of HAp nanoparticles had a good match with the molecule, which causes aggregation. Good diffusion is one of the good fertilizer properties due to plants can uptake the nutrient efficiency, the good size distribution can be controlled-release fertilizer, environmentally friendly. Thus, it can be sustainable

fertilizers in agriculture. The rerelease behavior of phosphorus and calcium is considered to investigate in the next experiment.

4.2.2 Dissolution of HAp nanoparticles

In this study, dissolutions of HAp nanoparticles were analyzed to observe the release of phosphate and calcium in 30 days at various concentrations including 100, 500, and 1,000 mg/L. The dissolution of HAp nanoparticles at low concentrations has been shown to increase in 30 days (Table 4.6). The results showed that 100 mg/L of HAp nanoparticles can increase the released phosphate from 2.31 mg/L on the first day to 3.30 mg/L on day 30 and the release of calcium increased from 2.45 mg/L from the first day to 3.18 mg/L on day 30. Percentages of the increase were 30% and 42% for calcium and phosphate.

Table 4.6 Dissolution of calcium ion (Ca^{2+}) and phosphate (PO_4^{3-}) from HAp nanoparticles in solutions.

Samples mg/L	Calcium ion 1 day mg/L	Calcium ion 30 days mg/L	% increase	Phosphate 1 day mg/L	Phosphate 30 days mg/L	% increase
HA100	2.45	3.18	30	2.31	3.30	42
HA500	5.46	5.31	-2.7	6.97	6.55	-7
HA1,000	5.57	5.59	0	7.35	7.91	7

Our results showed phosphorus and calcium slow-released continuously within 30 days, similar to Kottegoda and colleagues (Kottegoda et al., 2017) reported that the nanohybrid containing HAp nanoparticles decorated with urea in a 6:1 ratio

(urea: HAp nanoparticles) showed significant slow release of nitrogen leading to higher efficiency in releasing for nitrogen for agronomic use. The application of nanoparticles as slow-release is a promising strategy toward enhancing the efficiency of fertilization, complying with the concept of precision agriculture. The slow-releasing of nutrients was supported by its distribution, hydrodynamic size, pH, and conductivity in colloidal solution.

The results from the analyses of size and distribution and dissolution supported that at 100 mg/L HAp nanoparticles can provide greater dissolution and release of Ca^{2+} and PO_4^{3-} than other tested concentrations. There are many factors involved in better dissolution such as small particle size, small hydrodynamic size, pH, conductivity, and the particle rod shape. Misra and colleagues reported that spherical CuO nanoparticles could dissolve significantly higher than rod shapes due to the particle radius in nanoscales (Misra et al., 2012). HAp nanoparticles have rod shapes so they can slowly dissolve and release their component like the results about the slow release of nitrogen of Kottegoda and colleagues (Kottegoda et al., 2017). So, the slow-released nutrient decreases adverse environmental outcomes. Including, the plant can get nutrient efficiency for growth. In this study, we can conclude that at 100 mg of HAp is good distribution, it caused slowly released calcium and phosphate ion continuously. Overall, this study suggested the potential of HAp nanoparticles synthesized from aloe vera extract and sol-gel method had improved the stability nanoparticles in solution, it has property on sustainable fertilizers in agricultural can be releasing phosphate and calcium ion.

4.3 Germination and Seedling Growth

The first physiological process of plant growth is seed germination, beginning with dry seed, water uptake, and ending with radicle protrusion (Li et al., 2014). Measuring the water state is finding the ratio of the fresh weight of plant tissue and turgid weight. Thus, the relative water content was referred to as the plant status investigation technique (Smart, 1974). The relative water content (RWC) measurement followed Gonzalez and Gonzalez-Vilar (2003) formula:

$$\% \text{ RWC} = (\text{FW} - \text{DW}) \times 100 / \text{TW} - \text{DW}$$

Where FW is fresh weight, DW is dry weight and TW is turgid weight. Furthermore, the root and shoot length measurement allowed the investigation of HAp nanoparticles' ability to enhance rice seedling as well as its induction of plant toxicity. This research compared the potential of HAp nanoparticles with commercial fertilizers 18-46-0 and 15-15-15 at 100, 500, and 1,000 mg/L and control treatment (DI water). Germination percentage, relative water content, roots, and shoot length were examined. The data of all parameters are shown in Table 4.7. In this study, we propose that the diffusion coefficient to results has directly affected the release rate

Table 4.7 Effect of HAp nanoparticles and commercial fertilizers at different concentrations on germination, relative water content, root and shoot length.

Treatment	Germination	RWC	Root length	Shoot length
Control	90±3.16 ^{bc}	81.65±1.45 ^{abc}	7.65±0.30 ^{bcde}	4.32±0.26 ^{ab}
HA 100 mg/L	98±2.00 ^c	79.31±0.81 ^{ab}	8.06±0.30 ^{de}	3.97±0.34 ^{ab}
HA 500 mg/L	76±4.00 ^{ab}	79.86±2.69 ^{ab}	8.47±0.33 ^e	4.10±0.36 ^{ab}
HA 1,000 mg/L	74±2.44 ^{ab}	88.73±2.41 ^c	6.50±0.25 ^b	4.40±0.27 ^{ab}
Fertilizer1 100 mg/L	88±4.89 ^{abc}	79.03±2.90 ^{ab}	7.80±0.65 ^{cde}	4.39±0.11 ^{ab}
Fertilizer1 500 mg/L	80±5.47 ^{abc}	80.19±1.33 ^{ab}	6.56±0.27 ^{bc}	4.42±0.18 ^{ab}
Fertilizer1 1,000 mg/L	80±6.32 ^{abc}	81.67±3.65 ^{abc}	3.30±0.21 ^a	4.83±0.35 ^b
Fertilizer2 100 mg/L	76±13.63 ^{ab}	74.83±2.94 ^a	7.03±0.50 ^{bcd}	3.79±0.25 ^a
Fertilizer2 500 mg/L	68±5.83 ^a	82.10±2.11 ^{abc}	4.37±0.52 ^a	4.18±0.05 ^{ab}
Fertilizer2 1,000 mg/L	84±6.78 ^{abc}	82.75±1.87 ^{bc}	4.42±0.46 ^a	4.45±0.41 ^{ab}

Note: Fertilizer 1 = Nitrogen =18, Phosphorus =46, Potassium 0 Fertilizer 2= Nitrogen =15, Phosphorus =15, Potassium 15

The percentage of germination of rice upon exposure to the HAp nanoparticles and commercial fertilizers at various concentrations ranged between 68 to 98%. The results showed that germinating of rice plant was detected to be highest at 100 mg/L HAp nanoparticles. It was 98±2.00%. The lowest germination was observed in treatment at 500 mg of 15-15-15 fertilizer which was 68±5.83%. Germination tended to decrease with increasing concentration of HAp nanoparticles. The germination of the seed exposed to HAp nanoparticles is shown in Figure 4.19.

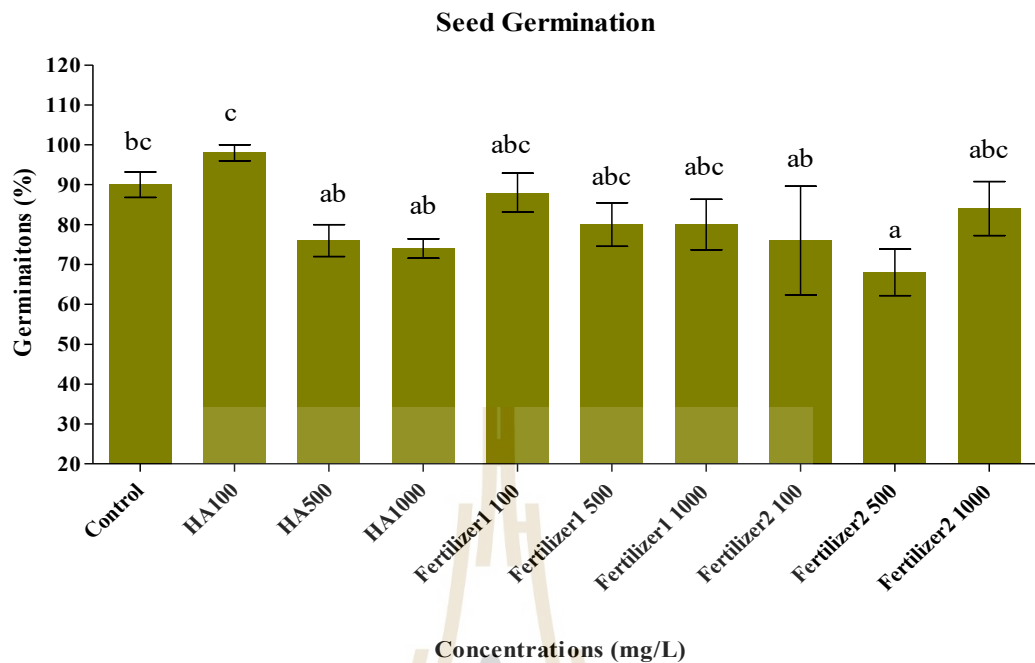


Figure 4.19 Effect of HAp nanoparticles and commercial fertilizers at different concentrations on seed germination.

Our results indicated that concentration at 100 mg/L of HAp nanoparticles has suitable for stimulating seed germination. Due to it has small particles sized can acts uptake and translocation cross biological barriers more efficiently in a plant. In addition, this positive effect could due to the greater bioavailability of phosphorus and calcium to the seed radicals and the high solubility of HAp nanoparticles in suspension. Notably, considering the releasing of phosphorus and calcium and size distribution in solution was supported better stimulating rice germination. This study is similar to Pradhan and colleagues (Pradhan et al., 2021) studied. Urea doped hydroxyapatite nanoparticles and found that they could promote rice seed germination. In contrast, a high concentration of the particles decreased the germination of rate. Jiang described that a high concentration of nanoparticles may

lead to aggregation of particles, which were unable to pass the protection that covered the seeds (Jiang et al., 2018).

On the other hand, the report of (Marchiol, 2019) showed the germination percentage was not influenced by concentration increasing of CMC nHA (200-2000 mg/L). Khodakovskaya supported that carbon nanotubes (CNTs) can penetrate tomato seeds and affect their germination and growth rates. The germination was found to be dramatically higher for seeds that germinated on a medium containing CNTs (10–40 $\mu\text{g/mL}$) compared to control. Analytical methods indicated that the CNTs can penetrate the thick seed coat and support water uptake inside seeds, a process that can affect seed germination and growth of tomato seedlings. In addition, it well knows that calcium and phosphorus could uptake into the seed coat and exert a helpful effect on the process of seed germination (Khodakovskaya et al., 2009).

In addition, some reports are showing that nanoparticles have positive effects on seed germination. Some nanoparticles have inhibited germination in the seedling. However, these effects depend on the nanoparticle's physical-chemical properties such as size, zeta potential, and concentration (Jiang et al., 2018). At 100 mg/L of HAp, this concentration is a good distribution, and a surface charge is highly negatively charged. Positively or negatively charged nanoparticle properties can be taken up by the leaves and translocate to the roots (Sun et al., 2019). Su and colleagues reported that negatively charged nanoparticles can up by the roots than positive charges, due to positive charges induce the production of mucilage, which prevents their uptake by plants. However, a complete understanding of the dynamics of plant-nanoparticle interaction is still not clear (Su et al., 2019).

We do not have data to directly support the hypothetical mechanism for the stimulation of rice seed germination by HAp nanoparticles. But it is a well-known fact that phosphorus and calcium are essentially required for plant growth and their ions play an important role in the activation of enzymes involved in seed germination. With more water absorbed, gibberellin acid (GA) could be better solubilized in the embryo and got transported to seed tissue and aleuronic cytoplasm. GA serves to generate the amylase enzyme. Further, the amylase enzyme hydrolyses the seed starch into sugars and supplies energy to the seed cells required for germination. By nanoparticles can help to increase the level of nitrate reeducated in embryos. It is enhancing the seeds' ability to absorb and utilize water and other nutrients thereby promoting seed antioxidant systems and seed germination. In addition, nanoparticles help in the reduction of the antioxidant stress by reducing ROS, which enhances the activities of key enzymes involved in seed germination (Maarouf-Bouteau et al., 2008). The possible reason for such a beneficial role is the increase in activity of growth hormone gibberellins. As HAp nanoparticles are found to be biocompatible they may be used as nano fertilizer (Shinde et al., 2020).

Water is one of the most important factors to plant growth and productivity. Plants retain less than 5% of the water absorbed by roots for cell expansion and plant growth. The remainder passes through plants directly into the atmosphere, a process referred to as transpiration. Relative water content (RWC) was used as a measure of plant leaf water status (Caig and Romagosa, 1991). In this research, relative water content (RWC) was analyzed to understand the impact of HAp nanoparticles on water status in rice plants. According to our RWC results,

1,000 mg/L of HAp nanoparticles affected significantly the water status of rice. The highest RWC of $88.73 \pm 2.41\%$ was attained as shown in Figure 4.20.

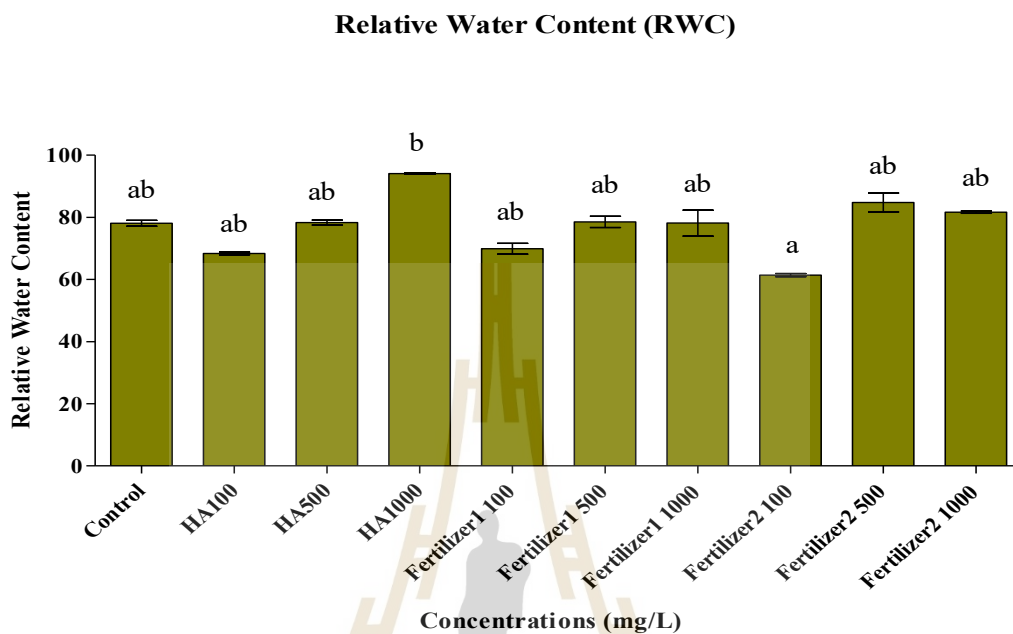


Figure 4.20 Effect of HAp nanoparticles and commercial fertilizers at different concentrations on relative water content.

The result of relative water content is correlated with root length because the root acts to absorb nutrients to stimulate the growth of roots and shoots (Kumar et al., 2013). Our results showed the high concentration of HAp (1,000 mg/L) supported uptake of water more than other concentrations significantly. The purpose of this study is consistent with the findings of (Khodakovskaya et al., 2009) mentioned that the nanoparticles might help stimulate water absorption to pass through water channels (aquaporin) into the seed. This study is similar to Mondal has shown that MWCNTs and OMWCNTs enhanced seed germination and plant growth rate of mung bean planted due to increased activity of aquaporin. A plant use water potential to transport water to the leaves so that photosynthesis can take place (Mondal et al.,

2011). Water potential has quantified the tendency of water to move from one area to another due to osmosis, gravity, mechanical pressure, and matrix effects such as capillary action. A common flow of water will move from an area of higher water potential to an area that is lower potential. High concentration has negative water potential, relative to the pure water reference. The water will move from the locus of greater potential (pure water) to the locus of lesser (the solution). This study similar to Patakas and colleagues (Patakas et al., 2002) in that the high concentration has osmotically adjusted by reducing the water potential (resulting in a negative Ψ_w). It led to the passive accumulate of solutes as a consequence of dehydration of cells decreased.

In this research, HAp nanoparticles potential was evaluated the potential of stimulation of the root and shoot length including root morphology were studied. The results demonstrated that HAp nanoparticles at 100 and 500 mg/L increased significantly root length and root length decreased at 1,000 mg/L. While, the shoot length in all HAp treatments was not significantly different ($P < 0.05$) from the other treatments as shown in Table 4.7 and Figure 4.22.

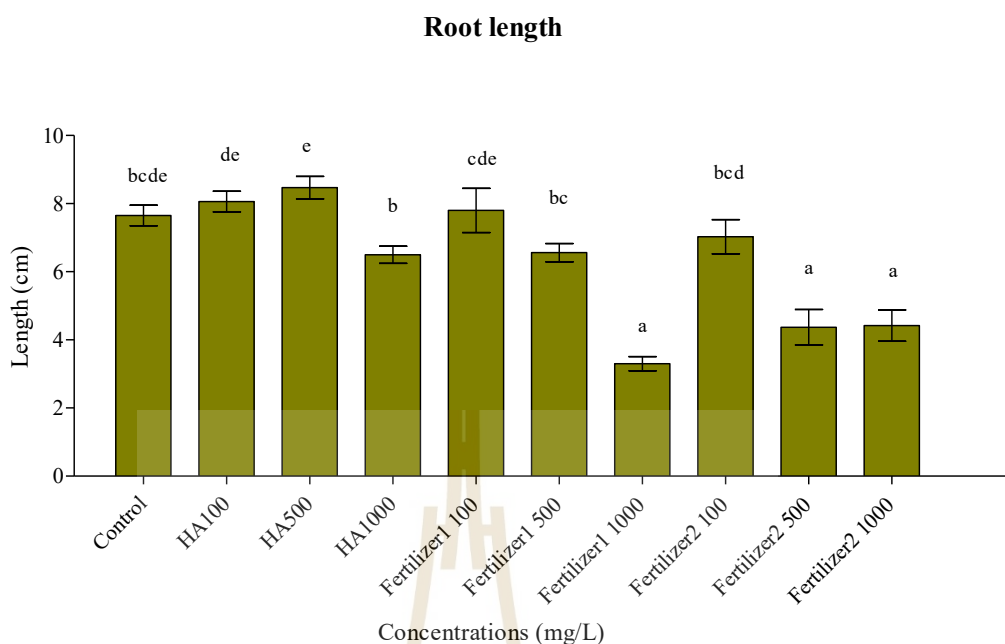


Figure 4.21 Effect of HAp nanoparticles and commercial fertilizers at different concentrations on root length.

We observed a good response of HAp nanoparticles at quite low concentrations (100 and 500 mg/L) over the other treatments, whereas at 1,000 mg/L of HAp was decreased. Similar to results Bala reported that studied the effect of hydroxyapatite nanorod on seed germination and growth of chickpea plant. It was found that the enhancement of both germination rate and plant growth radically (Bala et al., 2020). The plant growth rate's maximum increase was observed in the presence of 1 mg/ml Hap-nanorod where the plant growth rate was more than two times over the control and decreased in 1.5 mg/L of Hap- nanorod. Similar to Marchiol and colleagues who studied HAp nanoparticles solutions stabilized with carboxymethylcellulose (CMC) on root length in *Solanum lycopersicum* L. It was found that 200-2000 mg-1 of HAP can stimulate root length (Marchiol et al., 2019).

Thus, our results indicated that the low concentration has great potential to be used as a nano-fertilizer. Szameitat studied that the mechanistic HAp nanoparticles could penetrate the roots through the apoplast of mature epidermal and cortical cells, and dissolve here due to the acidic environment of the cell wall matrix. Then, the root cap prevents by the mucilage layer surrounding them (Szameitat et al., 2021). Then, HAp nanoparticles gradually dissolve without penetrating deeper cell layers. At a high concentration of 1,000 mg of HAp nanoparticles, the root was inhibited more than the other treatments. It was possible that large particles were formed at high concentration and they adhered on the surface of the root leading to the blocking of the root openings and absorption of nutrients by root was inhibited. These results similar were to Wang and co-worker who studied the effect of HAp nanoparticles on the root length of tomato and cucumber (Wang et al., 2012). It was found that the HAp at 500 and 1,000 mg/L reduced the root length of tomato and cucumber. On other hand, the report of Marchiol and colleagues to study the HAp solutions stabilized with carboxymethylcellulose (CMC) on root elongation it was found that root elongation is strongly stimulated when concentration increasing. Overall, these results provide that HAp has a nontoxic affected on the plant (Marchiol et al., 2019).

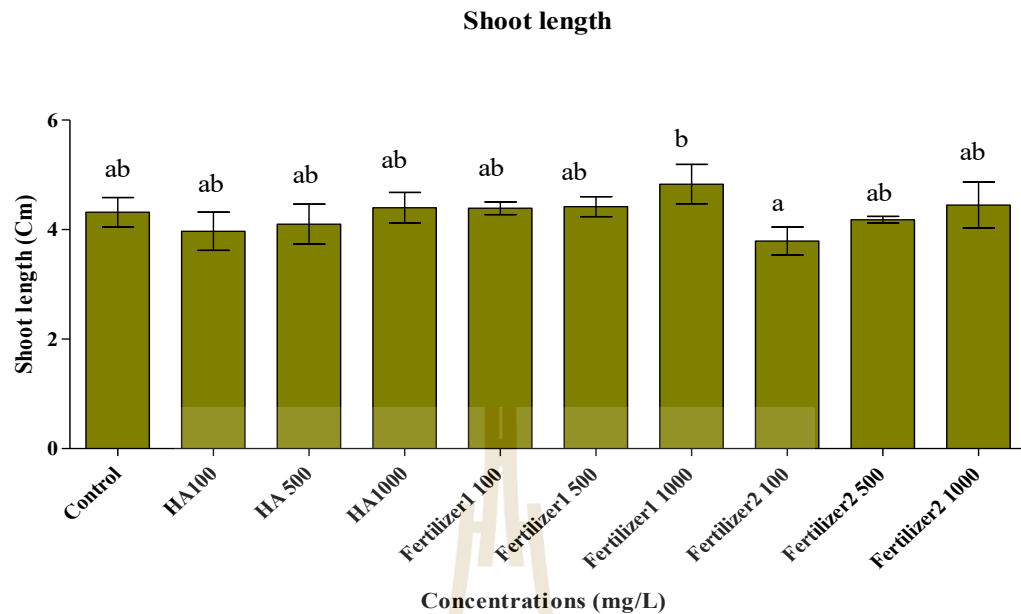


Figure 4.22 Effect of HAp nanoparticles and commercial fertilizers at different concentrations on shoot length.

While 1,000 mg/L of HAp nanoparticles was inhibited root. On the other hand, the results in shoot growth were found HAp nanoparticles did not inhibit shoot growth as shown in Figure 4.22. The shoot length was positively enhanced highest averaged 4.83 at 1,000 mg of commercial fertilizer (18-46-0) and the lowest was found averaged 3.79 cm at 100 mg of commercial fertilizer. These results in appreciably increased changes in shoot length. Especially, at high concentration can be observed that shoots had the stimulated length well. Similar to the findings of Jiang who have reported that HAp nanoparticles were reported to inhibit hypocotyl growth in mung bean sprouts. They found that hypocotyls length reduced in mung bean exposed to nanoparticles at 5 mg/L of concentration. Hypocotyls length decreased from 18.9 cm to 12 cm (Jiang et al., 2014). Nanoparticles penetrate the cell wall and cell membrane of root epidermis accompanied by a complex series of events to enter

the plant vascular bundle (xylem), and move to the stele symplastically, to be translocated to leaves. However, to cross the intact cell membrane, NPs move via pores on the cell membrane, which indicates that uptake of nanomaterial is size-specific (Ma et al., 2010; Rico et al., 2011). Nanoparticles, before reaching the stele, must be integrated passively through the apoplast of the endodermis (Judy, 2013). Xylem serves as the most important vehicle in the distribution and translocation of nanoparticles (Aslani et al., 2014). The cell wall, through which the acquisition of water molecules and other solutes occurs, is usually a porous network of polysaccharide fiber matrices (Carpita et al., 1993).

Thus, to use nanofertilizers efficiently, accurate knowledge of carrier release kinetics is required. At the same time, it is also necessary to know what are the effects produced by the carriers themselves on the plants. In this regard, no systematic studies concerning the effects of HAp nanoparticles on plants have been carried out, so far (Marchiol et al., 2019).

The morphology of roots and shoots is extremely important for the growth and development of plants. In this study, nanoparticles that have affected the changes in morphology were investigated. The morphology of root after having been stimulated in the exposure of HAp nanoparticles and commercial fertilizer 18-46-0 and 15-15-15 for 7 days was observed. HAp nanoparticles treatments led to the development of a greater number of root hairs than did other treatments. 100 and 500 mg/L of HAp nanoparticles treatments more root hairs were observed in (Figure 4.23-4.25). Similar to Ma and co-worker who studied that the response of root hair density on phosphorus (P) availability in *Arabidopsis thaliana* was analyzed starting at 7 days of growth. It was found that the root hair density has highly increased at low

phosphorus availability. The low phosphorus (1 mmol m^{-3}) can increase root hair density about five times greater than in high phosphorus ($1,000 \text{ mmol m}^{-3}$) (Ma et al., 2001). Root hairs are subcellular from the root epidermis which helps the uptake of immobile nutrients such as phosphorus by increasing the absorptive surface area of the root (root hair). It helps to allow the root to explore a greater soil volume. Root hair grows longer may be a strategy for enhanced phosphorus acquisition when phosphorus availability is low. Phosphorus uptake per unit root length is increased with longer root hairs (Bates et al., 1998; Bates et al., 2001). Plants often improve their phosphorus acquisition in soil by changing their root morphology, including root elongation, root axis thinning, and increases in the number and density of root hairs (Linkohr et al., 2002; Miguel et al., 2015).

However, it is not clear how changes in root anatomy are associated with these responses. Some nanoparticles at low can induce root and shoot length, while high concentration can inhibit their growth. These conditions are not depending on all types of nanoparticles due to some nanoparticles at higher concentrations can increase the roots and shoots length. Thus, the plant morphology, seed germination, root and shoot development depend on different factors such as size, reactivity chemical formula, and effective dosages (Talebi et al., 2018).

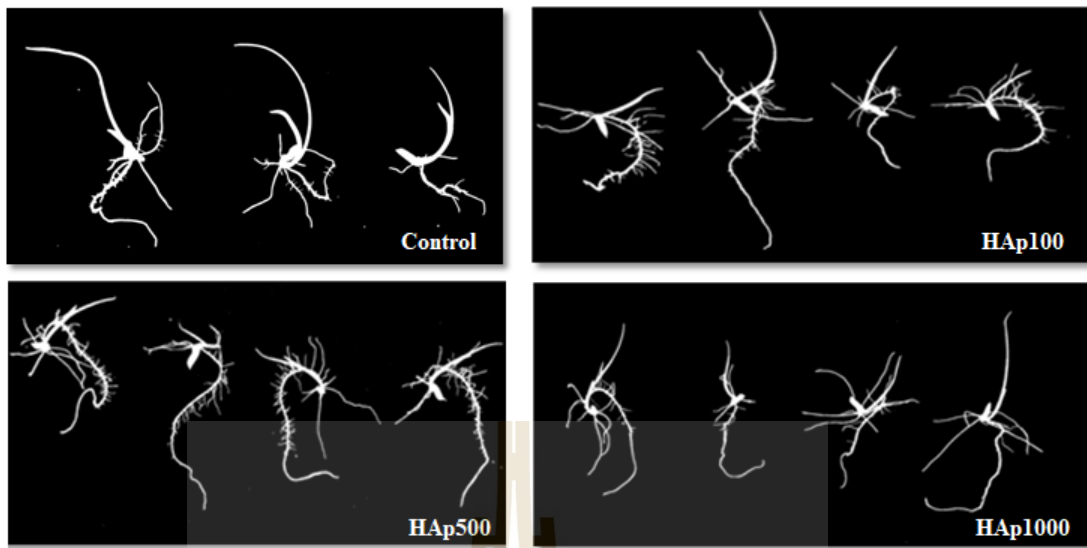


Figure 4.23 Roots of seeds exposed to the control condition and treatments with 100, 500 and 1,000 mg/L.

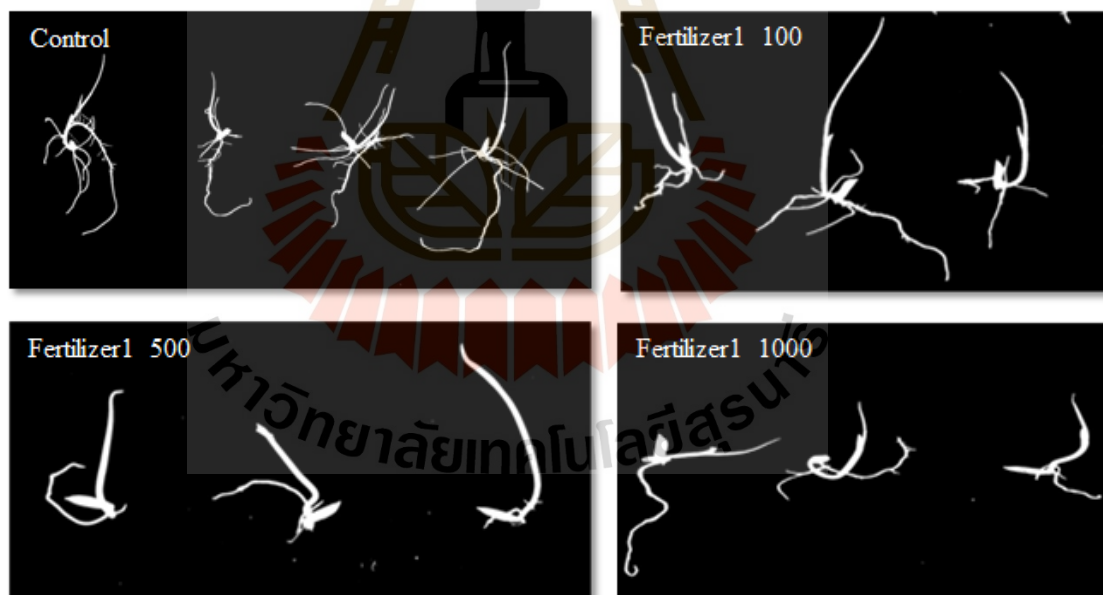


Figure 4.24 Roots of seeds exposed to the commercial fertilizer 18-46-0 at 100, 500 and 1,000 mg/L

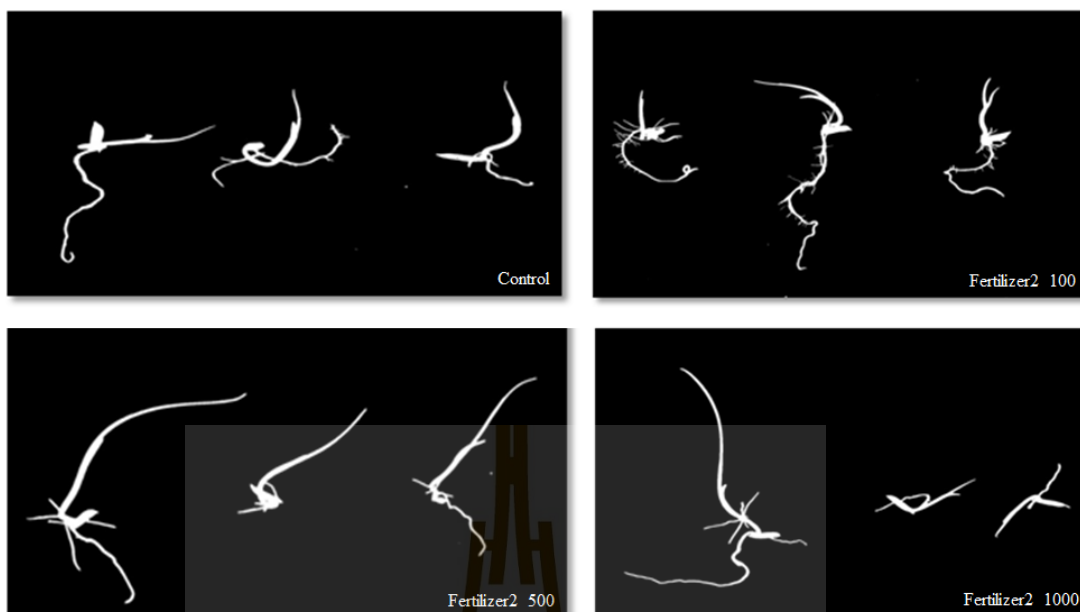


Figure 4.25 Roots of seeds exposed to commercial fertilizer 15-15-15 at 100, 500 and 1,000 mg/L.

4.4 Plant Stress

Lipid peroxidation is processed under oxidants such as free radicals attack lipids containing carbon-carbon double bond(s), especially polyunsaturated fatty acids (PUFAs). The polyunsaturated fatty acids are affected by lipid peroxidation mostly and their decomposition is identified as oxidative damage of the cell. The levels of lipid peroxidation were measured by determining the levels of malondialdehyde (MDA). Malondialdehyde is a product of lipid peroxidation and was assayed by thiobarbituric acid reactive substrate (TBARS) contents using the method of Hodges and colleagues with some modifications (Hodges et al., 1999).

The following formula was applied to calculate malondialdehyde content using UV-Vis spectrophotometer absorption coefficient (ϵ) and expressed as nmol

malondialdehyde g^{-1} fresh mass (FW) following the formula: $\text{MDA (nmol g}^{-1} \text{ FM)} = [(A_{532} - A_{600}) \times V \times 1,000 / \epsilon] \times W$, where ϵ is the specific extinction coefficient ($=155 \text{ mM cm}^{-1}$), V is the volume of the crushing medium, W is the fresh weight of the leaf, A_{600} is the absorbance at 600 nm wavelength, and A_{532} is the absorbance at 532 nm wavelength. The MDA contents in roots of rice seedlings exposed to HAp nanoparticles and commercial fertilizers ranged between 7.50 ± 0.14 to 21.77 ± 0.314 mg/L. The results showed that the highest MDA content of 21.77 ± 0.314 mg/L was detected at 500 mg/L of HAp nanoparticles treatments as shown in Table 4.8 and Figure 4.26.

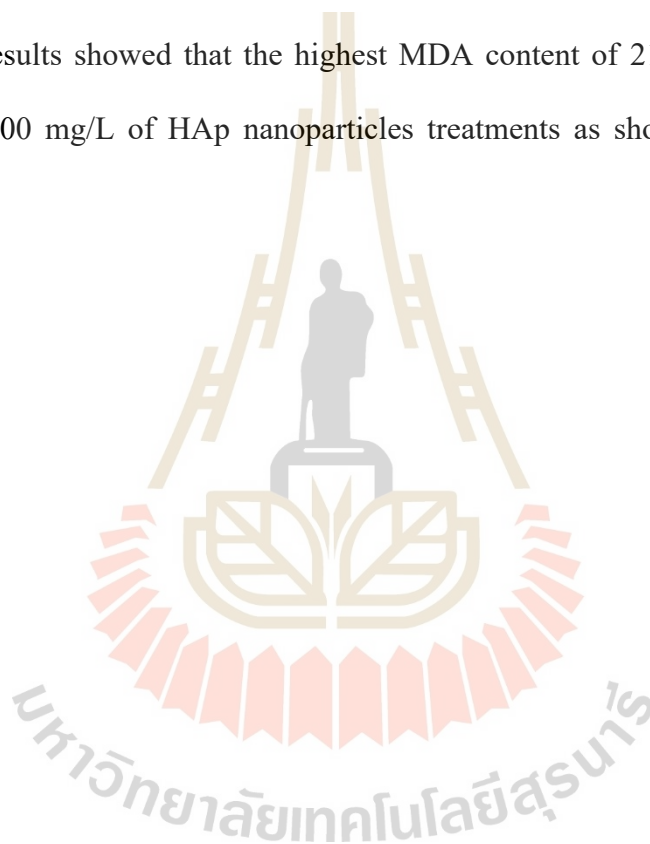


Table 4.8 Effect of HAp nanoparticles and commercial fertilizers at different concentrations at 100, 500, 1,000 mg/L on Malondialdehyde (MDA) and cell death.

Treatments (mg/L)	Malondialdehyde MDA±Std. Error (mg/L)	Cell death ±Std. Error
Control	14.62±0.18 ^e	1.27±0.06 ^c
HA 100 mg/L	15.22±0.57 ^e	1.23±0.03 ^c
HA 500 mg/L	21.77±0.314 ^f	1.25±0.06 ^c
HA 1,000 mg/L	13.96±0.20 ^{de}	1.17±0.03 ^c
Fertilizer1 100 mg/L	12.81±0.14 ^d	0.83±0.01 ^a
Fertilizer1 500 mg/L	7.50±0.14 ^a	0.98±0.02 ^b
Fertilizer1 1,000 mg/L	9.74±0.59 ^b	1.81±0.03 ^d
Fertilizer2 100 mg/L	11.08±0.67 ^c	1.83±0.03 ^d
Fertilizer2 500 mg/L	11.36±0.35 ^c	1.76±0.08 ^{bc}
Fertilizer2 1,000 mg/L	12.75±0.59 ^d	1.89±0.05 ^e

Note: Fertilizer 1 = Nitrogen =18, Phosphorus =46, Potassium 0

Fertilizer 2= Nitrogen =15, Phosphorus =15, Potassium 15

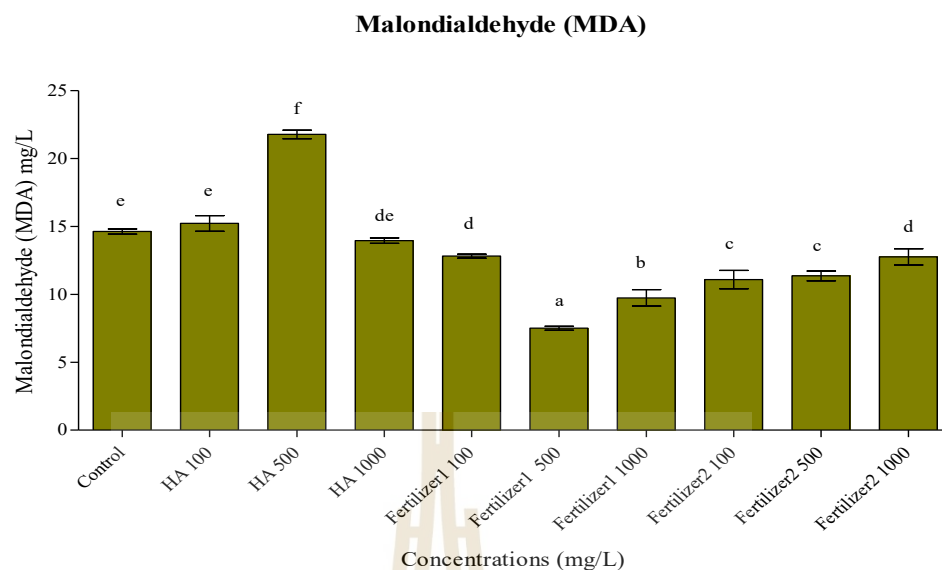


Figure 4.26 Effect of HAp nanoparticles and commercial fertilizer at different concentrations 100, 500, and 1,000 mg/L on malondialdehyde (MDA).

The changes in MDA which is an indicator of lipid peroxidation of plant cells are presented in Figure 4.26. Data clearly show at 500 mg/L of HAp nanoparticles gave a significantly different ($P < 0.05$) MDA level compared to other treatments. Increased production of MDA indicates that the damage biomembrane proteins and phospholipids leading to cell membrane destabilization when plants are subjected to stress this concentration. Rio and colleagues (Rio et al., 2013) and Siddiqui and colleagues (Siddiqui et al., 2015) who observed that nCeO₂ at concentration 62.5, 125, 250 and 500 mg/L can induce the generation of ROS and oxidative damage in *Oryza sativa* L. Similar to Lin and colleagues (Lin et al., 2019) reported that the multiwall carbon nanotubes penetrated through the cell wall of rice and induce phytotoxicity due to oxidative stress. However, Li and co-worker (Li et al., 2014) evaluated the effect of HAp nanoparticles on Cd-induced stress in pakchoi (*Brassica*

Chinensis L.) It was found that HAp nanoparticles can decrease the content of MDA in plant shoots, HAp nanoparticles did not exert a harmful effect on the growth. Similar to our results of cell death, we occurred the results in concentration 500 mg/L of HAp nanoparticles did not increase the level of the cell death as shown in Figure 4.27.

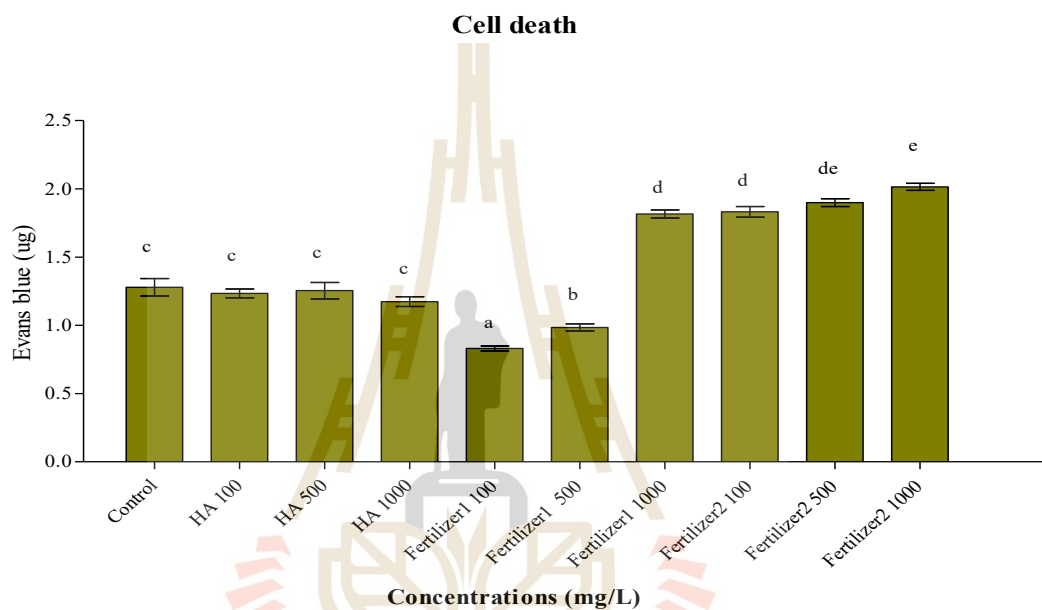


Figure 4.27 Effect of HAp nanoparticles and commercial fertilizer at different concentration 100, 500, and 1,000 mg/L on cell death.

Although, these results showed that 500 mg/L of HAp nanoparticles can stimulate the production of MDA increasing in the cell which is leading to lipid peroxidation, but did not affect cell death and it also can grow and develop in the root. On the other hand, results in the commercial fertilizers at 1,000 mg of (18-46-0) and all treatment of (15-15-15) were found effected to dead more than HAp nanoparticles treatments (Figure 4.27). Our results indicated that the high concentration at 1,000 mg/L of HAp, has the ability of ion absorptions in a plant, did not aggregate in a cell,

it causes to not dead in the cell as shown in Figure 4.31. On the other hand, commercial fertilizer treatments at 1,000 mg of 18-46-0 and all concentrations of 15-15-15 had low concentrations MDA content but finding that its cell was highly damage compared to the HAp and control trial. Nanoparticles can increase toxicity in the plant, it depends on many factors such as the concentration, shape, size, surface features, crystal chemistry (Rico et al., 2015; Tripathi et al., 2016).

Morphology of cell death in root tissue was observed as shown in Figure 4.28-4.33. The membrane is consists of lipids and glycoproteins and acts as a physical, protective barrier. MDA levels associated with oxidative stress can act on membrane lipids to decrease membrane stability. MDA contents cannot be used to assess the instantaneous damage to membranes in plants. We used Evan's blue staining technique to assess cell death or membrane damage for monitoring the plant stress (Vijayaraghavareddy et al., 2017) Cell death evaluations were analyzed by following Zanardo and colleagues (Zanardo et al., 2009), this protocol measured Evans blue stain was released, using a UV spectrophotometer at wavelength 600 nm. Evan's blue is acidic, which stains dead or damaged cells. The dye does not enter live cells with stable membranes (Nv et al., 2017). Thus when plant cells are subject to stress that compromises membrane integrity, the number of cells that are permeated by Evan's blue will be increase compared to control cells that are not stressed. In contrast, live healthy cells that are capable of maintaining membrane integrity do not take up Evan's blue dye. Morphology in cell death of root was presented by microscopes as shown in Figure 4.28-4.33. The amount of cells that are stained with Evan's blue dye under various conditions can be used as an indicator of cellular stress. Our results

could conclude that a high concentration of HAp did not toxicity in root tissue and its can growth in the seedling.

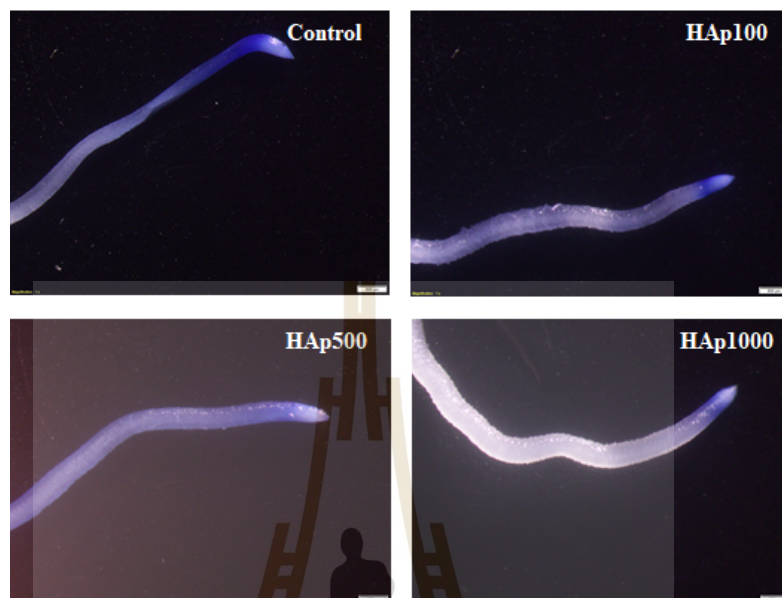


Figure 4.28 Cell death of root in control (DI water) and HAp nanoparticles at 100, 500, and 1,000 mg/L.

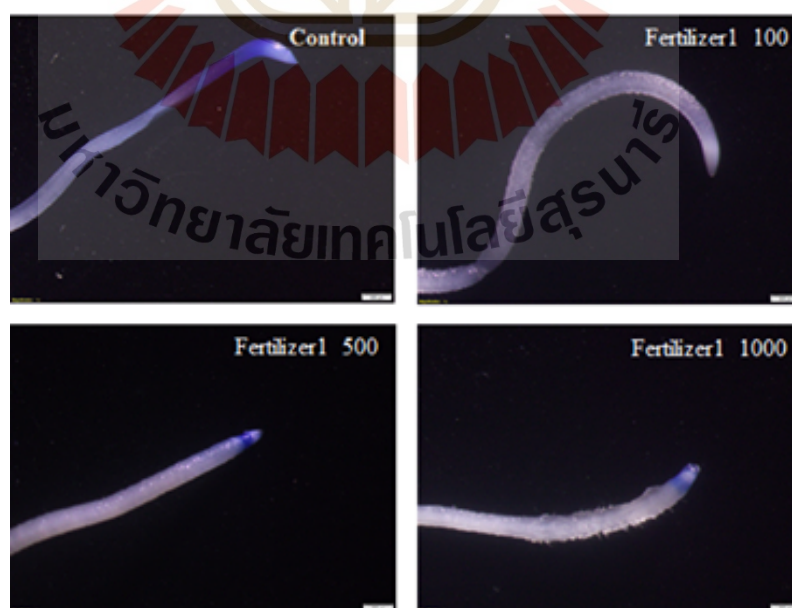


Figure 4.29 Cell death of root in commercial fertilizer1 18-46-0 at 100, 500, and 1,000 mg/L.

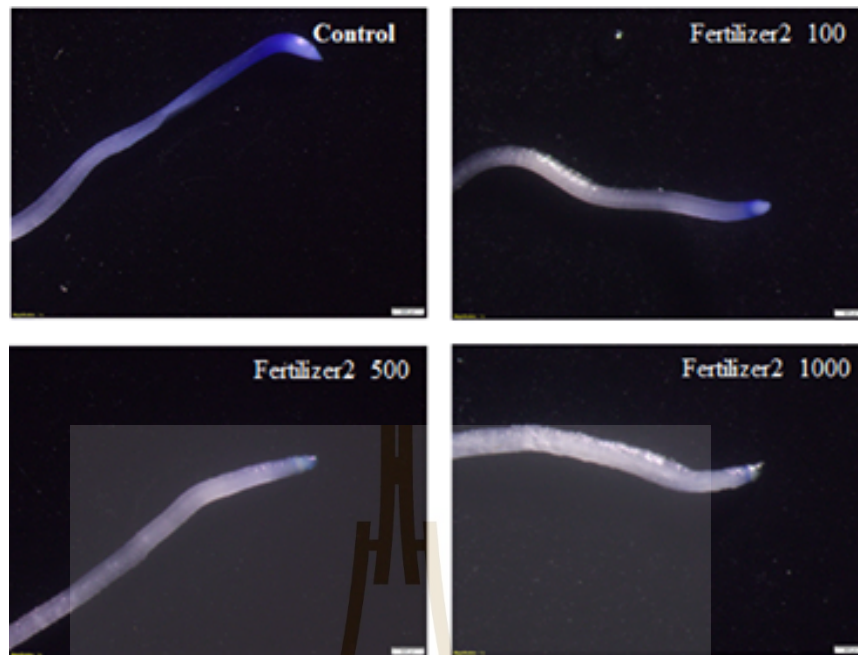


Figure 4.30 Cell death of root in commercial fertilizer1 15-15-15 at 100, 500, and 1,000 mg/L.

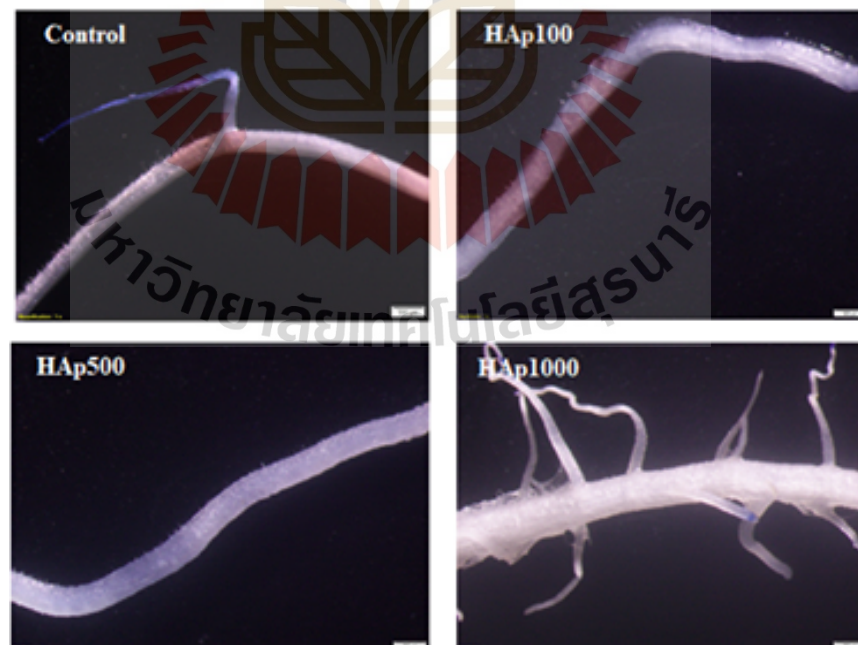


Figure 4.31 Cell death of root in control and HAp nanoparticles at 100, 500, and 1,000 mg/L.

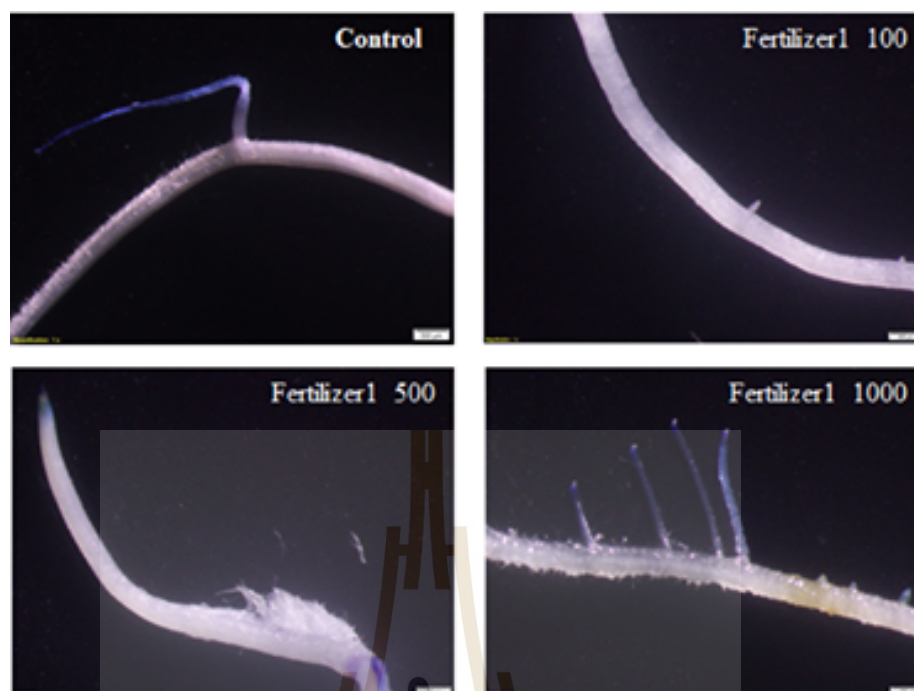


Figure 4.32 Cell death of root in commercial fertilizer1 (18-46-0) at 100, 500, and 1,000 mg/L.

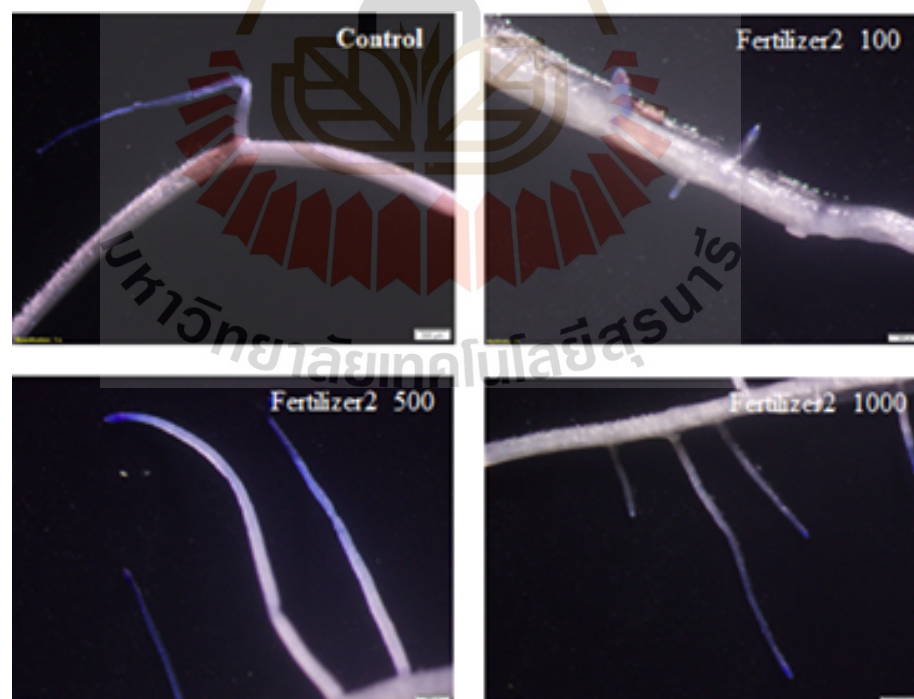


Figure 4.33 Cell death of root in commercial fertilizer 2 (15-15-15) at 100, 500, and 1,000 mg/L.

4.5 Growth

Phosphorus is considered one of the essential elements for plant nutrition. Plants need phosphorus for growth. Phosphorus stimulates the root development of the young plant, increasing its ability to absorb other nutrients from the soil. Phosphorus is related to the photosynthetic energy process, it is the metabolism of carbohydrates that are stored in phosphate compounds such as ATP and ADP for later use in growth and reproduction (Badawi et al., 2017). In addition, phosphorus is related to help plant growth such as in flower, pollination, seeding, and strengthening of stems, root germination, synthesis of proteins, fats, and various carbohydrates (Marschner et al., 1995; Hawkesford et al., 2012). The growth of the rice plant is divided into three phases such as the vegetative phase which runs from germination to panicle initiation, the reproductive stage which runs from panicle initiation to flowering, and the ripening phase which runs from flowering to maturity as shown in Figure 4.34.

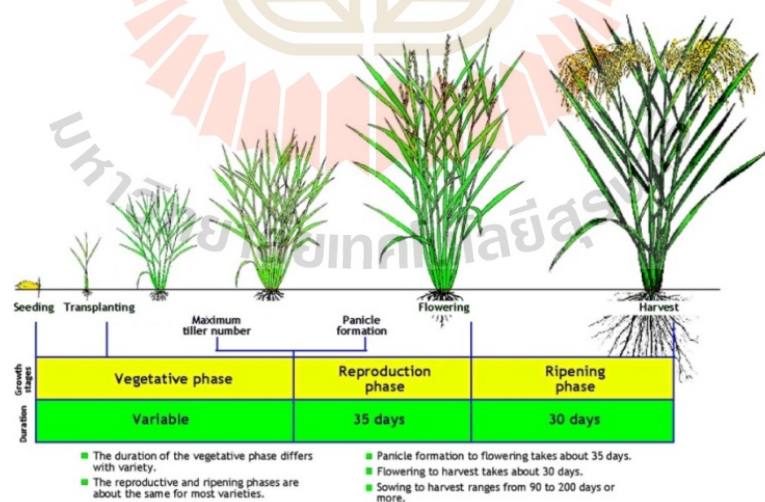


Figure 4.34 Growth phases and stages in rice plant (International Rice Research Institute; IRRI).

The growth of rice in response to HAp in the soil was investigated. Height, leaf width, number of panicles, and number of grains per panicle were measured as indicators for vegetative growth (Figure 4.35). HAp nanoparticles were used in the treatments in comparison with commercial fertilizers with formula 18-46-0 and 15-15-15 at 100, 500, and 1,000 mg/kg in soil. The commercial fertilizers were without calcium. The nutrients included were nitrogen; phosphorus and potassium. The soil used was Suranaree University. It consisted of phosphorus 250000 ppm and potassium 1400 ppm. The number of panicle and the grains per panicle were recorded in 130 days as shown in Figure 4.36.

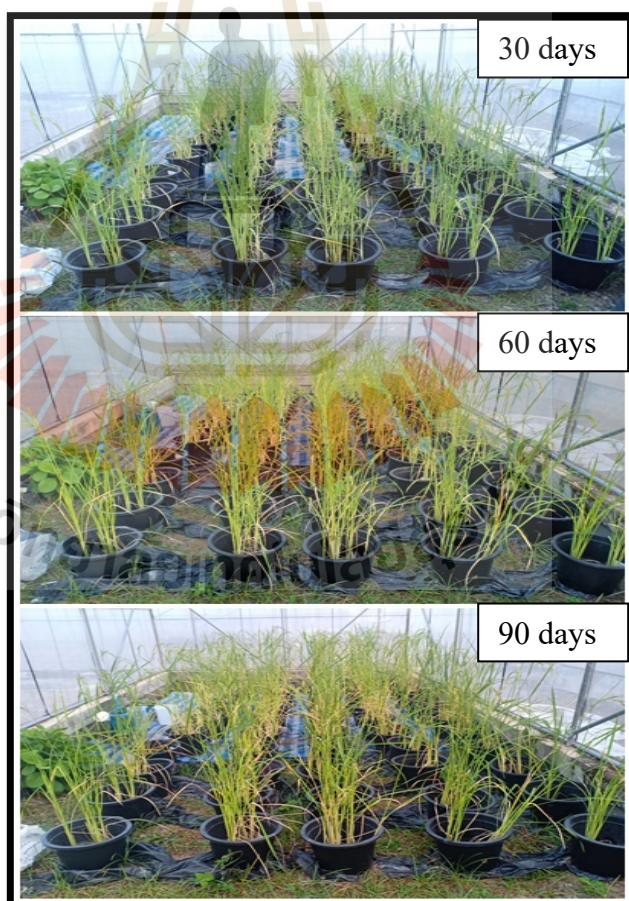


Figure 4.35 Physiology of rice after 35, 60, and 90 days.

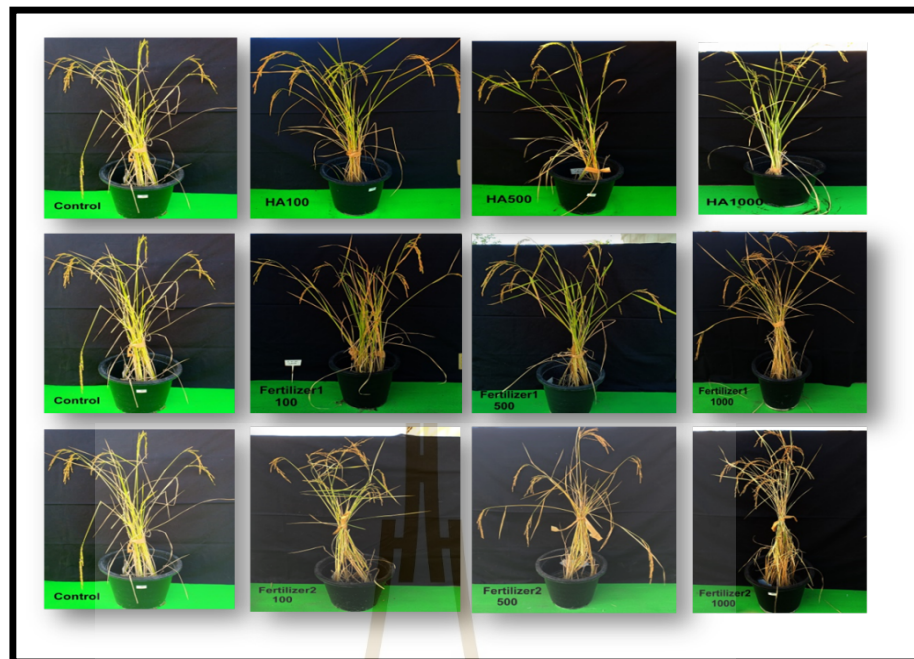


Figure 4.36 Physiology of rice after 130 days.

The rice plants were exposed to HAp nanoparticles and both commercial fertilizers with soil treatment in different concentrations. The vegetative phase was recorded in 35 days such as height and leaf width length. Height and leaf width was found to be insignificantly different ($P < 0.05$) in all treatments (Table 4.9 and Figure 4.37-4.38). Similar to Ye and colleagues (Ye et al., 2019) was found that the phosphorus application had no significant effect on plant height and flag leaf width. Phosphorus is essential for the production and functioning of the photosynthetic apparatus (Hammond and White, 2011). Phosphorus deficiency may be reduced leaf expansion. In addition, it has impacted root and plant growth and development including the role of photosynthesis decreasing.

Table 4.9 Height and leaf width, number of panicle of rice in the experiment.

Treatments (mg/L)	Height of rice (cm)	Width of rice (cm)	No. of panicle per pots
Control	59.71±5.23 ^a	0.57±0.03 ^a	9.2±0.66 ^a
HAp 100 mg	64.45±1.01 ^a	0.54±0.03 ^a	9.4±2.29 ^a
HAp 500 mg	67.40±1.69 ^a	0.61±0.01 ^a	8.4±0.6 ^a
HAp 1,000 mg	64.59±2.31 ^a	0.62±0.03 ^a	8.8±1.11 ^a
Fertilizer1 100 mg	63.73±1.42 ^a	0.58±0.02 ^a	15.0 ±0.7 ^c
Fertilizer1 500 mg	63.70±1.95 ^a	0.57±0.01 ^a	14.0±1.3 ^{bc}
Fertilizer1 1,000 mg	64.57±1.91 ^a	0.59±0.02 ^a	12.0±1.61
Fertilizer2 100 mg	64.00±1.29 ^a	0.59±0.01 ^a	11.20±0.91
Fertilizer2 500 mg	62.93±2.35 ^a	0.58±0.02 ^a	13.80±1.31 ^{bc}
Fertilizer2 1,000 mg	61.29±2.80 ^a	0.57±0.03 ^a	10.60±1.63 ^{ab}

Note: Fertilizer 1 = Nitrogen =18, Phosphorus =46, Potassium 0

Fertilizer 2= Nitrogen =15, Phosphorus =15, Potassium 15

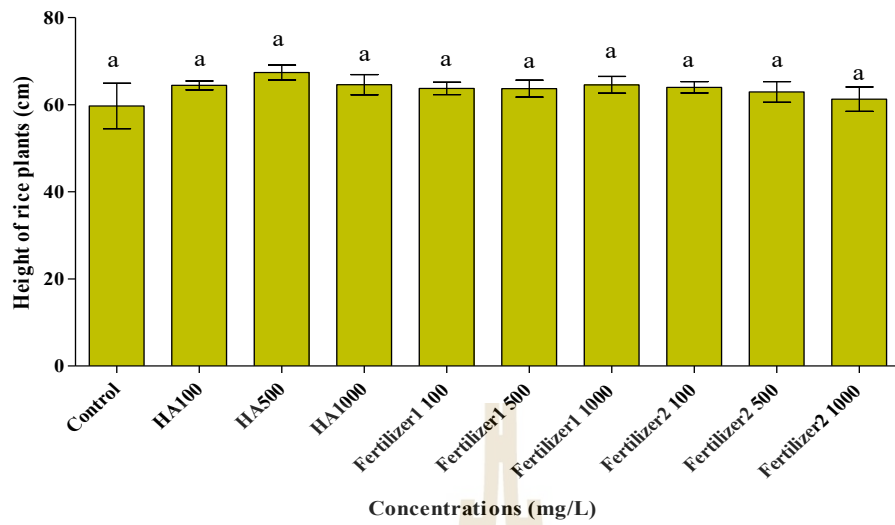


Figure 4.37 Height of rice plants exposed to HAp nanoparticles and commercial fertilizers in soil.

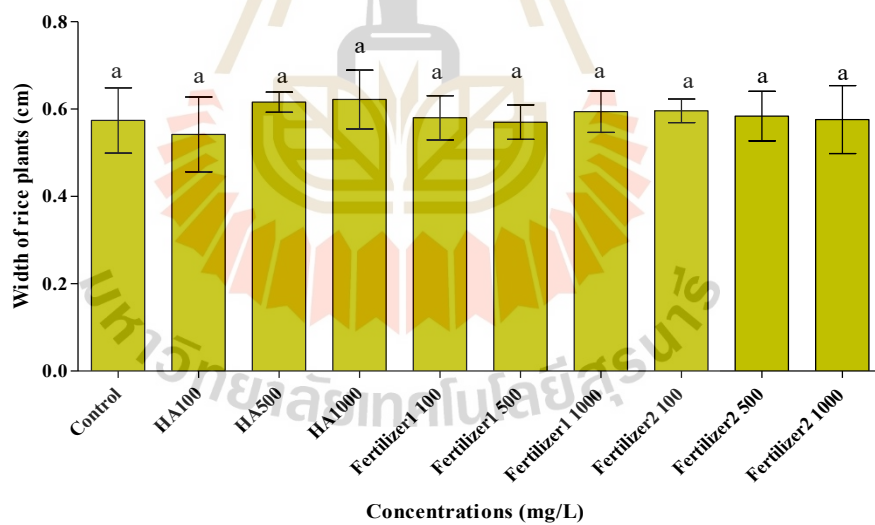


Figure 4.38 Leaf width of rice plants exposed to HAp nanoparticles and commercial fertilizers in soil.

The number of panicles ranged from 8.4 ± 0.6 to 15.0 ± 0.7 as shown in Table 4.9 and Figure 4.39. At 100 mg of commercial fertilizer (18-46-0) was highest, while HAp nanoparticles at 500 mg/L were lowest. It is possible that HAp nanoparticles at the concentrations tested did not provide sufficient phosphate to plants to uptake for early growth; this led to the decreased number of panicles (Figure 4.39). Chang and colleagues demonstrated that the effect of CuO nanoparticles at a concentration of 600 mg/L can inhibit root absorption or clogging the root opening in uptake nutrient. However, there are no detailed photosynthesis and growth studies on the response to the supply of phosphorus in rice (Chang et al., 2012).

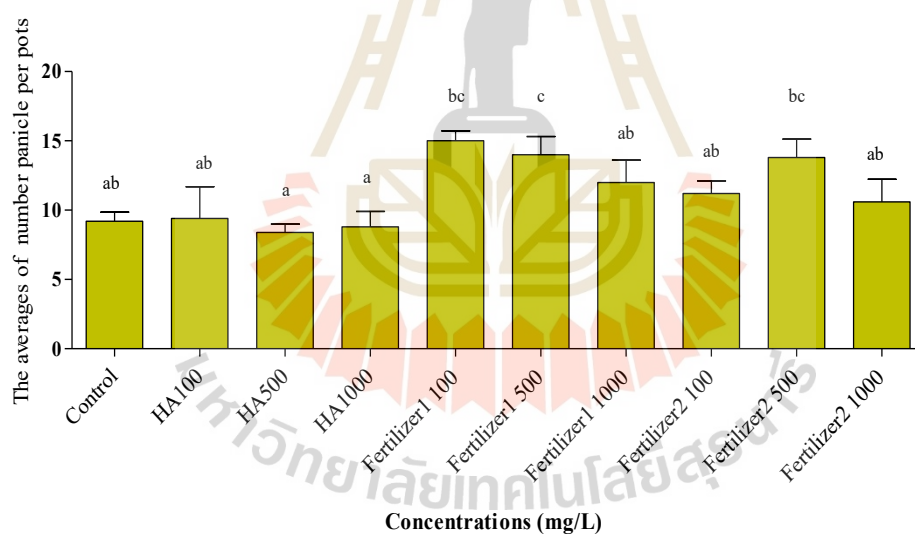


Figure 4.39 The number of panicle exposed to HAp nanoparticles and commercial fertilizers in soil.

The rice plants were exposed to HAp nanoparticles and both commercial fertilizers with soil treatment in different concentrations. The reproductive phase was recorded in 130 days such as the number of grains per panicle, weight 1,000 grains, and weight of grains per pots. At 1,000 mg/L of HAp nanoparticles was found to be significantly different ($P<0.05$) in all treatments (Table 4.10 and Figure 4.40-4.42).

Table 4.10 Weight of 1,000 grains and grains per panicle of rice in the experiments.

Concentrations (mg/L)	No. of grains per panicle	Weight 1,000 grains	Weight of grains per pots
Control	69.26±2.78 ^a	26.23±0.07 ^d	83.58
HA 100 mg	68.08±2.9 ^a	27.41±0.07 ^f	87.71
HA 500 mg	67.87±4.02 ^a	26.29±0.09 ^{de}	74.95
HA 1,000 mg	91.94±6.42 ^b	27.50±0.09 ^f	111.26
Fertilizer1 100 mg	69.20±2.34 ^a	26.62±0.25 ^e	138.19
Fertilizer1 500 mg	67.82±2.81 ^a	25.25±0.11 ^b	119.90
Fertilizer1 1,000 mg	70.66±1.98 ^a	25.30±0.16 ^b	107.28
Fertilizer2 100 mg	68.18±2.34 ^a	25.78±0.15 ^c	98.44
Fertilizer2 500 mg	61.64±3.59 ^a	23.65±0.07 ^a	100.60
Fertilizer2 1,000 mg	65.62±3.0 ^a	23.53±0.06 ^a	81.84

Note: Fertilizer 1 = Nitrogen =18, Phosphorus =46, Potassium 0

Fertilizer 2= Nitrogen =15, Phosphorus =15, Potassium 15

The number of grains per panicle upon exposure to the HAp nanoparticles and commercial fertilizers at various concentrations ranged between 61.64±3.59 to

91.94±6.42 as shown in Table 4.10 and Figure 4.40. HAp nanoparticles at 1,000 mg/L gave the highest value and 500 mg of commercial fertilizer 2 (15-15-15) gave the lowest value. Similarly, Liu and Lal reported that HAp nanoparticles increased the yield of soybean by 20% in comparison with commercial phosphate fertilizer (Liu and Lal, 2014). The number of grains per panicle is determined by variety and stand density. Most California varieties commonly produce 70–100 grains per panicle (Espino et al., 2014)

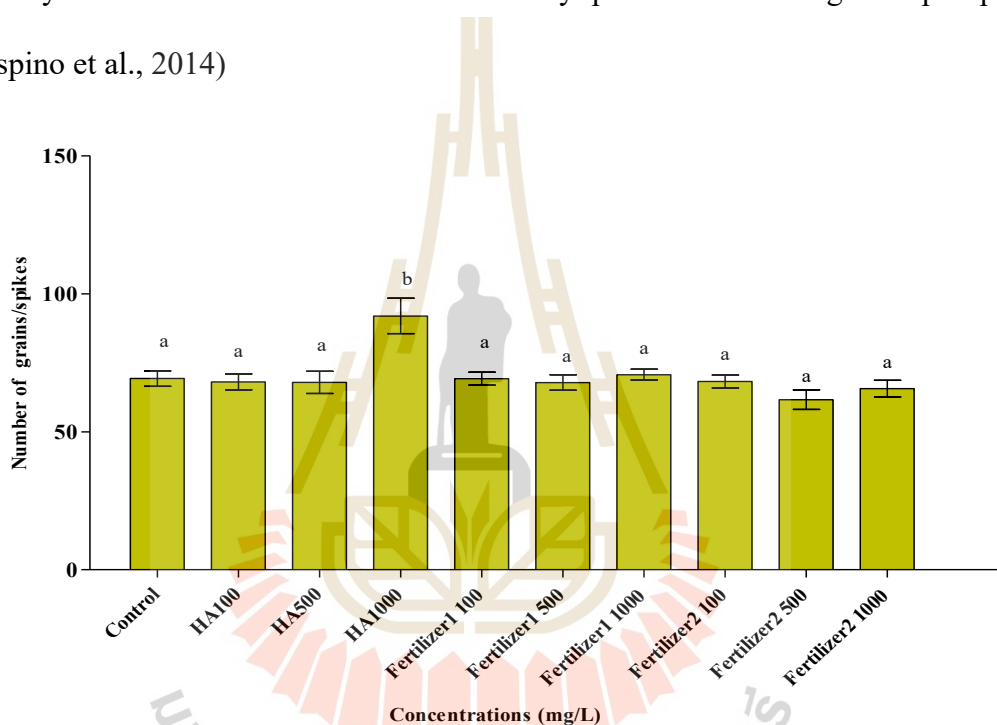


Figure 4.40 Number of grain per panicle of rice exposed to HAp nanoparticles and commercial fertilizers in soil.

The results of the weight of 1,000 grains of rice upon exposure to the HAp nanoparticles and commercial fertilizers ranged between 23 to 27 g (Table 4.10). The weight of 1,000 grain was the highest at 100 mg/L and 1,000 mg/L of HAp nanoparticles giving the values of 27.50±0.09 g and 27.41±0.07 g respectively. The lowest value was 23.53±0.06 g resulted from the treatment with 1,000 mg/L of

commercial fertilizer 2 (15-15-15) observed as shown in Figure 4.41. Standard of the weight of 1,000 grains of rice was 25g (IRRI). Gharib and colleagues studied that the effect of different concentrations of nitrogen at 50, 100, 150, and 200 kg of nitrogen per hectare and foliar application with ascobien for stimulating grain yield of hybrid rice, it was found that 1,000 grain weight were ranged 22-23 g. The weight of 1,000 grains revealed the response of early flowering was induced (Gharib et al., 2011). Lawre and colleagues demonstrated that the influence of zinc oxide nanoparticles on growth and seed productivity in onion. It was found that nanoparticles can increase the number of flowers and seed per umbel, which might be caused by higher seed weight per umbel and 1,000 seed weight (Lawre et al., 2014).

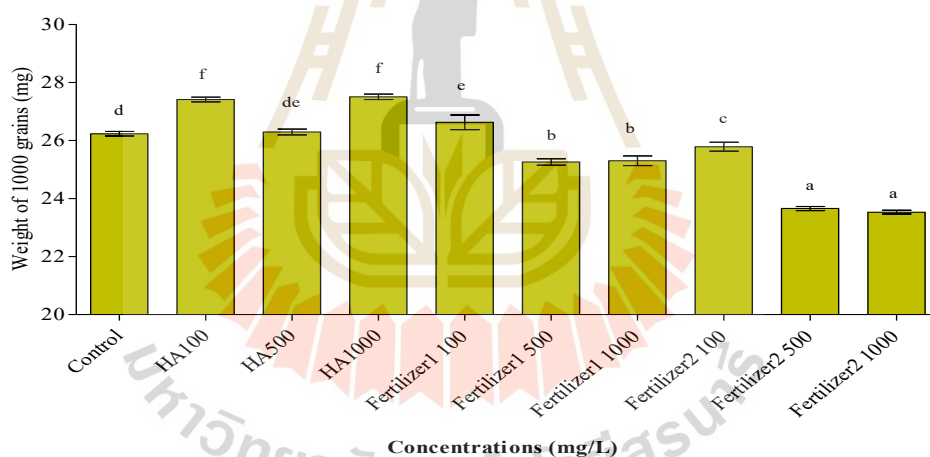


Figure 4.41 Weight of 1,000 grains of rice exposed to HAp nanoparticles and commercial fertilizers.

4.6 Yield Quality

To obtain high yield quality, nanofertilizers practices are essential due to their influence not only on crop yield and weight but also on increasing the seed quality and physiological quality. This study aimed to evaluate the effects of HAp

nanoparticles compared to commercial fertilizer with formula 18-46-0 and 15-15-15 at 100, 500, and 1,000 mg/L were analyzed on grain yield quality such as starch, amylose content, and seed aroma.

4.6.1 Starch in seed

Photosynthesis is the process by which plants convert solar energy into chemical energy, stored in carbohydrates. Starch is a complex carbohydrate, also known as polysaccharides. A polysaccharide is a single sugar molecule that is long chains of sugar glucose molecules linked together like a chain called a monosaccharide. Glucose is a sugar molecule made up of carbon (C), hydrogen (H), and Oxygen (O). The glucose in the starch is in 2 forms as Amylose (water-insoluble) and Amylopectin (water-soluble). In this study, we focused on elemental carbon and oxygen, which are the main elements of starch in seed by using SEM coupled with energy-dispersive X-ray spectroscopy (EDX) was identified (Power et al., 2014). There are reports as Newman and co-worker identified that the basic chemical of starch is $(C_6H_{10}O_5)_n$ consist of carbon, oxygen, and hydrogen, and where “n” is the number molecule present from 300 to 1,000, starch consists of carbon approximately 42.1%, hydrogen was 65% and oxygen 51.4% (Newman et al., 1996).

At 500 mg of HAp nanoparticles in the outer grain (outer layers of pericarp) showed highly of carbon at 68.92% in the seed. However, oxygen was lowest found at 29 weight %. The carbon and oxygen indicated that a carbohydrate molecule was produced from the photosynthesis process. The plant would convert solar energy with the photosynthesis process into chemical energy form to build carbohydrate molecules. This study indicated that HAp can increase the starch in

seed that means carbohydrates increasing, due to carbohydrates are naturally occurring in sugar and starches. Which is a sugar molecule linked together from starches.

Table 4.11 Starch content in seed.

Treatments	Outer layers	
	Carbon weight %	Oxygen weight %
Control	66.71	31.13
HA100 mg/L	66.49	33.11
HA500 mg/L	68.92	29.59
HA1,000 mg/L mg/L	63.73	33.76
Fertilizer1 100 mg/L	61.03	36.38
Fertilizer1 500 mg/L	61.96	33.83
Fertilizer1 1,000 mg/L	56.44	35.10
Fertilizer2 100 mg/L	63.33	33.20
Fertilizer2 500 mg/L	61.43	34.74
Fertilizer2 1,000 mg/L	63.14	31.58

Note: Fertilizer 1 = Nitrogen =18, Phosphorus =46, Potassium 0

Fertilizer 2= Nitrogen =15, Phosphorus =15, Potassium 15

4.6.2 Amylose in seed

Starch consists of two constituents, amylose and amylopectin, which are high molecular weight polymers of D-glucose bound by α -1,4-glycoside linkages. It means that the first and fourth carbon atoms of each glucose molecule are linked to the carbon atoms of a neighboring glucose molecule through an oxygen atom. The amylose content has affected physical and chemical properties such as viscosity, shear

resistance, gelatinization, texture, solubility, tackiness, gel stability, cold swelling, and retrogradation properties of starch. All these properties have high importance in the suitability of the starch of a given crop for various processing and use (Seung et al., 2020). Amylose is considered to be a linear polymer, containing the α -1,4-glycosidic linkages. It contains 300–1,000 glucose molecules. Though there is evidence that amylose is not completely linear, its behavior is that of a linear polymer. Amylose forms an intense blue complex with iodine, with maximum absorption at 660 nm. Pure amylose is considered to have an iodine binding capacity of 20 percent. This iodine coloration is employed as a method to quantify amylose (Juliano et al., 1984). Typically, amylose content, rice is classified as waxy (0-2% amylose), very low amylose content (2-12% amylose), low amylose content (12-20%) intermediate (20-25% amylose) and high (>25 amylose) (Bhattacharya et al., 1982). The amylose content of the Khaodakmali 105 are low amylose content (<19%).

The amylose content upon exposure to the HAp nanoparticles and commercial fertilizers 18-46-0, 15-15-15, and control (DI water) at various concentrations 100, 500, and 1,000 mg/L. The results showed amylose contents all treatment has ranged from 9 to 13% (Table 4.12)

Table 4.12 Amylose content of rice grains from different treatments.

Samples	Absorbance (620 nm)	Amylose content (%)
Control	0.22±0.00 ^d	11.37
HAp100 mg	0.23±0.00 ^e	11.90
HAp 500 mg	0.25±0.00 ^f	12.73
HAp 1,000 mg	0.26±0.00 ^g	13.34
Fertilizer1 100 mg	0.17±0.00 ^a	9.09
Fertilizer1 500 mg	0.26±0.00 ^g	13.34
Fertilizer1 1,000 mg	0.22±0.00 ^d	11.45
Fertilizer2 100 mg	0.19±0.00 ^b	9.96
Fertilizer2 500 mg	0.20±0.00 ^c	10.61
Fertilizer2 1,000 mg	0.25±0.00 ^f	12.80

HAp nanoparticle at 1,000 mg/L was highly 13% and lowest at 100 commercial fertilizers 18-46-0 mg/L was 9%. These results indicated that HAp could increase amylose content in seed. Amylose content is the most important because it determines cooked rice texture. Rice varieties with very low amylose content (10-19%) become very sticky, moist, and tender on cooking, whereas varieties with intermediate amylose content (20-25%) become fluffy, soft, moist, and tender, and those with high amylose content (>25%) become fluffy and dry and harden on cooling. Similar to the reported Thao and colleagues (Thao et al., 2015) study on the effect of nitrogen (N), phosphorus (P), and potassium (K) fertilizers on amylose contents. Results showed the application of phosphorus and potassium has provided higher amylose content more than nitrogen fertilizer. Phosphorus and potassium at 80 ha⁻¹ would be produced the highest amylose level at 20.9%. Jane and co-worker demonstrated about the increasing of amylose content is possible the analysis of the coloration with the IOD

caused by the amount of glucan reacts with iodine and thus a complex compound capable of absorbing light at the analytical wavelength (Jane et al., 1999). As a result, the absorbance is the total sum of the glucan molecules as shown in Figure 4.43. In addition, the difference in the amylose may also be due to the amylose content of HAp nanoparticles was increased which may be since starch is mostly concentrated in the endosperm and less in the bran as shown in Figure 4.44

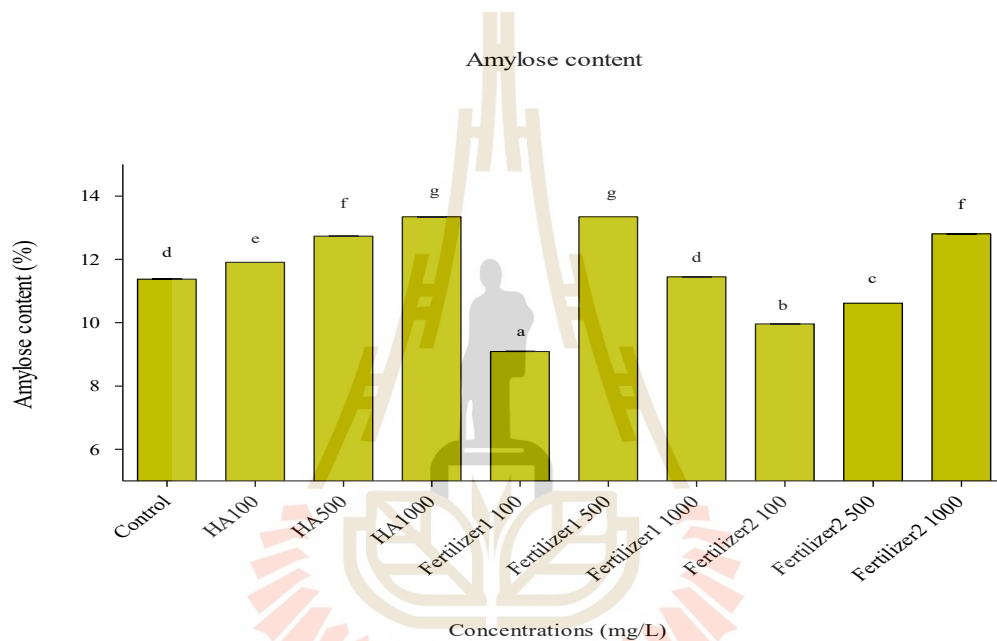


Figure 4.42 Effect of HAp nanoparticles and commercial fertilizer1 (18-46-0) and fertilizer2 (15-15-15) at different concentrations 100, 500, and 1,000 mg/L on amylose content in seed.

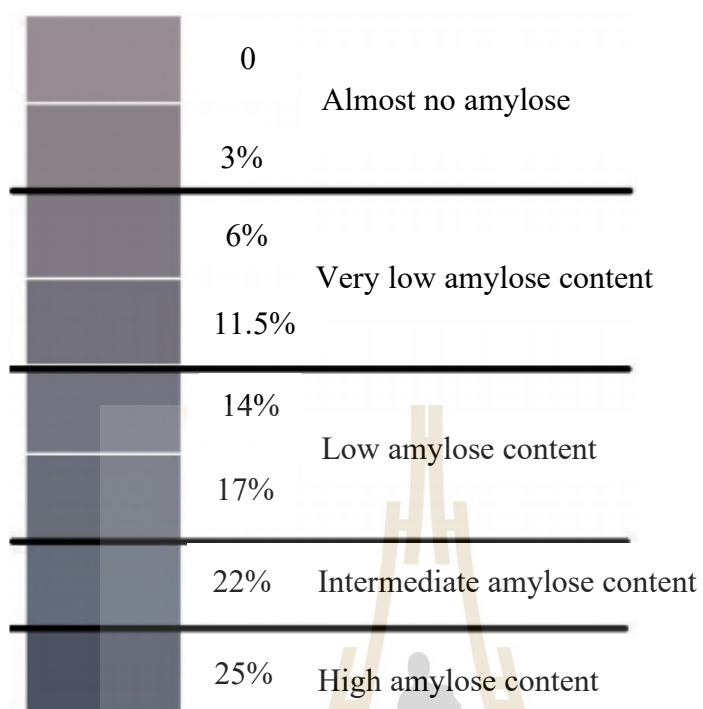


Figure 4.43 Relative color board derived from apparent amylose content characterization.



Figure 4.44 Amylose in seed with the iodine solution.

4.6.3 Acetyl-1-pyrroline in rice grains

Rice is the most important cereal crop and staple food consumed by more than half of the world's population. Rice is classified as aromatic and non-aromatic rice (Singh et al., 2019). Aromatic in rice is one of the most economically important factors. The fragrances has controlled by a major gene *osBadh2* (also recognized as *fgr/badh2/os2-AP/osbadh2,LOC_Os08g0424500*) (Bradbury et al., 2005). The aroma in rice is caused by 2-acetyl-1-pyrroline which is the major fragrant compound. 2-AP contents can be increased due to genetic control, environmental conditions such as climate, production sites, nutrients, and soil conditions. Nonetheless, too much abiotic stress hindered crop productivity and grain quality. Thus, good management practice is important to regulate the aroma quality. This research evaluated the effect of HAp nanoparticles compared with commercial fertilizer 18-46-0 and 15-15-15 at 100, 500, and 1,000 mg/L on 2-AP in the seed. The 2-AP content in rice seeds was measured using gas chromatography (GC) following Sansenya and co-worker (Sansenya et al., 2018). 2- AP content of 43 Thai local Rice Cultivars was studied by Sansenya and co-worker it was found that KDML 105 showed higher than all Thai local rice cultivars. 2-AP content of KDML 105 was 17.60 ug/g, while the local rice cultivar was ranged from 0.09 to 13.47 ug/L of 2-AP content. Our results showed that 2-AP in seed after being treated with HAp nanoparticles and both commercial fertilizers were found to be higher than the control. At 100, 500 and 1,000 mg/L of HAp nanoparticles 2-AP contents were 335.7µg/g, 407.1µg/g, and 396.5µg/g respectively (Table 4.13).

Table 4.13 2-Acetyl-1-Pyrroline (2- AP) in rice seed from different treatments.

Concentration	2 – Acetyl -1-Pyrroline in rice grains	
	2- AP Area	2 AP ($\mu\text{g/g}$)
Control	794	174.4
HA100	1525	335.7
HA500	1855	407.1
HA1,000	1803	396.5
Fertilizer1 100	1047	229.8
Fertilizer1 500	1519	334.4
Fertilizer1 1,000	1323	289.7
Fertilizer2 100	1231	270.9
Fertilizer2 500	1253	275.4
Fertilizer2 1,000	1358	298.4

Our results indicated that HAp nanoparticles at 100, 500, and 1,000 mg/L can increase 2-AP content in the seed of KDML 105 more than control and both commercial fertilizers (18-46-0, 15-15-15). Similar to Monggoot and colleagues studied the effect of some nutrient elements such as N, P, Ca, Zn, Mn, and Mg on 2-AP contents in rice reported that all single elements can increase 2-AP content (Monggoot et al., 2014). In particular, calcium and phosphorus can increase 2-AP by 2 folds more than what nitrogen can do. This indicates that adding a suitable single nutrient element has to enhance the effect on 2-AP production in rice plants. Some reported, Ca play a role in regulating and activating various enzymes in the pathway of 2-AP formation, which may be due to osmotic adjustment by Ca^{2+} related to the functional integrity of secondary messenger's molecule important for 2-AP biosynthesis (Cicek and Cakirlar, 2002). Furthermore, Bhattachary and co-worker

demonstrated that phosphorus might be an active co-factor in enzymes; it led to the activity of several enzymes by phosphorylation to 2-AP synthesis (Bhattacharya et al., 2019). In addition, Salinas suggested that an adequate phosphorus level could enhance proline accumulation in green bean leaves, seeds, roots, and pods (Salinas et al., 2013). Previous reports suggest that the level of 2-AP is related to the level of proline. The proline is one of the amino acids and is the first precursor in the 2-AP synthesis in the biochemical pathway (Yoshihashi et al., 2002). The compound of 2-AP has been synthesized via L-proline metabolism by the protein associated with recessive betaine aldehyde dehydrogenase gene (*badh2*), located on chromosome 8 (Zanan et al., 2014). The *badh2* gene encoding inactive betaine aldehyde dehydrogenase (*BADH2*) activates the synthesis of 2-AP and is only found in fragrant rice (Bradbury et al., 2005 ; Chen et al., 2008). In the biochemical pathway of 2-AP synthesis, when there is a presence of non-functional *BADH2*, the substrate D- aminobutyraldehyde (*GABald*) is converted to form D1- pyrroline and finally acetylated to form 2-AP (Chen et al., 2008). The synthesis and accumulation of 2-AP content in rice have many environmental factors such as drought, salinity, and shading treatments. For example, 2-AP formation increased due to an increase in salt concentration (Gay et al., 2010; (Poonlaphdecha et al., 2012). Moreover, drought stress affects increasing 2-AP concentration in grains during a period of grains formation (Yoshihashi et al., 2004) reported that. Recently, one of the environmental factors, the level of solar radiation from shading treatment, has been studied, where the results showed that 2-AP content in grains of all shading treatments was significantly increased, compared to rice without shading treatment. In addition, Mo and co-worker found that decreasing solar intensity can increase proline content and 2-AP content in rice (Mo et

al., 2015). Furthermore, the gamma ray can reduce grain weigh rice, but it can increase 2-AP content in grain rice higher than non-irradiated rice. Increasing in 2-AP content was observed in irradiated rice grains with 11.62 ug/g⁻¹ to 25.08 ug/g compared to non-irradiated rice grains (8.76 ug/g). Accumulation of metabolites often occurs in plants subjected to stress including various elicitors or signal molecules (Sansenya et al., 2017). In addition, secondary metabolite also contributes to the specific odors, tastes, and colors in the plant (Cicek and Cakirlar, 2002). Normally occurs in the cytosol where it contributes substantially to cytoplasmic osmotic adjustment and is correlated with stress tolerance. However, there are still various enzymes in the biochemical pathway of 2-AP biosynthesis yet to be identified and there has been no explicit explanation about the role of phosphorus and calcium in the process of 2-AP formation, and this is substantially needed to be further studied.

4.6.4 Morphology in seed

Scanning electron microscopy (SEM) proved itself to be a valuable method in the study of the granulate microstructure, surface characteristics of starch and starch granules. The endosperm is the starch-rich component (about 70%) of the cereal seed. It plays an important role in determining the nutritional value of rice through its parts; starch, protein, lipids, and fiber (Kang et al., 2006). The goal of our work is to reveal, by SEM observations of the inner endosperm of grain rice, the surface morphology of starch granules in the endosperm of rice aleurone was studied. All treatments of HAp and commercial fertilizers 18-46-0, 15-15-15, and control (DI water) were shown in Figure 4.45-4.54.

The aleurone layer (AL) is considered as the botanical part of the endosperm, although it is processed as part of the bran that differs in thickness. Which

are usually one to seven cell layers depending on varieties. The aleurone layer is found on the outside of the endosperm and it has protein bodies. It is important for seed development and seed dormancy. Due to it accumulated large quantities of oils, lipids, and mineral stores that are useful during seed development. In addition, it is to help the synthesis and secretion of α -amylase enzymes in the endosperm. The diffusion of gibberellins (GA) in aleurone would be induced the synthesis of the amylase broken down the starchy in endosperm to be used germinate in the growing embryo in the early stages.

Figure 4.45-4.54 shows the aleurone layer and endosperm in rice grain (scanning electron micrographs 15 kV \times 2000 =10 μ m). Rice grown were treated with HAp nanoparticles and commercial fertilizer found that at 500 mg/L of HAp nanoparticles has only one- cell thick and was a degraded cell in the starchy endosperm. In contrast at 100 and 1,000 mg/L of HAp and both commercial fertilizers were observed the multiple cells of aleurone layers. The difference in morphology, which is maybe concerned with chemical intermediate or hormone functions, has not been investigated.

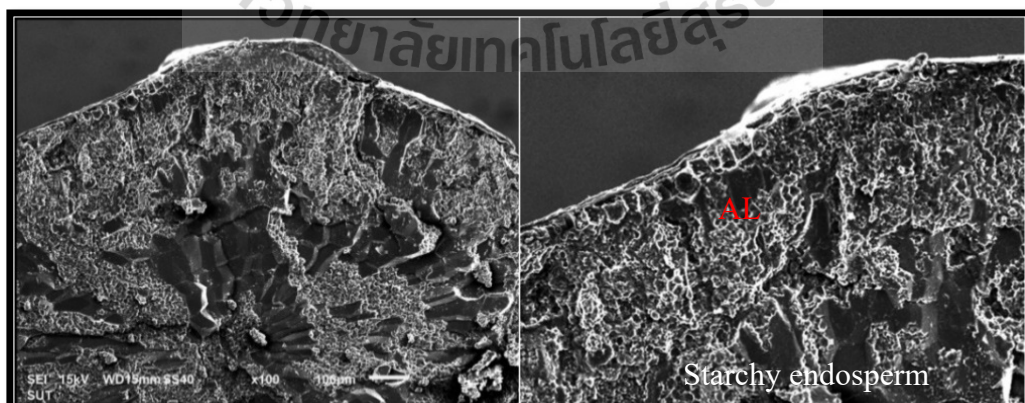


Figure 4.45 Morphology of seed treated in control and aleurone of starch in rice (scanning electron micrographs 15 kV \times 2000 =10 μ m).

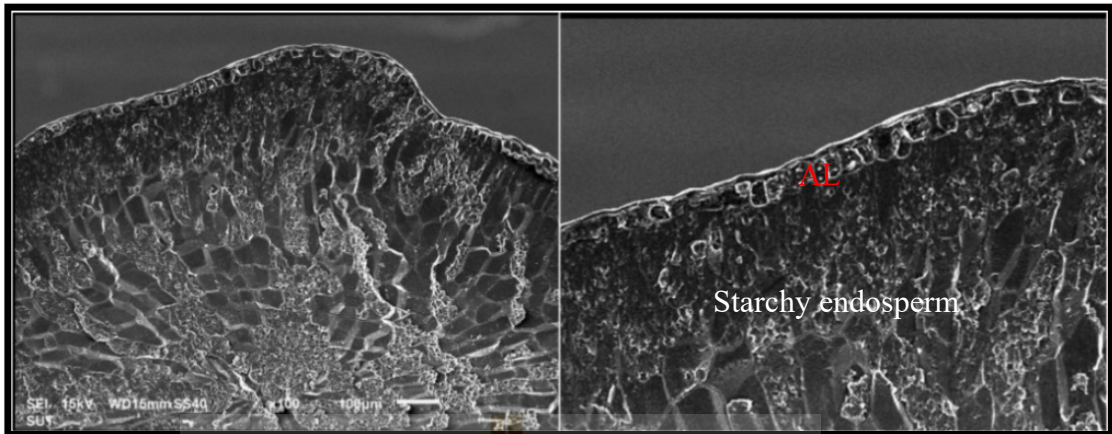


Figure 4.46 Morphology of seed treated in HAp 100 mg and aleurone starch (scanning micrographs 15 kV \times 2000 = 10 μ m).

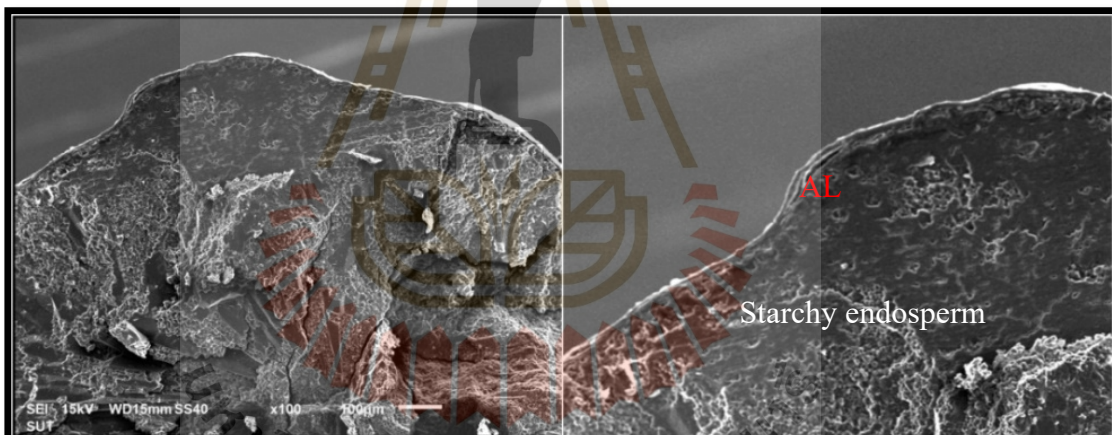


Figure 4.47 Morphology of seed treated in HAp 500 mg and aleurone of starch (scanning electron micrographs 15 kV \times 2000 = 10 μ m).

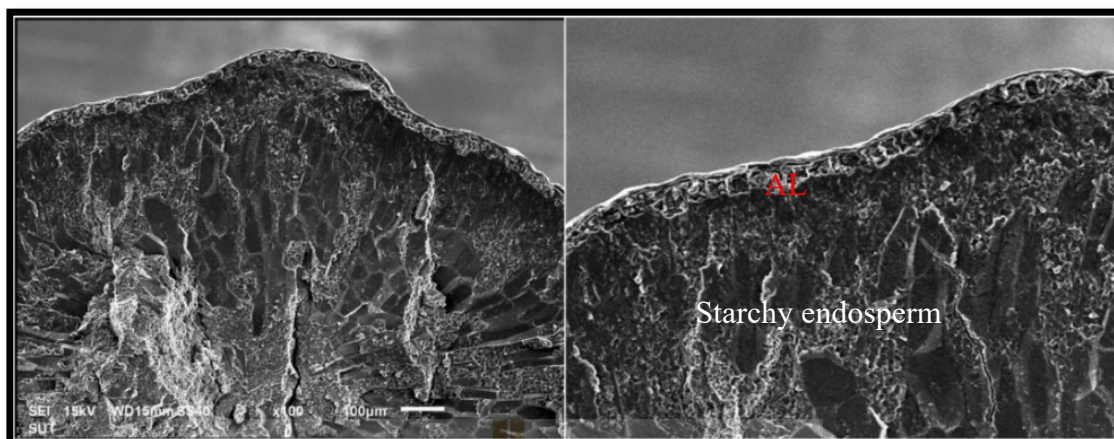


Figure 4.48 Morphology of seed treated in HAp 1,000 mg and aleurone of starch (scanning electron micrographs 15kV×2000=10 μm).

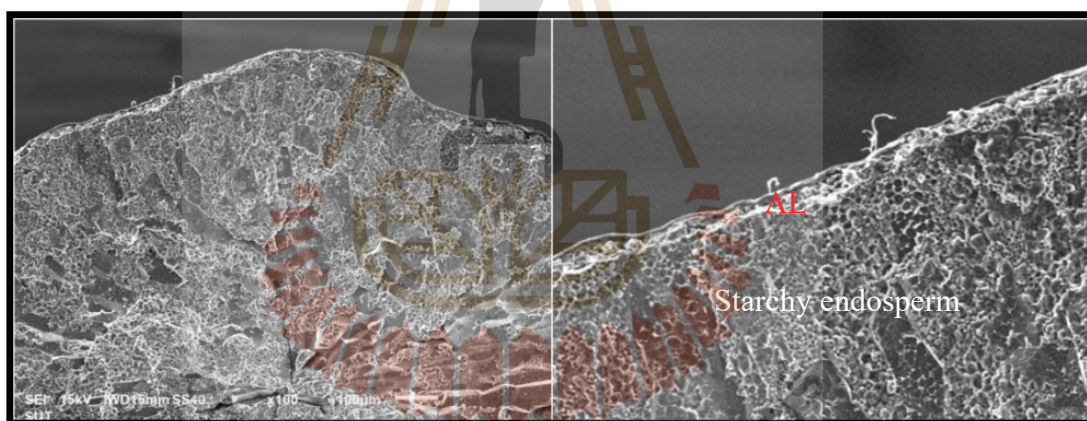


Figure 4.49 Morphology of seed treated in fertilizer I 100 (18-46-0) and aleurone of starch (scanning electron micrographs 15kV×2000=10 μm).

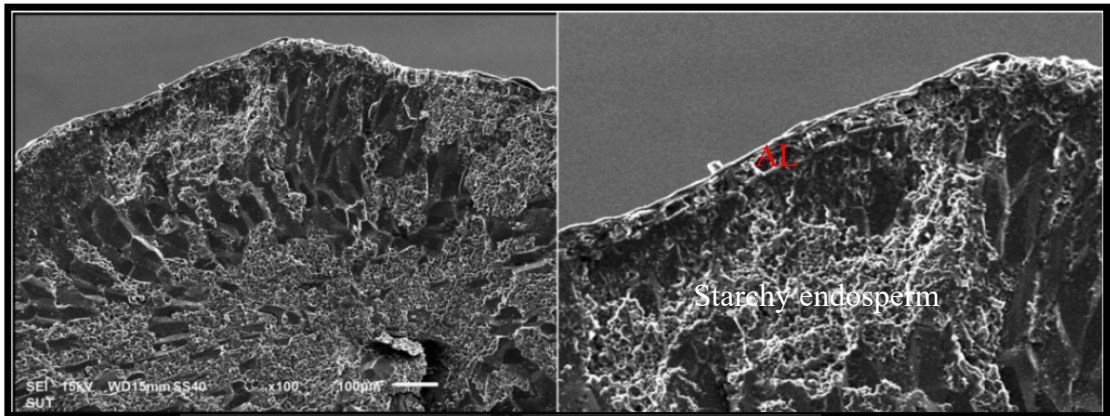


Figure 4.50 Morphology of seed treated in fertilizer 1 500 (18-46-0) and aleurone of starch in rice(scanning electronmicrographs15kV×2000=10µm).

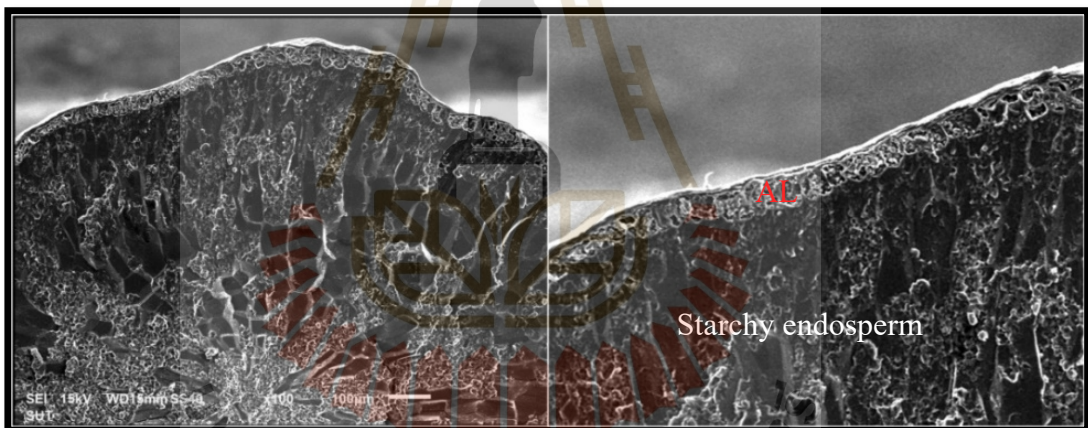


Figure 4.51 Morphology of seed treated in fertilizer 1 1,000 (18-46-0) and aleurone of starch in rice (scanning electronmicrographs15kV×2000=10µm).

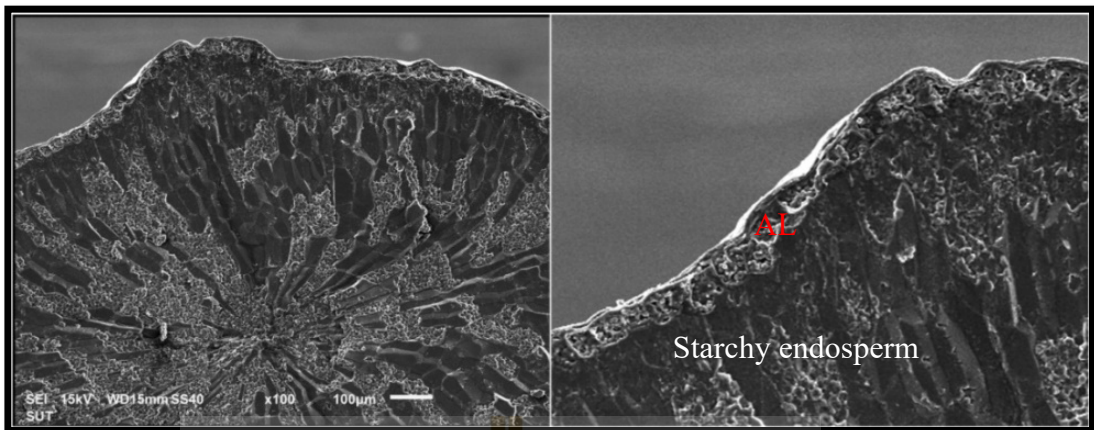


Figure 4.52 Morphology of seed treated in fertilizer 2 100 (18-46-0) and aleurone of starch in rice (scanning electronmicrographs 15kV×2000=10μm).

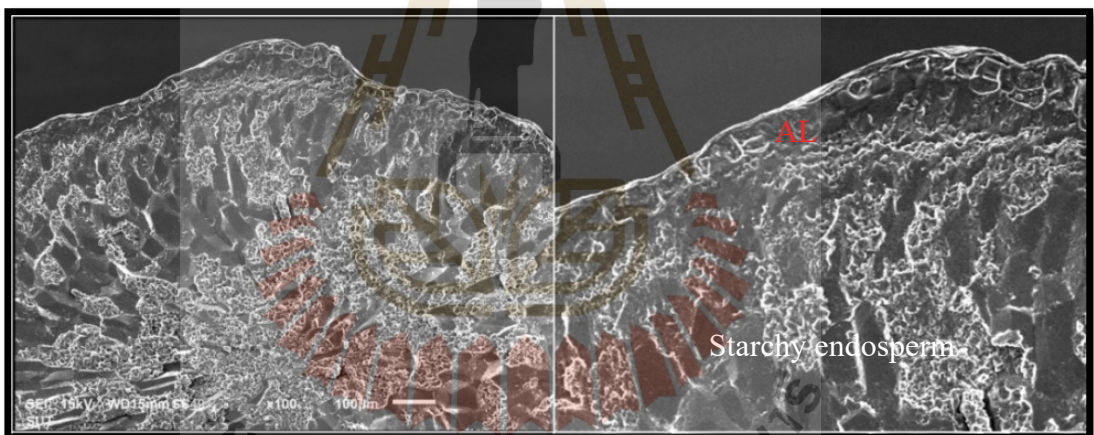


Figure 4.53 Morphology of seed treated in fertilizer 2 500 (18-46-0) and aleurone of starch in rice (scanning electronmicrographs 15kV×2000=10μm).

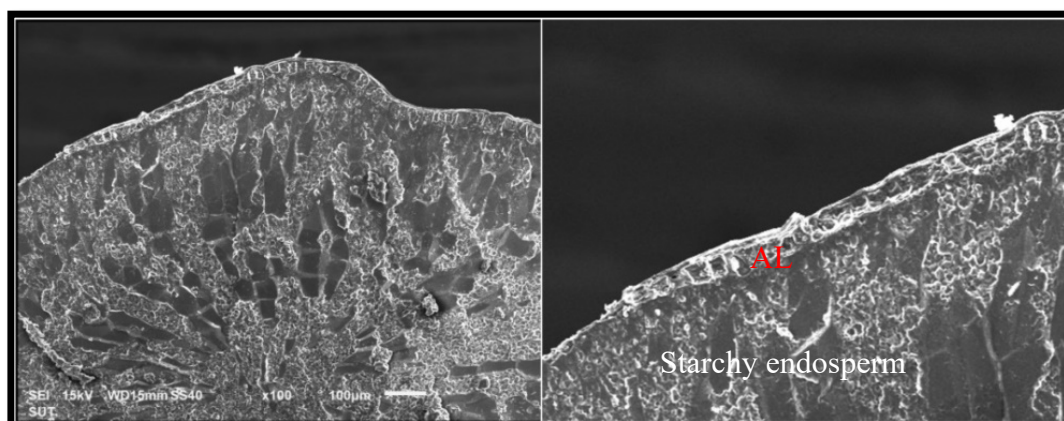


Figure 4.54 Morphology of seed treated in fertilizer 2 1,000 (18-46-0) and aleurone of starch in rice (scanning electronmicrographs15kV×2000=10µm).



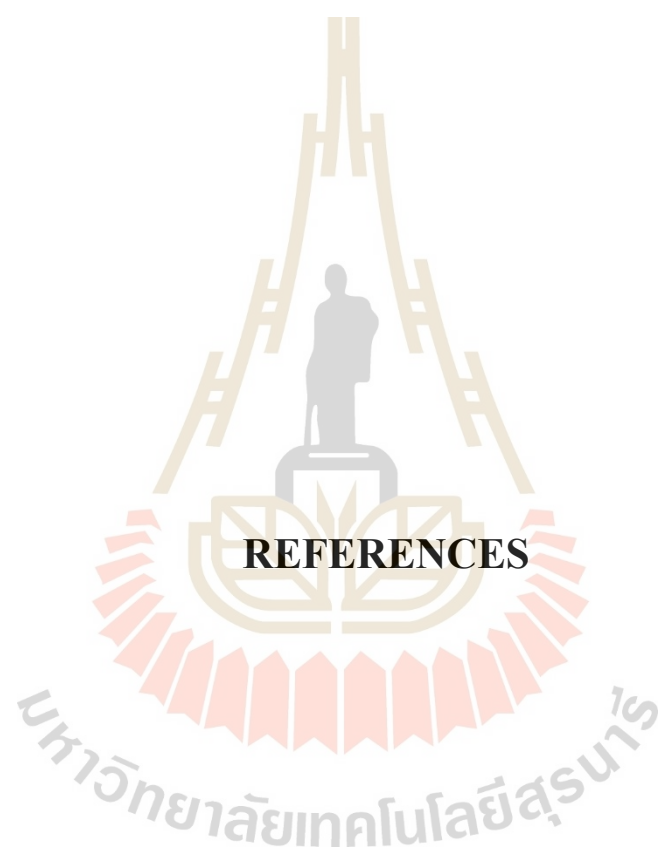
CHAPTER V

CONCLUSION

From our findings, it appeared that HAp nanoparticles have potential as nano phosphate and calcium fertilizer by using aloe vera extract as a reducing agent. HAp nanoparticles had the potential to stimulate certain responses for germination and the effects of growing plants. At 100 mg of HAp nanoparticles proved to be the higher dissolution and it led to slowly release continuously, including that it proved to be the best stimulated germination and root length according to our findings. While, at 1000 mg of HAp nanoparticles inhibited root length due to it was blocked on the surface of roots, it led to toxic in the cell membrane directly affects root development. But, it was not negatively affected on shoot length. In addition, from results plant stress treated with HAp nanoparticles experiments indicated that plant can tolerance to HAp nanoparticles. It was seen in the levels of higher MDA, while the cell death experiment was decreased in the HAp treated seedling. HAp nanoparticles and both commercial fertilizers showed no adverse impact on vegetative growth such as height and leaf width length. However, HAp nanoparticles also showed toxicity on the number of the panicle. The yield quality was tested indicates that the best of results at 1000 mg of HAp nanoparticles than both commercial fertilizer and control treatments such as the number of grains per panicle, weight of 1000 grains, starch content,

amylose content. In addition, the stimulating effect of seed aroma (2-AP) at 100, 500, and 1000 mg of HAp were proved to be better than the other treatments. Therefore, we concluded that HAp nanoparticles synthesized with aloe vera extracts might be an interesting point on stimulating seed germination and high quality in seed boosting. In addition, it enables farmers to ensure that use of HAp nanoparticles as nanofertilizer, the plant can uptake the nutrients derived from fertilizers throughout the growth cycle. The farmers have wisely used this fertilizer and gain more usefulness. Further studies on the HAp nanoparticle is suggested to include the monitoring of effects on the environment, leaching through soil and possible adverse effect on soil microorganism. Moreover, the design fertilizers to get attached in the soil with hydrogen bonds is interesting. Including, there have been no conclusive reports of the potential for uptake through the seed membrane and increase the ability to absorb, including the use of water that stimulates germination enzymes is another interesting factor.

-



REFERENCES

REFERENCES

- Abdulla Abdulaziz Alshehddi, L., and Bokhari, N. (2020). Influence of gold and silver nanoparticles on the germination and growth of *Mimusops laurifolia* seeds in the South-Western regions in Saudi Arabia. **Saudi Journal of Biological Sciences**. 27(1): 574-580.
- Al-Mamun, M.R., Hasan, M.R., Ahommed, M.S., Bacchu, M.S., Ali, M.R., and Khan, M.Z.H. (2021). Nanofertilizers toward sustainable agriculture and environment. **Environmental Technology & Innovation**: 101658.
- Albaum, H.G. (1952). The metabolism of phosphorylated compounds in plants. **Annual Review of Plant Physiology**. 3(1): 35-58.
- Alexandratos, N., and Bruinsma, J. (2012). **World agriculture towards 2030/2050: the 2012 revision**. Earthscan, Ltd, London.
- Ali, S., Rizwan, M., Noureen, S., Anwar, S., Ali, B., Naveed, M., Abd Allah, E.F., Alqarawi, A.A., and Ahmad, P. (2019). Combined use of biochar and zinc oxide nanoparticle foliar spray improved the plant growth and decreased the cadmium accumulation in rice (*Oryza sativa* L.) plant. **Environmental Science and Pollution Research**. 26(11): 11288-11299.
- Andrade, Â., Ferreira, J., and Domingues, R. (2004). Zeta potential measurement in bioactive collagen. **Materials Research-Ibero American Journal of Materials**. 7(4): 26-29.

- lani, F., Bagheri, S., Muhd Julkapli, N., Juraimi, A.S., Hashemi, F.S.G., and Baghdadi, A. (2014). Effects of engineered nanomaterials on plants growth: An overview. **The Scientific World Journal**. 2014: 641759.
- Aswathy Aromal, S., and Philip, D. (2012). Green synthesis of gold nanoparticles using *Trigonella foenum-graecum* and its size-dependent catalytic activity. **Spectrochimica Acta Part A: Molecular and Biomolecular Spectroscopy**. 97: 1-5.
- Badawi, M.A., Seadh, S.E., Naeem, E.S.B., and El-Iraqi, A.S.E.I. (2017). Effect of phosphorus fertilizer levels on productivity and grains quality of some rice cultivars. **Journal of Plant Production**. 8(3): 411-415.
- Bala, N., Dey, A., Das, S., Basu, R., and Nandy, P. (2014). Effect of hydroxyapatite nanorod on chickpea (*Cicer arietinum*) plant growth and its possible use as nano-fertilizer. **Iranian Journal of Plant Physiology**. 4(3): 1061-1069.
- Berg, J.M., Romoser, A., Banerjee, N., Zebda, R., and Sayes, C.M. (2009). The relationship between pH and zeta potential of ~ 30 nm metal oxide nanoparticle suspensions relevant to in vitro toxicological evaluations. **Nanotoxicology**. 3(4): 276-283.
- Bhattacharya, K.R., Sowbhagya, C.M., and Swamy, Y.M.I. (1982). Quality profiles of rice: A tentative scheme for classification. **Journal of Food Science**. 47(2): 564-569.
- Boonyanitipong, P., Kositsup, B., Kumar, P., Baruah, S., and Dutta, J. (2011). Toxicity of ZnO and TiO₂ nanoparticles on germinating rice seed. **International Journal of Bioscience, Biochemistry and Bioinformatics**. 1: 282-285.

- Borm, P., Klaessig, F.C., Landry, T.D., Moudgil, B., Pauluhn, J., Thomas, K., Trottier, R., and Wood, S. (2006). Research strategies for safety evaluation of nanomaterials, part V: role of dissolution in biological fate and effects of nanoscale particles. **Toxicological Sciences**. 90(1): 23-32.
- Borm, P.J.A., Robbins, D., Haubold, S., Kuhlbusch, T., Fissan, H., Donaldson, K., Schins, R., Stone, V., Kreyling, W., Lademann, J., Krutmann, J., Warheit, D., and Oberdorster, E. (2006). The potential risks of nanomaterials: a review carried out for ECETOC. **Particle and Fibre Toxicology**. 3(1): 1-11.
- Bradbury, L.M.T., Fitzgerald, T.L., Henry, R.J., Jin, Q., and Waters, D.L.E. (2005). The gene for fragrance in rice. **Plant Biotechnology Journal**. 3(3): 363-370.
- Bruinsma, J. (2003). **World agriculture: towards 2015/2030: an FAO perspective**. Earthscan, Ltd, London.
- Buttery, R.G., Ling, L.C., Juliano, B.O., and Turnbaugh, J.G. (1983). Cooked rice aroma and 2-acetyl-1-pyrroline. **Journal of Agricultural and Food Chemistry**. 31(4): 823-826.
- Carpita, N.C., and Gibeaut, D.M. (1993). Structural models of primary cell walls in flowering plants: consistency of molecular structure with the physical properties of the walls during growth. **The Plant Journal**. 3(1): 1-30.
- Cengiz, B., Gokce, Y., Yildiz, N., Aktas, Z., and Calimli, A. (2008a). Synthesis and characterization of hydroxyapatite nanoparticles. **Colloids and Surfaces A: Physicochemical and Engineering Aspects**. 322(1): 29-33.
- Cengiz, B., Gokce, Y., Yildiz, N., Aktas, Z., and Calimli, A. (2008b). Synthesis and characterization of hydroxyapatite nanoparticles. **Colloids and Surfaces A: Physicochemical and Engineering Aspects**. 322(1-3): 29-33.

- Chang, Y.-N., Zhang, M., Xia, L., Zhang, J., and Xing, G. (2012). The toxic effects and mechanisms of CuO and ZnO nanoparticles. **Materials**. 5(12): 2850-2871.
- Chen, H. (2018). Metal based nanoparticles in agricultural system: behavior, transport, and interaction with plants. **Chemical Speciation & Bioavailability**. 30(1): 123-134.
- Chen, S., Yang, Y., Shi, W., Ji, Q., He, F., Zhang, Z., Cheng, Z., Liu, X., and Xu, M. (2008). Badh2, encoding betaine aldehyde dehydrogenase, inhibits the biosynthesis of 2-acetyl-1-pyrroline, a major component in rice fragrance. **Plant Cell**. 20(7): 1850-1861.
- Chunguang, L., Dai, Z., and Sun, H. (2017). Potential of duckweed (*Lemna minor*) for removal of nitrogen and phosphorus from water under salt stress. **Journal of Environmental Management**. 187: 497-503.
- Çiçek, N., and Çakırlar, H. (2002). The effect of salinity on some physiological parameters in two maize cultivars. **Bulgarian Journal of Plant Physiology**. 28: 1-12.
- Cordell, D., Drangert, J.-O., and White, S. (2009). The story of phosphorus: Global food security and food for thought. **Global Environmental Change**. 19(2): 292-305.
- Destainville, A., Champion, E., Bernache-Assollant, D., and Laborde, E. (2003). Synthesis, characterization and thermal behavior of apatitic tricalcium phosphate. **Materials Chemistry and Physics**. 80(1): 269-277.
- do Espirito Santo Pereira, A., Caixeta Oliveira, H., Fernandes Fraceto, L., and Santaella, C. (2021). Nanotechnology potential in seed priming for sustainable agriculture. **Nanomaterials (Basel)**. 11(2).

- El-Maarouf-Bouteau, H., and Bailly, C. (2008). Oxidative signaling in seed germination and dormancy. **Plant signaling & behavior**. 3(3): 175-182.
- Eliaz, N., and Metoki, N. (2017). Calcium phosphate bioceramics: A review of their history, structure, properties, coating technologies and biomedical applications. **Materials**. 10(4): 1-16.
- FAO. (2017). **World fertilizer trends and outlook to 2020**. Food and Agriculture Organization of the United Nations (FAO), Rome, Italy.
- Femenia, A., García-Pascual, P., Simal, S., and Rosselló, C. (2003). Effects of heat treatment and dehydration on bioactive polysaccharide acemannan and cell wall polymers from *Aloe barbadensis* Miller. **Carbohydrate Polymers**. 51(4): 397-405.
- Gao, J., Wang, Y., Folta, K.M., Krishna, V., Bai, W., Indeglia, P., Georgieva, A., Nakamura, H., Koopman, B., and Moudgil, B. (2011). Polyhydroxy fullerenes (fullerols or fullerlenols): Beneficial effects on growth and lifespan in diverse biological models. **PLOS ONE**. 6(5): e19976.
- Giroto, A.S., Guimarães, G.G.F., Foschini, M., and Ribeiro, C. (2017). Role of slow-release nanocomposite fertilizers on nitrogen and phosphate availability in soil. **Scientific Reports**. 7: 46032-46032.
- Jan, A.T., Kamli, M.R., Murtaza, I., Singh, J.B., Ali, A., and Haq, Q.M.R. (2010). Dietary flavonoid quercetin and associated health benefits—An Overview. **Food Reviews International**. 26(3): 302-317.
- Jiang, X., Du, B., Huang, Y., and Zheng, J. (2018). Ultrasmall noble metal nanoparticles: Breakthroughs and biomedical implications. **Nano Today**. 21: 106-125.

- Kaviya, S., Santhanalakshmi, J., and Viswanathan, B. (2011). Green synthesis of silver nanoparticles using *Polyalthia longifolia* leaf extract along with D-sorbitol: Study of antibacterial activity. **Journal of Nanotechnology**. 2011: 152970.
- Khodakovskaya, M., Dervishi, E., Mahmood, M., Xu, Y., Li, Z., Watanabe, F., and Biris, A. (2009). Carbon nanotubes are able to penetrate plant seed coat and dramatically affect seed germination and plant growth. **American Chemical Society-Nano**. 3: 3221-3217.
- Khodakovskaya, M.V., Kim, B.S., Kim, J.N., Alimohammadi, M., Dervishi, E., Mustafa, T., and Cernigla, C.E. (2013). Carbon nanotubes as plant growth regulators: effects on tomato growth, reproductive system, and soil microbial community. **Small**. 9(1): 115-123.
- Klinkaewnarong, J., and Maensiri, S. (2010). Nanocrystalline hydroxyapatite powders by a polymerized complex method. **Chiang Mai Journal of Science**. 37(2): 243-251.
- Klinkaewnarong, J., Swatsitang, E., Masingboon, C., Seraphin, S., and Maensiri, S. (2010). Synthesis and characterization of nanocrystalline HAp powders prepared by using aloe vera plant extracted solution. **Current Applied Physics**. 10(2): 521-525.
- Kottegoda, N., Munaweera, I., Adassooriya, N., and Karunaratne, V. (2011). A green slow-release fertilizer composition based on urea-modified hydroxyapatite nanoparticles encapsulated wood. **Current Science**. 101: 73-78.
- Kottegoda, N., Munaweera, I., Madusanka, N., and Karunaratne, V. (2011). A green slow-release fertilizer composition based on urea-modified hydroxyapatite nanoparticles encapsulated wood. **Current Science**. 101(1): 73-78.

- Kottegoda, N., Sandaruwan, C., Priyadarshana, G., Siriwardhana, A., Rathnayake, U.A., Berugoda Arachchige, D.M., Kumarasinghe, A.R., Dahanayake, D., Karunaratne, V., and Amaratunga, G.A.J. (2017). Urea-hydroxyapatite nanohybrids for slow release of nitrogen. **American Chemical Society-Nano**. 11(2): 1214-1221.
- Koutsopoulos, S. (2002). Synthesis and characterization of hydroxyapatite crystals: A review study on the analytical methods. **Journal of Biomedical Materials Research**. 62(4): 600-612.
- Liu, R., and Lal, R. (2014). Synthetic apatite nanoparticles as a phosphorus fertilizer for soybean (*Glycine max*). **Scientific Reports**. 4(1): 5686.
- Liu, R., and Lal, R. (2014). Synthetic apatite nanoparticles as a phosphorus fertilizer for soybean (*Glycine max*). **Scientific Reports**. 4: 5686.
- López, A., de Tangil, M.S., Vega-Orellana, O., Ramírez, A.S., and Rico, M. (2013). Phenolic constituents, antioxidant and preliminary antimycoplasmic activities of leaf skin and flowers of *Aloe vera* (L.) Burm. f. (syn. *A. barbadensis* Mill.) from the *Canary Islands* (Spain). **Molecules**. 18(5): 4942-4954.
- Maensiri, S., Laokul, P., Klinkaewnarong, J., Phokha, S., and Seraphin, S. (2008). Indium oxide (In_2O_3) nanoparticles using aloe vera plant extract: Synthesis and optical properties. **Optoelectronics and Advanced Materials-rapid Communications**. 2: 161-165.
- Mani, P.K., and Mondal, S. (2016). Agri-nanotechniques for plant availability of nutrients. In: Kole, C., D. S. Kumar and M. V. Khodakovskaya (Ed.). **Plant nanotechnology: Principles and practices**. Cham, Springer International Publishing, pp. 263-303

- Marchiol, L., Filippi, A., Adamiano, A., Degli Esposti, L., Iafisco, M., Mattiello, A., Petrusa, E., and Braidot, E. (2019). Influence of hydroxyapatite nanoparticles on germination and plant metabolism of tomato (*Solanum lycopersicum* L.): Preliminary evidence. **Agronomy**. 9(4): 161.
- Merghany, M., Shahein, M., Sliem, M.A., Abdelgawad, K., and Radwan, A.F. (2019). Effect of nano-fertilizers on cucumber plant growth, fruit yield and it's quality. **Plant Archives**. 19(2): 165-172.
- Mikhak, A., Sohrabi, A., Kassae, M.Z., and Feizian, M. (2017). Synthetic nanozeolite/nanohydroxyapatite as a phosphorus fertilizer for *German chamomile* (*Matricaria chamomilla* L.). **Industrial Crops and Products**. 95: 444-452.
- Misra, S., Nuseibeh, S., Dybowska, A., Tetley, T., Berhanu, D., and Valsami-Jones, E. (2013). Comparative study using spheres, rods and spindle-shaped nanoplatelets on dispersion stability, dissolution and toxicity of CuO nanomaterials. **Nanotoxicology**. 8: 1-12.
- Montalvo, D., McLaughlin, M.J., and Degryse, F. (2015). Efficacy of hydroxyapatite nanoparticles as phosphorus fertilizer in andisols and oxisols. **Soil Science Society of America Journal**. 79(2): 551-558.
- Mukhopadhyay, S.S. (2014). Nanotechnology in agriculture: prospects and constraints. **Nanotechnology, Science and Applications**. 7: 63-71.
- Nasiri-Tabrizi, B., Fahami, A., and Ebrahimi-Kahrizsangi, R. (2013). A comparative study of hydroxyapatite nanostructures produced under different milling conditions and thermal treatment of bovine bone. **Journal of Industrial and Engineering Chemistry**. 20(1): 245-258.

- Palmer, L.C., Newcomb, C.J., Kaltz, S.R., Spoerke, E.D., and Stupp, S.I. (2008). Biomimetic systems for hydroxyapatite mineralization inspired by bone and enamel. **Chemical reviews**. 108(11): 4754-4783.
- Palomas, J., Boonsalee, S., and Jongprateep, O. (2018). Morphology and chemical compositions of hydroxyapatite powder synthesized by solution combustion and solid state reaction techniques. **Kasetsart Engineering Journal**. 31(106): 1-8.
- Pradhan, S., Durgam, M., and Mailapalli, D.R. (2021). Urea loaded hydroxyapatite nanocarrier for efficient delivery of plant nutrients in rice. **Archives of Agronomy and Soil Science**. 67(3): 371-382.
- Razaq, M., Zhang, P., Shen, H.-l., and Salahuddin. (2017). Influence of nitrogen and phosphorous on the growth and root morphology of i. **PLOS ONE**. 12(2): e0171321.
- Ruiqiang, L., and Rattan, L. (2015). Effects of molecular weight and concentration of carboxymethyl cellulose on morphology of hydroxyapatite nanoparticles as prepared with one-step wet chemical method. **Frontiers of Environmental Science & Engineering**. 9(5): 804-812.
- Shang, Y., Hasan, M.K., Ahammed, G.J., Li, M., Yin, H., and Zhou, J. (2019). Applications of Nanotechnology in Plant Growth and Crop Protection: A Review. **Molecules (Basel, Switzerland)**. 24(14): 2558.
- Shang, Y., Hasan, M.K., Ahammed, G.J., Li, M., Yin, H., and Zhou, J. (2019). Applications of nanotechnology in plant growth and crop protection: A review. **Molecules**. 24(14): 1-23.

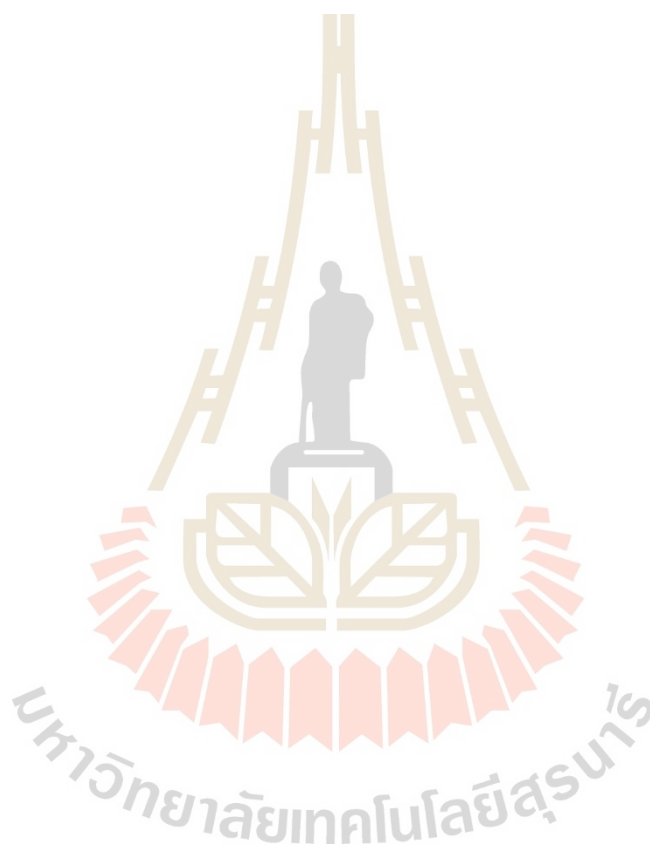
- Shuai, C., Yu, L., Yang, W., Peng, S., Zhong, Y., and Feng, P. (2020). Phosphonic Acid Coupling Agent Modification of HAP Nanoparticles: Interfacial Effects in PLLA/HAP Bone Scaffold. **Polymers**. 12(1): 199.
- Siddiqui, M.H., and Al-Whaibi, M.H. (2014). Role of nano-SiO₂ in germination of tomato (*Lycopersicon esculentum* seeds Mill.). **Saudi Journal of Biological Sciences**. 21(1): 13-17.
- Silva, B.L., Freire, P., Melo, F., Guedes, I., M.A. A., Filho, J.M., and Moreno, A.J.D. (1998). Polarized raman spectra and infrared analysis of vibrational modes in L-threonine crystals. **Brazilian Journal of Physics**. 28: 1-12.
- Smith, V.H., and Schindler, D.W. (2009). Eutrophication science: Where do we go from here? **Trends in Ecology & Evolution**. 24(4): 201-207.
- Soliman, A.S., Hassan, M., Abou-Elella, F., Ahmed, A.H., and El-Feky, S.A. (2016). Effect of nano and molecular phosphorus fertilizers on growth and chemical composition of baobab (*Adansonia digitata* L.). **Journal of Plant Sciences**. 11: 52-60.
- Sun, J., Wang, F., Sui, Y., She, Z., Zhai, W., Wang, C., and Deng, Y. (2012). Effect of particle size on solubility, dissolution rate, and oral bioavailability: Evaluation using coenzyme Q₁₀ as naked nanocrystals. **International journal of nanomedicine**. 7: 5733-5744.
- Suresh, C.M., Raj, S., and Trivedi, R. (2020). Nanotechnology a novel approach to enhance crop productivity. **Biochemistry and Biophysics Reports**. 24: 100821.
- Tarafdar, J.C., Raliya, R., and Rathore, I. (2012). Microbial synthesis of phosphorous nanoparticle from tri-calcium phosphate using *Aspergillus tubingensis* TFR-5. **Journal of Bionanoscience**. 6(2): 84-89.

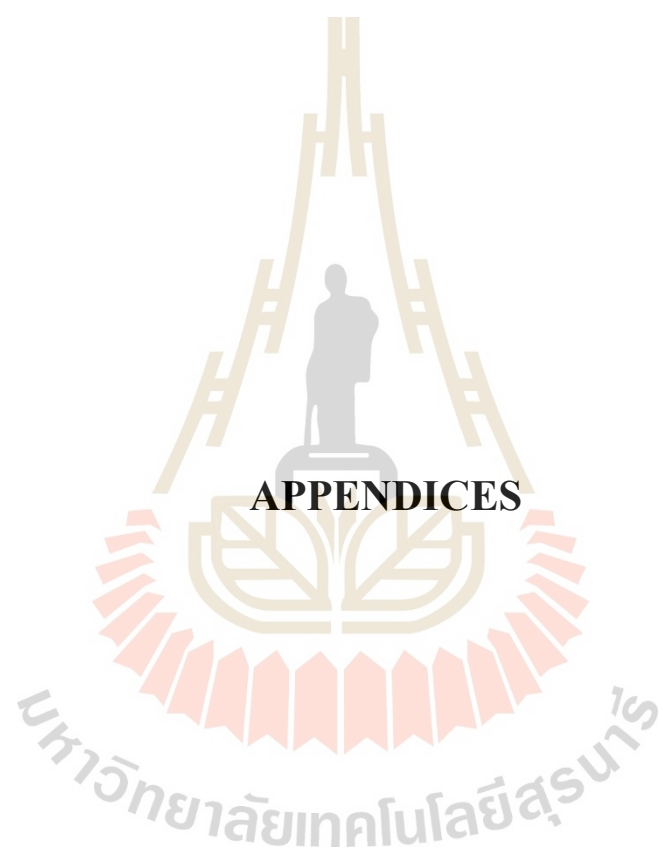
- Taşkın, M.B., Şahin, Ö., Taskin, H., Atakol, O., Inal, A., and Gunes, A. (2018). Effect of synthetic nano-hydroxyapatite as an alternative phosphorus source on growth and phosphorus nutrition of lettuce (*Lactuca sativa* L.) plant. **Journal of Plant Nutrition**. 41(9): 1148-1154.
- Thin, M.M., Sacchi, E., Setti, M., and Re, V. (2020). A dual Source of phosphorus to lake sediments indicated by distribution, content, and speciation: Inle lake (Southern Shan State, Myanmar). **Water**. 12(7): 1993.
- Tippayawat, P., Phromviyo, N., Boueroy, P., and Chompoosor, A. (2016). Green synthesis of silver nanoparticles in aloe vera plant extract prepared by a hydrothermal method and their synergistic antibacterial activity. **PeerJ**. 4: e2589.
- Tuong, T., and Bouman, B. (2003). Rice production in water-scarce environments. **Water productivity in agriculture: Limits and opportunities for improvement**. 1: 13-42.
- Tuteja, N., and Mahajan, S. (2007). Calcium signaling network in plants: an overview. **Plant signaling & behavior**. 2(2): 79-85.
- Watanabe, Y., Yamada, H., Ikoma, T., Tanaka, J., Stevens, G.W., and Komatsu, Y. (2014). Preparation of a zeolite NaP1/hydroxyapatite nanocomposite and study of its behavior as inorganic fertilizer. **Journal of Chemical Technology & Biotechnology**. 89(7): 963-968.
- Wilkinson, J. (2015). Food security and the global agrifood system: Ethical issues in historical and sociological perspective. **Global Food Security**. 7: 9-14.
- Wongpornchai, S., Sriseadka, T., and Choonvisase, S. (2003). Identification and quantitation of the rice aroma compound, 2-acetyl-1-pyrroline, in bread flowers

- (*Vallaris glabra* Ktze). **Journal of Agricultural and Food Chemistry**. 51(2): 457-462.
- Xu, H.H., Moreau, J.L., Sun, L., and Chow, L.C. (2011). Nanocomposite containing amorphous calcium phosphate nanoparticles for caries inhibition. **Dental Materials**. 27(8): 762-769.
- Yuvakkumar, R., Elango, V., Rajendran, V., Kannan, N., and Prabu, P. (2011). Influence of nanosilica powder on the growth of maize crop (*Zea Mays* L.). **International Journal of Green Nanotechnology**. 3: 180-190.
- Zhao, Y., Zheng, H.-X., Xu, Y., and Lin, N. (2019). Estrogenic effect of the extract of Qingyan formula on reproductive tissues in immature mice. **Evidence-Based Complementary and Alternative Medicine**. 2019: 1-8.
- Zheng, Y., Wang, H., Yang, M., Peng, G., Dong, T.T., Xu, M.L., and Tsim, K.W. (2018). Prenylated flavonoids from roots of *Glycyrrhiza uralensis* Induce differentiation of B16-F10 melanoma cells. **International Journal of Molecular Sciences**. 19(8): 8.
- Zheng, Z.H., Han, Y., You, S.Y., Chen, Z., and Zheng, X.D. (2019). Improvement in post-partum uterine involution in rats treated with *Apios americana*. **Journal of Zhejiang University-SCIENCE B**. 20(7): 576-587.
- Zhu, Y., Yao, Y., Shi, Z., Everaert, N., and Ren, G. (2018). Synergistic effect of bioactive anticarcinogens from soybean on anti-proliferative activity in MDA-MB-231 and MCF-7 human breast cancer cells *in vitro*. **Molecules**. 23(7): 1557.
- Zubair, H., Bhardwaj, A., Ahmad, A., Srivastava, S.K., Khan, M.A., Patel, G.K., Singh, S., and Singh, A.P. (2017). Hydroxytyrosol induces apoptosis and cell

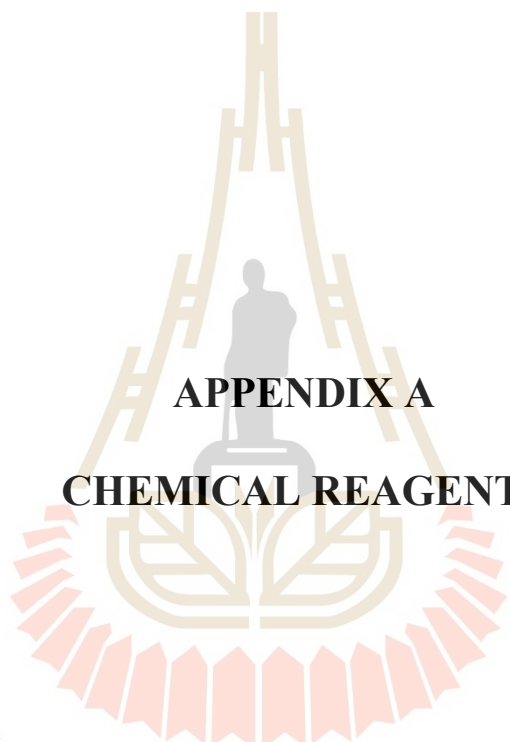
cycle arrest and suppresses multiple oncogenic signaling pathways in prostate cancer cells. **Nutrition and Cancer**. 69(6): 932-942.

Zyla, K., Ledoux, D.R., Garcia, A., and Veum, T. (2007). An *in vitro* procedure for studying enzymic dephosphorylation of phytate in maize-soyabean feeds for turkey poult. **BMC Complementary Medicine and Therapies**. 74(1): 3-17.





APPENDICES



APPENDIX A
CHEMICAL REAGENTS

มหาวิทยาลัยเทคโนโลยีสุรนารี

A.1 Aloe vera extracts

Aloe vera extract 35 g DI water 100 mL

A.2 Preparation of calcium nitrate and diammonium hydrogen phosphate

39.4 g of calcium nitrate ($\text{Ca}(\text{NO}_3)_2 \cdot 4\text{H}_2\text{O}$ (99 % purity, BDH)), and 11.5 g of diammonium hydrogen phosphate ($(\text{NH}_4)_2\text{HPO}_4$ (99% purity, BDH)) were added in 250 ml of DI water

A.3 Preparation of different concentrations of hydroxyapatite (HAp) solutions

100 mg /L or 0.01 g

500 mg/L or 0.05 g

1000 mg/L or 0.1 g

Preparation : Dissolve respective amounts in 100 mL of distilled water and ultrasonication for 30 minutes.

A.4 Preparation of different concentrations of fertilizers suspensions

(Fertilizer1 = N=18 and P=46 K=0)

(Fertilizer2 = N=15 and P=15 K=15)

Fertilizer1 100 mg /L or 0.01 g

Fertilizer1 500 mg/L or 0.05 g

Fertilizer1 1000 mg/L or 0.1 g

Fertilizer2 100 mg/L or 0.01 g

Fertilizer 2 500 mg/L or 0.05g

Fertilizer 2 1000 mg/L or 0.1 g

Preparation: Dissolve respective amounts in 100 mL of distilled water and ultrasonication for 30 minutes.

A.5 Reaction mixture for cell death

Preparation of 0.25 % v/v Evans blue

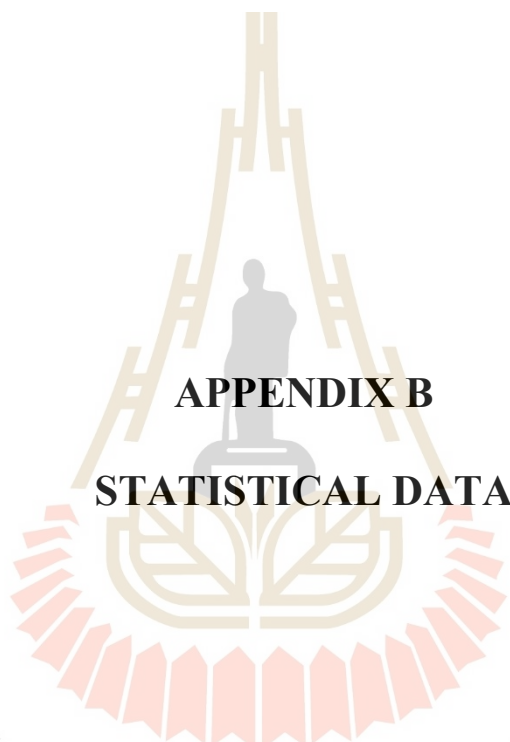
0.25 g of Evans blue powder in 100 mL in distilled water

A.6 Chemical for MDA extraction

0.25% (w/v) Thiobarbituric acid (TBA) 0.25 g

10 % Trichloroacetic acid (TCA) 10 g

Preparation: Dissolve 10 g of TCA and 0.25 g of TBA in distilled water and make up to respective volumes of 100 mL each.

The logo of Sakon Nakhon Vejjajit Rajabhat University is a circular emblem. It features a central figure of a person standing on a pedestal, surrounded by a stylized sunburst or gear-like border. The text 'มหาวิทยาลัยเทคโนโลยีสุรนารี' is written in Thai script around the bottom of the emblem.

APPENDIX B
STATISTICAL DATA

มหาวิทยาลัยเทคโนโลยีสุรนารี

Table 1 Effect of HAp nanoparticles and commercial fertilizers at different concentrations 100, 500, 1000 mg/L on germination percent.

Germinations (%)				
Concentrations	N	Subset for alpha = 0.05		
		a	b	c
Fertilizer2 500	5	68.0000		
HA1000	5	74.0000	74.0000	
HA500	5	76.0000	76.0000	
Fertilizer2 100	5	76.0000	76.0000	
Fertilizer1 500	5	80.0000	80.0000	80.0000
Fertilizer1 1000	5	80.0000	80.0000	80.0000
Fertilizer2 1000	5	84.0000	84.0000	84.0000
Fertilizer1 100	5	88.0000	88.0000	88.0000
Control	5		90.0000	90.0000
HA100	5			98.0000
Sig.		.059	.131	.082

Means for groups in homogeneous subsets are displayed.

a. Uses Harmonic Mean Sample Size = 5.000.

Average of values are means \pm Error (N=5) of relative water contents under different concentrations of hydroxyapatite nanoparticles and commercial fertilizers (18-46-0) and (15-15-15). Analysis significantly different at Duncan's test ($P \leq 0.05$).

Table 2 Effect of HAp nanoparticles and commercial fertilizers at 100, 500, 1000 mg/L on relative water content (%).

Relative Water Content (%)				
Concentrations Duncan ^a	N	Subset for alpha = 0.05		
		a	b	c
Fertilizer2 100 mg	7	74.8304		
Fertilizer1 100 mg	7	79.0396	79.0396	
HA100 mg	7	79.3170	79.3170	
HA500 mg	7	79.8675	79.8675	
Fertilizer1 500	7	80.1996	80.1996	
Control	7	81.6541	81.6541	81.6541
Fertilizer1 1000 mg	7	81.6757	81.6757	81.6757
Fertilizer2 500 mg	7	82.1098	82.1098	82.1098
Fertilizer2 1000 mg	7		82.7581	82.7581
HA1000 mg	7			88.7345
Sig.		.067	.352	.063

Means for groups in homogeneous subsets are displayed.

a. Uses Harmonic Mean Sample Size = 7.000.

Average of values are means \pm Error (N=7) of relative water contents under different concentrations of hydroxyapatite nanoparticles and commercial fertilizers (18-46-0) and (15-15-15). Analysis significantly different at Duncan's test ($P \leq 0.05$).

Table 3 Effect of HAp nanoparticles and commercial fertilizers at different concentrations 100, 500, 1000 mg/L on shoot length.

Concentrations	N	Shoot length (cm)	
		Subset for alpha = 0.05	
		a	b
Fertilizer2 100	3	3.7960	
HA100	3	3.9781	3.9781
HA500	3	4.1072	4.1072
Fertilizer2 500	3	4.1803	4.1803
Control	3	4.3235	4.3235
Fertilizer1 100	3	4.3960	4.3960
HA1000	3	4.4065	4.4065
Fertilizer1 500	3	4.4247	4.4247
Fertilizer2 1000	3	4.4593	4.4593
Fertilizer1 1000	3		4.8353
Sig.		.171	.081

Means for groups in homogeneous subsets are displayed.

a. Uses Harmonic Mean Sample Size = 3.000.

Average of values are means \pm Error (N=3) of relative water contents under different concentrations of hydroxyapatite nanoparticles and commercial fertilizers (18-46-0) and (15-15-15). Analysis significantly different at Duncan's test ($P \leq 0.05$).

มหาวิทยาลัยเทคโนโลยีสุรนารี

Table 4 Effect of HAp nanoparticles and commercial fertilizers at different concentrations 100, 500, 1000 mg/L on root length.

Treatments	N	Root length (cm)		
		Subset for alpha = 0.05		
		a	b	c
Fertilizer1 1000	3	3.3020		
Fertilizer2 500	3	4.3727		
Fertilizer2 1000	3	4.4257		
HA1000	3		6.5037	
Fertilizer1 500	3		6.5673	
Fertilizer2 100	3		7.0303	7.0303
Control	3		7.6592	7.6592
Fertilizer1 100	3		7.8097	7.8097
HA100	3		8.0607	8.0607
HA500	3			8.4779
Sig.		.132	.054	.068

Means for groups in homogeneous subsets are displayed.

a. Uses Harmonic Mean Sample Size = 3.000.

Average of values are means \pm Error (N=3) of relative water contents under different concentrations of hydroxyapatite nanoparticles and commercial fertilizers (18-46-0) and (15-15-15). Analysis significantly different at Duncan's test ($P \leq 0.05$).

Table 5 Effect of HA nanoparticles and commercial fertilizers at different concentrations 100, 500, 1000 mg/L on malondialdehyde (MDA).

		MDA					
Concentrations	N	Subset for alpha = 0.05					
Duncan ^a		a	b	c	d	e	f
Fertilizer1 500 mg	3	7.50					
Fertilizer1 1000 mg	3		9.74				
Fertilizer2 100 mg	3			11.08			
Fertilizer2 500 mg	3			11.36			
Fertilizer2 1000mg	3				12.75		
Fertilizer1 100mg	3				12.81		
HA1000 mg	3				13.96	13.96	
Control	3					14.62	
HA100 mg	3					15.22	
HA500 mg	3						21.77
Sig.		1.000	1.000	.657	.075	.061	1.000

Means for groups in homogeneous subsets are displayed.
a. Uses Harmonic Mean Sample Size = 3.000.

Average of values are means \pm Error (N=3) of relative water contents under different concentrations of hydroxyapatite nanoparticles and commercial fertilizers (18-46-0) and (15-15-15). Analysis significantly different at Duncan's test ($P \leq 0.05$).

Table 6 Effect of HAp nanoparticles and commercial fertilizers at different concentrations 100, 500, 1000 mg/L on cell death.

Cell death						
Concentrations Duncan ^a	N	Subset for alpha = 0.05				
		a	b	c	d	e
Fertilizer1 100 mg	8	0.83				
Fertilizer1 500 mg	8		0.98			
HA1000 mg	8			1.17		
HA100 mg	8			1.23		
HA500 mg	8			1.25		
Control	8			1.27		
Fertilizer1 1000 mg	8				1.81	
Fertilizer2 100 mg	8				1.83	
Fertilizer2 500 mg	8				1.89	
Fertilizer2 1000 mg	8					2.01
Sig.		1.000	1.000	.083	.157	1.000

Means for groups in homogeneous subsets are displayed.
a. Uses Harmonic Mean Sample Size = 8.000.

Average of values are means \pm Error (N=8) of relative water contents under different concentrations of hydroxyapatite nanoparticles and commercial fertilizers (18-46-0) and (15-15-15). Analysis significantly different at Duncan's test ($P \leq 0.05$).

Table 7 Effect of HAp nanoparticles and commercial fertilizers at different concentrations 100, 500, 1000 mg/L on number of panicle.

Number of panicle				
Concentrations Duncan ^a	N	Subset for alpha = 0.05		
		a	b	c
HA500 mg	5	8.4		
HA1000 mg	5	8.8		
Control	5	9.2		
HA100 mg	5	9.4		
Fertilizer2 1000 mg	5	10.6	10.6	
Fertilizer2 100 mg	5	11.2	11.2	11.2
Fertilizer1 1000 mg	5	12.0	12.0	12.0
Fertilizer2 500 mg	5		13.8	13.8
Fertilizer1 500 mg	5		14.0	14.0
Fertilizer1 100 mg	5			15.0
Sig.		.101	.110	.074

Means for groups in homogeneous subsets are displayed.
a. Uses Harmonic Mean Sample Size = 5.000.

Average of values are means \pm Error (N=5) of relative water contents under different concentrations of hydroxyapatite nanoparticles and commercial fertilizers (18-46-0) and (15-15-15). Analysis significantly different at Duncan's test ($P \leq 0.05$).

Table 8 Effect of HAp nanoparticles and commercial fertilizers at different concentrations 100, 500, 1000 mg/L on number of grain of panicle.

Grain per panicle			
Concentrations Duncan ^a	N	Subset for alpha = 0.05	
		a	b
Fertilizer2 500 mg	10	61.64	
Fertilizer2 1000 mg	10	65.62	
Fertilizer1 500 mg	10	67.82	
HA500 mg	10	67.87	
HA100 mg	10	68.08	
Fertilizer2 100 mg	10	68.18	
Fertilizer1 100 mg	10	69.20	
Control	10	69.26	
Fertilizer1 1000 mg	10	70.66	
HA1000 mg	10		91.94
Sig.		.122	1.000

Means for groups in homogeneous subsets are displayed.
a. Uses Harmonic Mean Sample Size = 10.000.

Average of values are means \pm Error (N=10) of relative water contents under different concentrations of hydroxyapatite nanoparticles and commercial fertilizers (18-46-0) and (15-15-15). Analysis significantly different at Duncan's test ($P \leq 0.05$).

Table 9 Effect of HAp nanoparticles and commercial fertilizers at at different concentrations 100, 500, 1000 mg/L on weight of 1000 seed.

		Weight of 1000 grains					
Concentrations Duncan ^a	N	Subset for alpha = 0.05					
		a	b	c	d	e	f
Fertilizer2 1000 mg	4	23.53					
Fertilizer2 500 mg	4	23.65					
Fertilizer1 500 mg	4		25.25				
Fertilizer1 1000 mg	4		25.30				
Fertilizer2 100 mg	4			25.78			
Control	4				26.23		
HA500 mg	4				26.29	26.29	
Fertilizer1 100 mg	4					26.62	
HA100 mg	4						27.41
HA1000 mg	4						27.50
Sig.		.501	.808	1.000	.746	.078	.618

Means for groups in homogeneous subsets are displayed.
a. Uses Harmonic Mean Sample Size = 4.000.

Average of values are means \pm Error (N=4) of relative water contents under different concentrations of hydroxyapatite nanoparticles and commercial fertilizers (18-46-0) and (15-15-15). Analysis significantly different at Duncan's test ($P \leq 0.05$).

CURRICULUM VITAE

Name Miss. Sirinapa Pongpeera

Date of Birth 15 June 1984

Place of Birth Ubon Ratchathani Province, Thailand.

Education She received the Bachelor's degree in Applied Biology from Ubon Ratchathani Rajabhat University in 2007 and the Master's degree in Biology from Khon Kaen University in 2010. She has pursued the Ph.D. degree in Environmental Biology at Suranaree University of Technology. Her research expertise is in the field of nano-biology applied for agriculture. During her study, she has attended international union of materials research societies' international conference in Asia (IUMRS-ICA)

Poster presentation: 1. Enhancing Effect of Released Calcium and Phosphorus from Hydroxyapatite Nanoparticles on Rice Germination and Growth (2019).

2. Effect of hydroxyapatite nanoparticles on vegetative growth and yield quality in rice (*Oryza sativa* L.) (2021).

Digital Research Information Center:

Wastewater treatment from fermented rice noodle factory by using *Spirulina sp.* and *Chlorella sp.* (2010).